National Library of Canada
Acquisitions and Bibliographic Services Branch
395 Wellington Street
Ottawa, Ontario
K1A 0N4

Bibliothèque nationale du Canada
Direction des acquisitions et des services bibliographiques
395, rue Wellington
Ottawa (Ontario)
K1A 0N4

Your file Votre référence

Our file Notre référence

NOTICE

The quality of this microform is heavily dependent upon the quality of the original thesis submitted for microfilming. Every effort has been made to ensure the highest quality of reproduction possible.

If pages are missing, contact the university which granted the degree.

Some pages may have indistinct print especially if the original pages were typed with a poor typewriter ribbon or if the university sent us an inferior photocopy.

AVIS

La qualité de cette microforme dépend grandement de la qualité de la thèse soumise au microfilmage. Nous avons tout fait pour assurer une qualité supérieure de reproduction.

S'il manque des pages, veuillez communiquer avec l'université qui a conféré le grade.

La qualité d'impression de certaines pages peut laisser à désirer, surtout si les pages originales ont été dactylographiées à l'aide d'un ruban usé ou si l'université nous a fait parvenir une photocopie de qualité inférieure.

Canada

Performance Evaluation of a Computer Simulation of an Artificial Arm Using the Principle of Extended Physiological Proprioception

Sébastien Philippe-Auguste

A thesis submitted to the School of Graduate Studies and Research in partial fulfillment of the degree of

Doctor of Philosophy

Ottawa-Carleton Institute for Electrical Engineering

Department of Electrical Engineering, Faculty of Engineering, University of Ottawa,
Ottawa, Ontario, Canada 1993

ISBN 0-315-95967-3

Canada

UNIVERSITÉ D'OTTAWA
UNIVERSITY OF OTTAWA

I hereby declare that I am the sole author of this document. I authorize the University of Ottawa to lend this document to other individuals or institutions for the purpose of scholarly research. I further authorize the University of Ottawa to reproduce this document

by photocopying or by other means, in total or in part, at the request of other institutions or individuals for the purpose of scholarly research.

Acknowledgement

I wish to express my sincere gratitude to my supervisor, Dr. David Gibbons for his constant guidance, encouragement, and support throughout my reseach. Dr. David Gibbons has been, a father and friend to me.

I also would like to thank Dr. M. O'Riain for his generous and invaluable help and support at all phases of this work.

Many thanks to my colleagues and friends, Genevieve Vinet, J. Lin, J. Wang, Y. Djadi, A. Zaabab, A. Sisirucca and Joe for their help with my tests and for support.

I would like to thank the faculty and staff of the Department of Electrical Engineering, University of Ottawa and Rehabilitation Engineering, The Rehabilitation Center, Ottawa, for their kind support. I would also like to acknowledge the financial support from the Natural Science and Engineering Research Council of Canada and from the University of Ottawa.

Merci à ma mère et à mon père.

Abstract

This research work investigates a control strategy for artificial arms called Extended Physiological Proprioception (EPP). EPP control relies on the fact that the body's natural position feedback, also called proprioception, can be "extended" outside the body to a tool or, in this case, an artificial arm. Hence, providing closed-loop operation without the use of visual feedback. The presence of a natural source of feedback is essential if subconscious operation of an artificial arm is desired.

A hardware artificial arm was not used in this research, instead, a software simulation based on a simple mathematical model was employed. The interface between the human operator and the artificial arm was a virtual reality. The immense exploratory potential of virtual reality combined with our simulation was used to: 1) prove that EPP is an adequate control strategy to "communicate the intent" of the operator to the artificial arm; 2) show that subconscious operation of the arm was possible, 3) demonstrate that several motions (realized through programmed linkages) could be learned, used and remembered, 4) show that adequate discrimination between the various linkages (motions) could be easily done; and finally 5) allow the formulation of various recommendations for future design of EPP controlled artificial arms.

Contents

List of Figures

List of Tables

Chapter 1

Introduction

The control of a man-machine system such as an artificial arm, has been a challenge for researchers for many decades. The difficulty arises from the fact that when operating the device, it must mimic as closely as possible the natural limb without requiring too much concentration from the user. Moreover, whether the artificial arm is used for fine and precise work such as radioactive element manipulation, satellite positioning in space or gross work like tractor back-hoe manoeuver, the operator needs to have a "feel" for the artificial terminal device[1]. This should enable him to accommodate easily to the operation of the device and, at some point, use it subconsciously. This "feel" can be made possible by feeding back various parameters to the operator. In the case of a man-machine system controlled via command sticks, for example, this feedback can be of various forms:

- Position sensation: The position of the "command sticks" could be directly related to the position of the terminal device.
- Force sensation: The command sticks could stiffen in proportion to the force encountered by the terminal device.
- Velocity and to a lesser extent acceleration sensations: In this case, the speed at which the terminal device moves corresponds to the speed at which the operator drives the inputs.

[1]Most artificial arms are made of a combination of members or links resembling the natural upperarm and of a terminal device that can be a hook, a gripper or an articulated hand.

As can be seen from the above statement, the feedback information coming from the output of the controlled process is what provides the natural "feel" that we get when we are using a machine as an extension of ourselves. In most cases when dealing with a "normal"[2] subject operating a machine in a situation where weight and space are not critical, this feedback information is easily offered to the operator via:

1. The command sticks (position, force, speed and acceleration sensations)

2. Video screens (for visual feedback).

3. Loud speakers or earphones (for sound feedback).

Thus the hands, eyes and ears of the operator can be used as natural interfaces to code the external information to corresponding biological signals that the central nervous system can understand and process. The problem becomes a lot more involved when it comes to realizing rehabilitative assistive devices[3] for amputees. In this case, the natural man-to-external-world interface (i.e. the hand) is not available anymore, it is now difficult to pass information from man to machine and even more difficult for the mechanical side to feedback information to the central nervous system.

There have been many strategies proposed to control artificial limbs and the most relevant ones will presented in the next chapter. This thesis presents an innovative system developed to analyze the possible use of the strategy which is known as extended physiological proprioception or e.p.p., for the control of an artificial arm and other remote manipulators capable of performing a multitude of different motions.

The author of the present thesis has already done some work in conjunction with D.T. Gibbons and M.D. O'Riain in the field of artificial arms using the principle of e.p.p. We designed

[2]The term "normal subject" is used in contrast with disabled subject or amputee as no better terminology exits to designate a person with no disability.

[3]The rehabilitative devices discussed in this dissertation will be restricted to those used as upper limb replacement for amputees.

and constructed a bench model around the Boston elbow. This artificial arm was electrically powered and controlled by a microprocessor. It offered a possible repertoire of 16 different preprogrammed input/output relationships or linkages. Linkages define the input/output relationship between the shoulder joint, the elbow joint and the terminal device. Tests were run using normal subjects and the results were published [20][34]. As a result of these tests, we have shown that the shoulder joint can be used efficiently to control an artificial joint and provide e.p.p. at the same time. We have also shown that an e.p.p. controlled assistive device can have different programed linkages and still be used and operated without loss of proprioceptive feedback. Simpson has shown that in an e.p.p. device having a fixed 1:1 relationship between input and output, subconscious control by the user was achieved. We have used a modified form of e.p.p. where the input is connected to the output by programmed linkages which means that one input can correspond to many outputs depending on the choice of the user. Our system is also different from that of Simpson in that we have realized that it is sometimes better to provide a user with a system in which a coordinated motion of the output joints can be obtained by the action of a single input. Thus some tasks, which would require the coordinated motion of many joints and hence require an increased concentration level to be performed, can now be executed in a much simpler manner using only one or a few inputs. Of course, the user will have to familiarize himself with such a system and we are expecting some loss of speed and probably also accuracy compared with Simpson's original e.p.p. system. This research is motivated by the desire to study and quantify the degree of skill acquisition and retention when subconciously operating a multi-linkage multiple degree of freedom artificial arm. The rationale for the research is that the thorough and systematic evaluation tool that was developed during this work enabled the following to be done:

- To choose an adequate number of preprogrammed motions or "linkages" for a particular individual.
- Via the Virtual Reality simulation (to be discussed in chapter 3) to choose useful linkages corresponding to the needs and learning capacity of each individual.

1.1 Objective and Approach

The global objectives of this study were:

1. To develop a fully animated Virtual Reality simulation of an artificial arm coupled with a data acquisition system that should allow us to address the following questions:
   - Can c.p.p. be used efficiently with more then one linkage ?
   - What is the loss of accuracy and speed resulting from the addition of new linkages ?
   - Can a subject pick from a set of linkages, the one that best fits the task he is about to undertake ?
   - Is the hardware unbeatable servo indispensable ?
2. To perform tests on the system to answer the above questions and:
   - To gain more knowledge about the behavior of a human operating a machine, in areas such as:
     (a) Average reaction time, trial time.
     (b) The kind of controller that the human being becomes when using this simulation and compare that to results obtained by other research groups [30].
   - To gain some insight into the control interface. To investigate ideas to define hardware to facilitate learning and the use of the artificial arm.
   - To determine the extent to which this control strategy is viable.

The system is based on a computer simulation of an artificial arm. A simulation was considered to be much more appropriate than a bench model for the purposes of the present work for several reasons:

Safety. When working with volunteers, who are usually unconnected with the research, this is a most important factor. There is no risk of accident since the only hardware involved is the digital computer and a small passive potentiometer used to measure limb angle.

Flexibility. This is also an important factor since it allows us to build a general model for the prosthesis and refine it as needed. For instance, the operation of various commercial artificial arms is very easily modeled. There is also a great ease in simulating various conditions:

- The arm operating in the presence or absence of gravity.
- The arm operating loaded or unloaded.
- Different types of actuators such as ones not yet developed or even "ideal" ones.
- The geometry of the mechanical arm can be altered as desired and various lengths of limbs can be tested.

Practical aspect and realism. When using this simulation we found many important advantages over a bench model, especially in the case of reaching a target in space. True positioning tests can be performed without the subjects getting any cues when they touch a target, since it is only an image. Also, motor sounds, that could be used as an avenue of feedback, are totally absent. Furthermore, it is simple to implement the unbeatable servo feature that prevents the input from exceeding the capabilities of the output. Finally, the data gathering process is made faster and more accurate, since the precise measurement of the distance between the terminal device and the target is done automatically without disturbing the subject. The risk of disturbing the subject was a problem with the bench model. The elapsed time between starting and ending of each test is also monitored by the system, thus reducing the risk of timing errors.

Comfort. The prosthetic harness of our bench model was not comfortable and weight distribution was not even. Subjects fatigued when wearing it for some time and accuracy in positioning was affected. The simulation, once again, resolved that problem.

In implementing this computer simulation, our goals were to be able to display on a computer monitor, the complete real-time motion of an above elbow artificial arm worn by an amputee. The image had to be realistic enough such that the test subject seated in front of

the screen had the impression that he was actually wearing the artificial arm. The achievement of this goal required three major steps. The first one was to write the software such that a comprehensive model of the artificial arm could be defined and used by the simulation. The second one was to implement a life-like image of the complete artificial arm that would move just like the real system. The third step was to implement various tasks incorporating preprogrammed linkages.

1.2 Organization of the thesis

Chapter 1 presents the motivation behind the work done in this research. The objective is presented through a series of questions and an approach is proposed to provide answers.

Chapter 2 of this thesis is a review of the different strategies used for the control of artificial arms. The two major schools of thoughts based on 1) electromyographic control (EMG) and 2) extended physiological proprioception (e.p.p.) are introduced and contrasted.

Chapter 3 provides the reader with some background on "Virtual Reality" as this field is not well known although very popular these days. A background on three dimensional computer graphics is given. The tools needed for the implementation of a good Virtual Reality simulation are discussed.

Chapter 4 describes the simulation environment as a whole. The computer generated image of the artificial arm and the background scene are discussed. The preprogrammed coordinated motions called "linkages" are presented. We then move on to expose the basic model (including the differential equations) used for the artificial arm and an analysis of its dynamics. Some but not all the mathematical derivations are included in this chapter in order to facilitate reading; the complete mathematics is reported in appendix A.

Chapter 5 presents the results obtained. The general testing protocol is outlined and then each category of test is presented and discussed. The purpose of each of the tests is also emphasized. We also included in this chapter the data gathering process for completeness.

A brief commentary on the acceptance of the Virtual Reality by the subjects is made. Results are then introduced. In order to facilitate analysis, a case study is done on three typical subjects and any salient point, not common to all subjects, is analyzed and explained. Answers are provided to the basic questions raised prior to the start of this work. Suggestions are provided for future work in the field, such as to serve as guidelines since such information was not available in the literature.

The last chapter concludes by summarizing the work that was done and future work is proposed.

1.3 Contribution

This research work is probably one of the first to combine the exploratory potential of Virtual Reality to the study of adequate control strategies for artificial arms. Futhermore, it is the first study to assess the capabilities of a human being to learn programmed linkages, remember them, and use them. This was achieved without testing real amputees wearing experimental arms, but rather by testing so-called "normal" subjects. This argument takes on real meaning when we realize the responsibility of researchers who are faced with the problem of ethics in ensuring that they do not to raise false hope among disabled patients. Other direct contributions of this work are:

- Development of a computer program incorporating the features of a Virtual Reality, as the main research tool. The requirements were to perform the simulation on a Personal Computer which should run in real-time. No commercial software could be used as none could really do what we wanted (in 1989) and moreover the speed constraint was so tight that we had to develop customized software. The software is writen in C and the fast graphics routines were written in Assembler. System dynamics including approximation to non-linear differential equations are computed in real-time. Most research grade Virtual Reality systems available now range from $45,275 up to $250,000+ [7][41] [32][12].

- Design of a platform for testing artificial arm parameters such as: geometry, size, weight, size of components, motors, motor minimum torque, arm dynamics etc...
- Offer the possibility of varying at will the environmental parameters such as: presence or absence of gravity (aerospace applications), different density of medium (under water operation such as sea bottom exploration).
- Formulation of recommendations for the design of future externally powered microprocessor-controlled artificial arms.

This research was done in conjunction with the Department of Rehabilitation Engineering at the Rehabilitation Center in Ottawa, which has been monitoring the expertise developed through this work.

Chapter 2

Background: Review of the Various Strategies used for the Control of Arm Prostheses

The control of multiple degrees of freedom artificial limbs has been the concern of researchers in the fields of prosthetics and cybernetics, for the past few decades. One of the main problems is to find a suitable way of communicating the intent of the user to the artificial arm. Various options have been investigated; the most popular and elegant ones have made use of activities of physiological sites located somewhere in the upper-trunk to control the prosthetic devices. These activities were either electrical (such as myoelectric activity) or mechanical (the mechanical displacement of a joint). The difference between these two physiological activities has brought about two completely separate schools of thought as far as control strategies were concerned. These different sets of ideas will be reviewed below.

2.1 Electromyographic Control

When using the electrical signals of the body to control the prosthesis, muscle activity (also called electromyographic [EMG] activity) or nerve activity (also known as neuroelectric [NE] activity) is used. EMG control is much more popular than ENG control. These approaches

were regarded as being highly desirable because the prosthetic device would receive commands directly from the central nervous system. EMG control started to receive great attention when myoelectric control of a powered hand was introduced in 1948 [10]. Since then, a tremendous amount of effort has been dedicated to the realization of a truly practical artificial arm. A typical myoelectric control system is represented in figure 2.1 (taken from [17]).

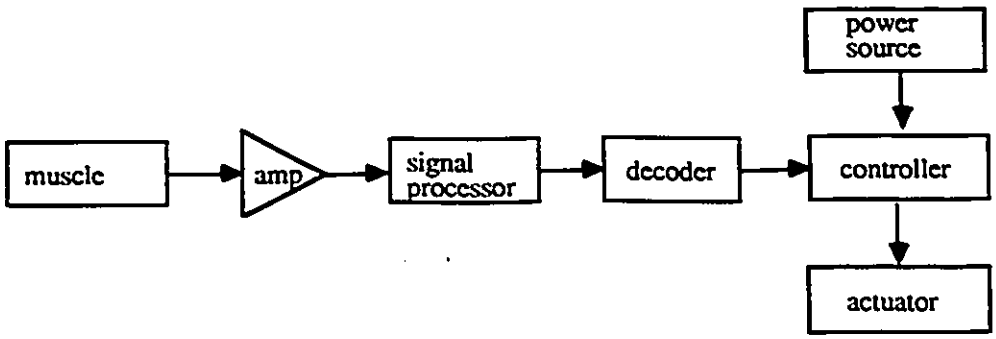

Figure 2.1: Schematic diagram of an EMG control system.

The EMG activity is picked up by electrodes, amplified, and processed through some sort of signal processor. A decoder interprets the signal received from the processor and sends the appropriate command to the controller that activates the actuators of the prosthesis.

Work on EMG controlled arm prostheses started initially with an inefficient use of the EMG signal with the so called one-muscle-for-one-motion approach; which means essentially that each degree of freedom was controlled by a distinct muscle [55]. For instance, the biceps and triceps muscles could be used to control elbow flexion/extension. Each muscle group had two states "on" or "off" which were characterized by the presence or the absence of electromyographic activity. Considering that an efficient multifunctional arm prosthesis should have between 3 to 5 degrees of freedom (depending on the level of amputation of the user) the number of muscle sites required would be excessive and the coordinated control of such a prosthesis would be difficult if not impossible for the amputee. Thus, researchers have moved

away from this approach and have tried to optimize the information utilization of the EMG signal. One particular approach is the one muscle 3-state system [42] where the muscle has two distinct levels of contraction and a no-contraction state. Research was mostly done in this direction by Scott, et al. at the University of New Brunswick. A variation of this system was the one muscle multi-state system used in multifunction prostheses. The advantage of this last approach was that one muscle group can control many different motions using different levels of EMG activity. However it must be mentioned that three (or more) state control is justifiable only when just one muscle site is available since this strategy will add to the problems of producing coordinated control. Some work parallel to the New Brunswick efforts was also done by Childress [8], Childress et al. [9] and by others.

A more recent EMG control philosophy is based on the assumption that a distinct control signal for the execution of each and every movement still exists on the surrounding musculature after amputation of a limb. Researchers have tried to extract this information from one or more muscle sites and thus use synergistic groups of muscles to control the operation of the prosthesis. In this case, the different control signals do not come from different electrode locations but from different patterns of EMG signals produced by the same electrodes attached to a number of locations. Work was done in this direction by Lyman, et al. [28], Graupe, et al. [21], Wirta, et al. [55] and others. The approach by both Lyman and Wirta used many electrode locations (10 or more) making sure that at each of these locations the EMG signal is strongly correlated with the single prosthesis function (in other words, the presence of a strong EMG signal at the chosen locations means that this particular motion is what the amputee wants to be executed). This method employs the low frequency characteristics of the myoelectric signals and of their distribution over the various electrode locations. The approach by Graupe et al. was slightly different, by making use of the complete spectrum of the EMG signal, identification and discrimination between different desired motions was made possible using only a few electrode locations (one to three). Graupe did not try to separate and identify each reference signal at each electrode location, instead he looked at the signal as a whole and extracted the wanted information from the "cross-talk" EMG signal emanating from separate electrode sites. This

approach required finer detection methods but it was accomplished using an Auto-regressive Moving Average (ARMA) identification algorithm which they claimed gave an 85% success rate under laboratory conditions. It is worth while mentioning that the 85% success rate that they claim is based on whether or not the required motion was executed, but not on the precision of the executed motion. This means that 15% of the time, the prosthesis is not performing the required motion. In fact, it could be doing something totally different. This could, in certain cases, be dangerous and this makes such a prosthesis inadequate for clinical or commercial use. Other EMG pattern recognition work reported more recently is that of Lee and Saridis [27].

As can be seen from the previous paragraphs there has been a lot of hope and work put into studying EMG signals to obtain control inputs for multifunctional prostheses. EMG control is indeed elegant as it lends itself to spectral and statistical analysis which allows mathematical models of EMG signal activity to be made (see Saridis [27]). With these models in hand, the relationship between a prosthesis command signal and its corresponding EMG pattern parameters can readily be analyzed under various conditions such as: electrode positions, speed of motion, and loading effects. However, there exist major drawbacks when using this type of control. It is known from elementary control theory that a position controller requires two distinct directions of information flow: one in the forward path and the other one in the feedback path, such that at any instant in time, the controller knows the state of the controlled process. In EMG control, only the forward path is present. A patient using such a controlled prosthesis, has no proprioceptive means of knowing where the terminal device is in space. Visual feedback has to be used all of the time if the control loop is to be closed, as shown in figure 2.2.

The problem of using visual feedback to operate a prosthesis is better explained or understood if we ask ourselves how efficient a baseball player would be if he had to keep looking at his bat to know where it was in space? Or how well a tennis player would perform if his eyes had to stay on his racquet while playing? These examples are not mere exaggerations but real illustrations of the weakness of EMG control and the importance of appropriate feedback in a

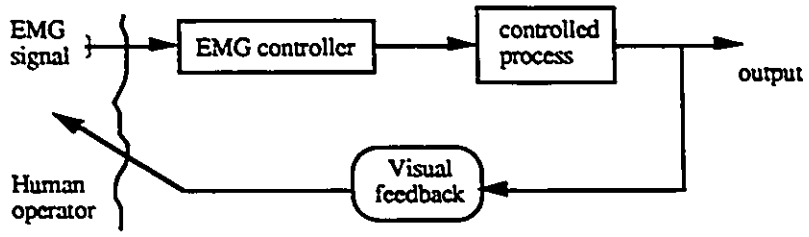

Figure 2.2: Closed-loop system using visual feedback.

man-machine process or in any other controlled process. But what makes these players so good at using the bat and the tennis racquet which are extensions of the body? How can they control the position, velocity and acceleration of these tools at will? The answer to these questions is complex but, nonetheless a basic explanation can be suggested. Let us assume that the intact joint (the hand of the player) is the input and that the tool (bat or racquet) is the output. Then the proprioceptive properties of the intact joint (i.e. the hand) can be exploited such that it can be used as a bidirectional channel passing command information from the biological side to the tool and returning back to the central nervous system information about motion, velocity and position of the tool. It must also be emphasized that for a person to subconsciously learn to use a tool, it must be of fixed length. These observations and, most of all, the ones demonstrating how well amputees handled their body powered cable-operated arm protheses are undoubtedly the foundations of the control strategy known as Extended Physiological Proprioception.

Simpson [44] was the first to propose the principle of Extended Physiological Proprioception (e.p.p) as a controlling method to achieve coordinated motions in a multifunctional (or multijointed) artificial arm. This principle involves using the position of an intact joint of the body as an input to the prosthetic system. The artificial arm is used as a mechanical extension of the body (just like the tennis racquet). In introducing the principle of e.p.p., Simpson specified two necessary conditions:

1. There should always be a one-to-one relationship between the input (the hand for in-

stance) and the output (the racquet). This will ensure that the operator never has to look to know exactly where the tool is in space. Since this one-to-one relationship has to be preserved at all times, Simpson added that:

2. The input should not be allowed to move faster or further than the output can follow. He called this "the unbeatable servo".

2.2 Extended Physiological Proprioception

The terminology "extended physiological proprioception" is mostly used in the field of prosthetics. The word proprioception relates to stimuli produced and perceived within an organism [50]. The system and control counterpart of proprioception would be the feedback. Physiology is the science of functions and phenomena of living organisms [50]. Thus extended physiological proprioception expresses the fact that the body's natural feedback perception is extended outside the limits of the body, and this is what we will be making use of. To better picture what we just explained we quote Polanyi [48]:

> "... The way we use a hammer or a blind man uses his stick, shows in fact that in both cases we shift outwards the point at which we make contact with the things that we observe as objects outside ourselves. While we rely on a tool or a probe, these are not handled as external objects. We may test the tool for its effectiveness or the probe for its suitability, e.g. in discovering the hidden details of a cavity, but the tool and the probe can never lie in the field of these operations; they remain necessarily on our side of it, forming part of ourselves, the operating person. We pour ourselves into them and assimilate them as part of our own existence."

Simpson is the first researcher to design and build a complete externally powered upper arm, forearm and hand system making use of the principle of e.p.p. [44] [45]. This device was successfully used to replace the complete physiological arm distally from the shoulder joint. The arm had four degrees of freedom plus hand prehension. These were respectively:

1) Shoulder protraction/retraction

2) Shoulder adduction/abduction

3) Elbow flexion/extension

4) Wrist rotation.

Simpson's artificial arm was gas powered using pneumatic actuators. Clavicular motion was used as the controlling input of the system. There was always a one-to-one relationship between the position of the clavicles and the position in space of the prosthesis, enabling the amputee to know where the terminal device was in space without looking at it. Simpson's device was designed according to the following constraints [47] considered to be the minimum requirements for an artificial arm.

- The physical dimension of the arm should not exceed those of the normal arm, including weight;
- The joints should be as far as possible in the correct anatomical position;
- The sphere of movement should be similar to that of the normal arm;
- The arm should be capable of unconscious control by the user;
- The energy demands of the arm should be low enough to allow them to be satisfied simply.

Simpson's arm prosthesis proved to be very effective and useful. It probably is the only one that fulfills the above requirements. However it had some limitations which were essentially:

1. The input/output relationships were mechanically fixed, making them difficult to change.
2. Coordinated motions were sometimes complex to execute.

As mentioned in the above paragraph, Simpson's design made a major contribution in the field of externally powered artificial limbs with built-in feedback. This showed empirically that e.p.p. was a really promising control modality. Some research done by Doubler and Childress [16] has supported the practicality and the potential effectiveness of applying the concept of e.p.p. to the control of artificial upper limbs. In their experiments, they made use

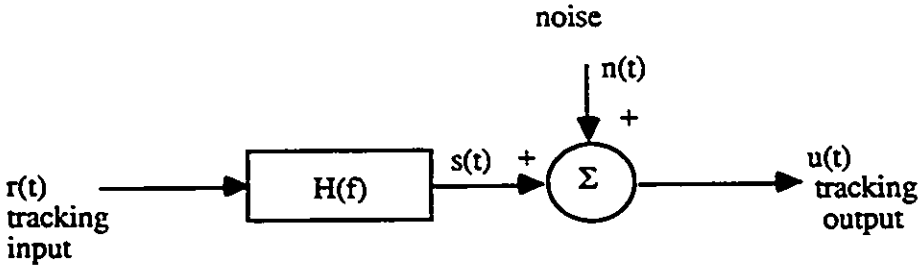

Figure 2.3: Quasi-linear representation of tracking system.

of the two orthogonal degrees of freedom of the shoulder joint (shoulder protraction/retraction and adduction/abduction) to control two prosthetic joints (i.e. wrist rotation and elbow flexion/extension). In order to be able to quantify the performance of e.p.p. as a control modality for a prosthesis, a tracking task performed on a computer screen was chosen. In order to have a control for the results obtained, the exact same tests were done using the physiological elbow and wrist. It is interesting to note that, in the experiment of Doubler and Childress [16], the target tracking was performed at 8 different tracking frequencies and in 1 and 2 dimensions. Data was gathered using the assistance of 5 subjects. Theoretically, Doubler and Childress modeled the tracking system as a quasi-linear model as given in figure 2.3 (taken from [16]). Their justification for using such a model was that: "For some time it has being known that when the input appears random, the input-output relationship for a pursuit manual control system can be represented by a linear element - whose characteristics remain constant as long as the input characteristics and task variables remain constant - in series with a source of random noise..." [16]. They then took advantage of been able to use linear control theory techniques to analyze and explain system operation. Channel capacity was calculated using Shannon's equation [43] assuming a continuous channel of bandwidth W in the presence of white Gaussian noise of power N and transmitted signal power S as given by equation (2.1).

$$C = W log_2(1 + S/N) \tag{2.1}$$

In the case of a non-constant signal-to-noise ratio over the channel bandwidth, equation (2.1) can be rendered more general by integrating over small portions of W where the S/N can be considered constant. Thus we get:

$$\dot{T} = \int_W \log_2 \left[1 + \frac{S(f)}{N(f)}\right] \tag{2.2}$$

The maximum information transmission rate can be experimentally calculated using the following equation:

$$\dot{T} = \frac{1}{NT} \sum_{k=0}^{k} \log_2 \left[\frac{\Phi_{uu}(f_k)}{\Phi_{uu}(f_k) - [H(f_k)]^2 \Phi_{rr}(f_k)}\right] \tag{2.3}$$

$$H(f_k) = \frac{\Phi_{ru}(f_k)}{\Phi_{rr}(f_k)} \tag{2.4}$$

Where:

$H(f_k)$ is the discrete transfer function,

Φ_{rr} is the input signal power spectra,

Φ_{uu} is the output signal power spectra,

Φ_{ru} is the cross-power spectrum relating the system input and output.

T is the sampling interval

N is the number of data samples in a segment (segments were used to separate data in order to find power and cross-power spectra).

Using equation (2.3) Doubler and Childress were able to determine the information transmission rates (in bits/sec) as a function of the input signal cut-off frequency as shown on figure 2.4 (taken from [43]). From these figures, one can see that there is a great similarity between "natural control" and e.p.p. in conveying information from operator to artificial arm. However, there are still some fundamental questions unanswered and unquantified. The possibility of tracking is one aspect required from an artificial arm and relies heavily on visual feedback. However positioning is another important aspect and this, whether the arm is used for rehabilitation of

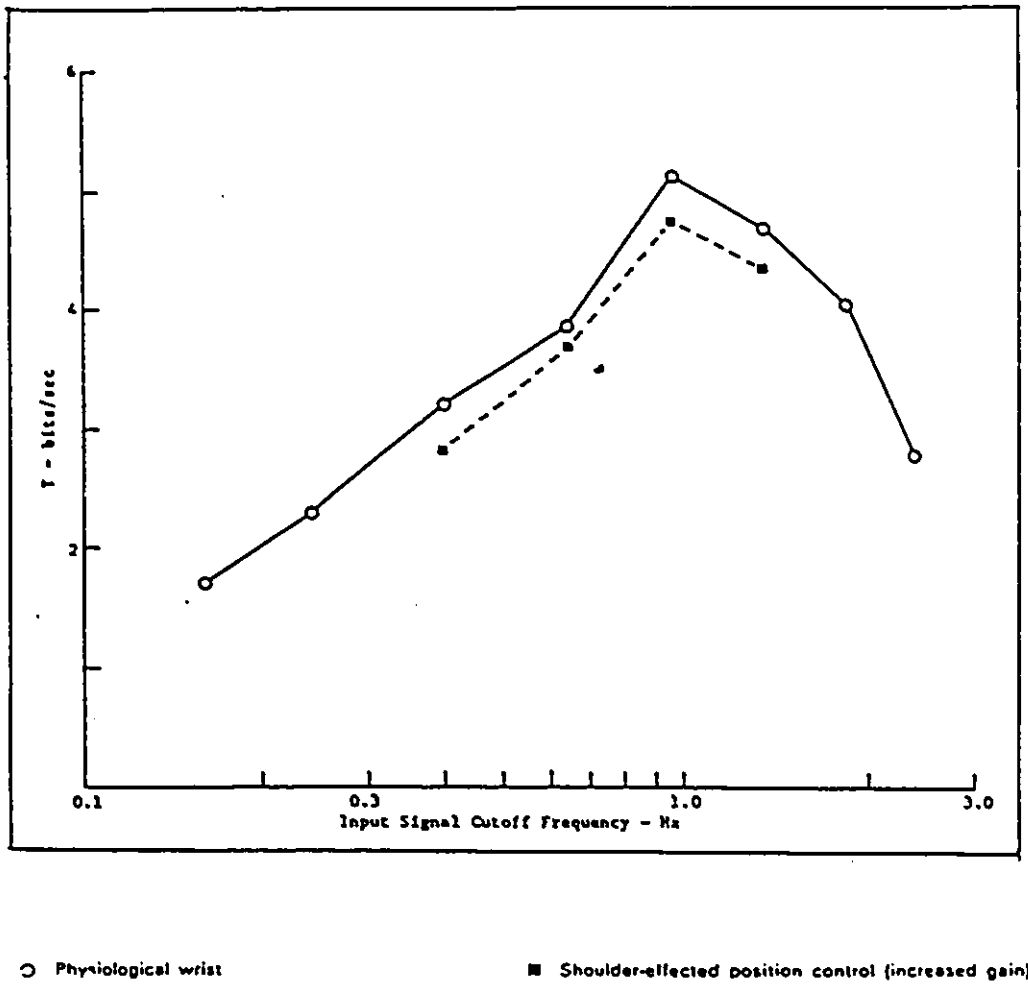

Figure 2.4: Comparison of the information transmission rates for one-dimensional tracking tasks performed by the same subject with the physiological wrist and shoulder-effected position control.

an amputee or tele-operation in space. One must consider that sometimes positioning has to be performed in the absence of visual feedback. Examples of this are: an amputee reaching for a tool while visually observing something else, or an astronaut positioning a satellite with two grippers one in front and one at the back of the satellite. Position proprioception is essential in these situations [1]. Moreover these situations require the capacity of transmitting information in two directions: man-machine and machine-man. Simpson has shown empirically that this can be done with an artificial arm having a single linkage.

[1]It is also interesting to note that even when visual feedback is available, proprioception is important to reduce the mental effort needed to control a prosthesis

Chapter 3

3-Dimensional Graphics and Virtual Reality

This chapter provides background information on one aspect of this research work which involves: three dimensional (3-D) interactive computer graphics, and Virtual Reality. It is not, however, meant to be an exhaustive treatment of this subject. Essentially, general ideas on what is routinely used in the field are presented to help understand problems and trade-offs such as: image quality versus screen refresh rate, hardware image generation accelerators, and basic cues for 3-D perception which will be encountered later in this work. In the first section, the basics of 3-D computer graphics are discussed and in the second section Virtual Reality is presented. Many different uses are reviewed, especially those pertinent to robotics and cybernetics.

3.1 3-D Computer Graphics

3.1.1 Background

Computer graphics began in the early 1960s at MIT with the work of Ivan Sutherland [51][52]. As a consequence of this work, he is generally accepted as being the father of computer graphics [11][7][33]. During his doctoral program, he wrote a series of interactive

graphics programs on a transistor experiment 2 (TX-2[1]) computer equipped with a vector-drawing CRT display. Since no graphics accelerator was available, the main processor had to do all the graphics calculations. The TX-2 could handle interactive 2-D graphics but not 3-D. In his dissertation, called "Sketch pad," Sutherland developed some of the concepts used in the field: object-oriented programming, constraint-based visual computing and real-time interactive programming. Sutherland and Danny Cohen, who developed the first 3-D flight simulator [11], conceived the first head-mounted display, in which miniature cathode-ray tubes acted as displays and mechanical linkages relayed head position and orientation to the computer so as to alter perspective view. Cohen wrote the software for this project which allowed a person to walk in a small simulated world. This "cyber" world featured objects as wire frame images. A little latter, in the 1970s, Myron Krueger [23][24][25] also worked in the field of synthetic worlds. He did not, like Sutherland, used a head-mounted display, his virtual environment was projected onto a wall-sized screen.

3.1.2 Evolution in 3-D Computer Graphics

Following the pioneering work of Sutherland, Cohen and others, there was a slow progress in 3-D techniques and technologies of computer graphics [29] mainly due to the lack of low cost high-processing power/high-speed hardware. However, the past 10 years have brought about a drastic change of that situation. Specialized high-performance graphics systems have been constructed [11], they are relatively expensive because the market is small, but demand is growing and the advent of digital television will considerably help in improving the situation. However, real-time interactive manipulation of true 3-D computer generated images has been a reality for the past few years.

3-D computer graphics evolved in two separate main streams: photo-realistic graphics and real-time graphics. The former focuses on creating a computer-generated image that approaches as closely as possible reality. Images are elaborately shaded to simulate the play of light and

[1]The first transistorized computer

shadow on the object. Also, object texture is rendered. It must be understood that in this case, image generation is extremely slow (minutes to hours) depending on the quality required and computing power. Originally, in photo-realistic computer-graphics, shading of objects was obtained by cleverly filling flat planes with polygons. Objects were broken down in a collection of flat surfaces such that hidden surface determination could be done in a reasonable amount of time. The quality of the image obtained using this technique was better than the wire frame line drawing but was a long way from camera quality pictures. Later in the 1970s Gouraud, Bui Tong Phong and Ed Catmull started the movement toward photo-realistic computer-generated images. Catmull walked away from polygonal approximation to more sophisticated algorithms to model smooth objects. It has been reported that the images produced by Catmull were among the best at that time. Other techniques and refinements called ray tracing and fractal methods followed and gave a real maturity to this stream of 3-D graphics.

The second main stream of 3-D computer graphics is mostly concerned with interactive speeds and good (but not perfect) image quality. Refresh rates must be at least 10 frames per second, preferably more, to avoid flicker. This kind of computer graphics allows real-time interaction with images opening the way for Virtual Reality, visual simulators for driving and flight training. Because of the processing power required, interactive 3-D graphics usually calls for dedicated hardware. According to Jim Clark[2] [11] all commercially available systems are based on the data flow architecture suggested by Henry Fuchs as shown in figure 3.1. This works as a traditional assembly line using the pipeline principle, each geometry engine does a bit of work and passes the data to the next stage. The geometry engines receive the data and manipulate raw surface geometry by performing rotations, translations, shading, subdivisions and pixel sampling. From the side of the data flow direction, via the pixel bus, pixels enter the image engine. This part does what is called the pixel processing (image accumulation, texture mapping etc.). Image engines are usually meshed in a group of 16 or more to form a block. Blocks of 16 are paralleled to increase system throughput. Based on Fuchs architecture newer

[2]Jim Clark is the founder and chairman of Silicon Graphics Computers, a leading manufacturer of 3-D computing systems.

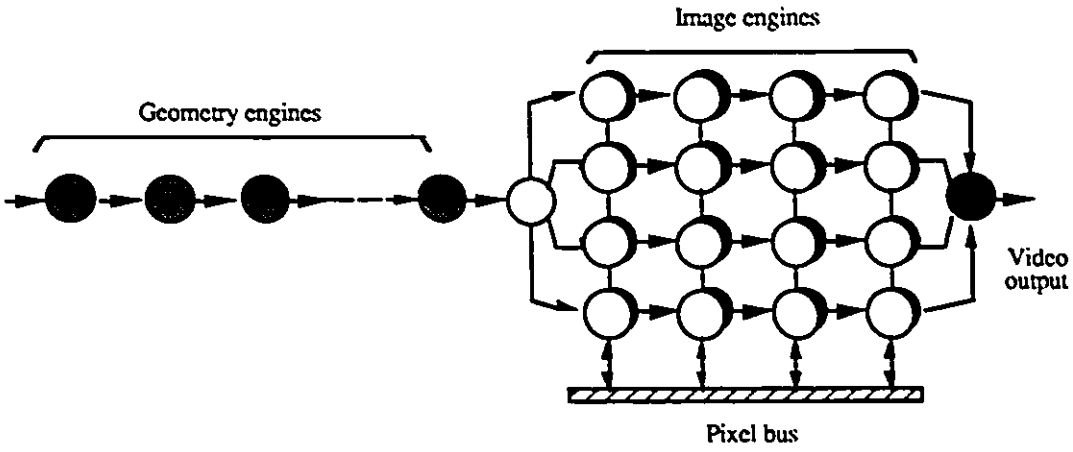

Figure 3.1: A real-time graphics architecture for interactive 3-D image generation (classic design).

systems were proposed by Jim Clark and others to allow real-time photo-realistic rendering.

As can be seen, what were originally two main streams: photo-realistic computer graphics and real-time computer graphics are now merging into one, thanks to progress in hardware architectures and submicron semi-conductor technologies allowing the clock rates to reach hundreds of mega-Hertz.

Having seen the technologies behind 3-D computer graphics, let us now see how this can be used to generate a fictitious environment called Virtual Reality.

3.2 Virtual Reality

The best description that could be given of Virtual Reality is that of William R. Nugent [33]: "Virtual Reality provides a simulated three-dimensional environment in which human participants appropriately interfaced, appear to be enveloped. They may move about and may

manipulate simulated physical elements in the environment and, in some versions, may engage and interact with representations of each other. An architect, for example, may invite a client to don video goggles and take a tour of a building which has been designed but not built". Watkinson [53] sees Virtual Reality as a sum of three illusions:

- The first illusion is depth (depth perception and cues will be discussed specifically in the next section). This is accomplished by inviting the user to don special goggles containing two small eye piece-size monitors mounted into a scuba mask/helmet to limit the peripheral vision. These monitors are now usually of the liquid-crystal display type; they provide perspectively different images to give the illusion of depth and hence three dimensions. This is also referred to as stereoscopic vision.

- The second illusion is that of place. The image displayed on the stereoscopic monitors provides the user with the entire scenery that he will encounter during his[3] Virtual Reality experience. The motion of the user is tracked from the floor or the ceiling with ultrasonic transducers or from a chair mounted with transducers. In this latter case the user would always be sitting in the chair. Also, attached to the headset, are other transducers (ultrasonic or mechanical) providing the computer with information about the user's head motion and orientation. All this is necessary so that if the user looks left or right, up or down the information is relayed in real-time to the computer which adjusts the image on the display, by changing the view point, to match the movement. The net effect seen through the miniature monitors is a replica of what would be seen in reality when the head is moved about, the major difference being that the entire field of view is computer generated. This is a major difference between the images in Virtual Reality and the ones in television or multimedia. In the former the view point is dynamic and user-tracked wereas in the latter it is static.

- The third illusion is that of interacting with the simulated environment. In order to participate in the Virtual Reality i.e. see his hand move and be able to manipulate

[3]The common usage of he and his has been adopted in the interests of a readable style, with no intend to insult females.

virtual objects, the user puts on a "datasuit" or a "data glove" as shown in figure 3.2. Unlike other input devices such as a mouse, the user body or hand is inside this interface, which is equipped with fiber optic sensors sending data to the computer about body motion (datasuit) or hand motion(data glove). When either of these input devices is used in conjunction with the headset, the user will see part of his body or his arm whenever they enter his field of vision. The exact motion that he does in real life will also be done in the Virtual Reality.

Besides these basic constituents of Virtual Reality, other features can be incorporated to simulate more closely reality.

- Audio feedback helps in localizing where objects are in space. When a person walks near by, without looking, we immediately get a lot of information about his displacement. The point of origin of the sound gives valuable cues on where the person is in the scene. We can also tell the direction in which he is heading, whether it is a fast pace or a moderate one or even the sex of the individual from the sound of the shoes on the floor. That pre-conditions us for the following moment when we will turn or raise our head to look at him. A comprehensive review of various work done in this field has been reported by Wenzel in [54] and her work on localization in virtual acoustic displays is also exposed.

- Tactile feedback could also be an important feature. It gives an assurance that an object has been found.

- Finally, force feedback is useful in informing on how much pressure is applied on a virtual object like an egg for instance. Some interesting work was done in this direction by Burdea [4][5][6].

All of these sources of information are important, however up to now very little effort has been invested in making them a normal constituent of Virtual Reality.

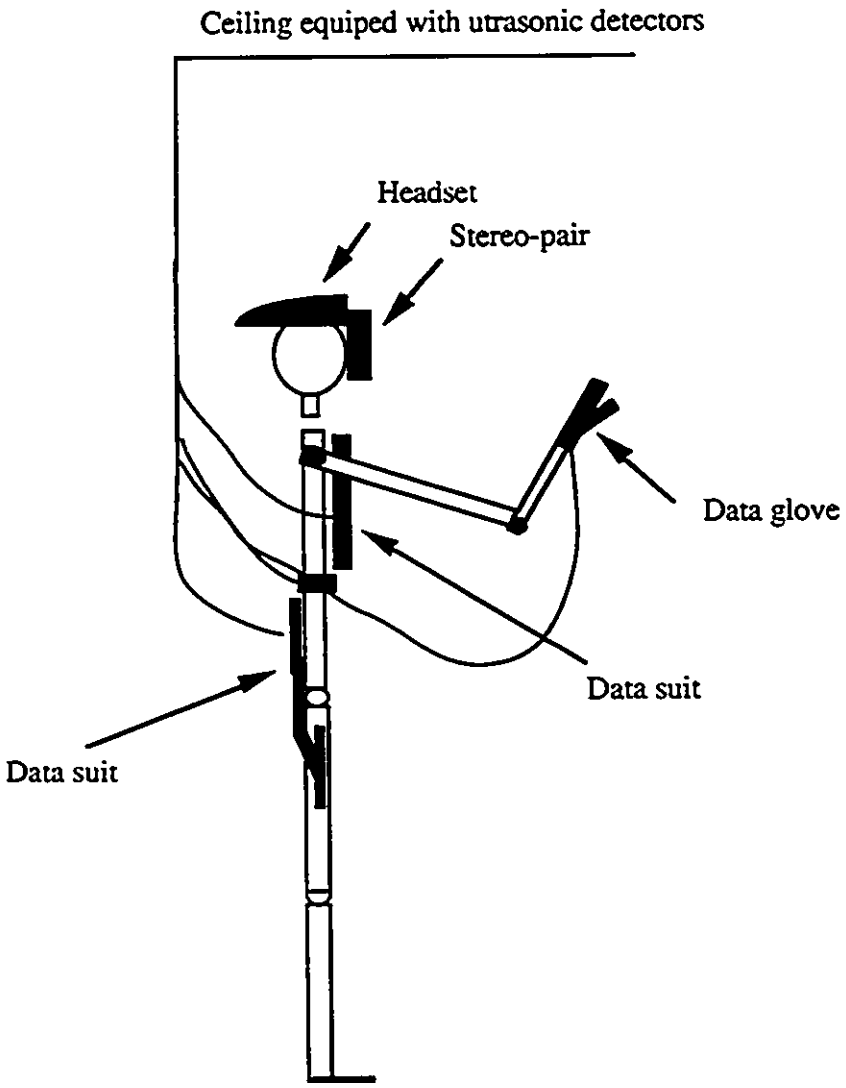

Figure 3.2: Schematic diagram representing an individual wearing a Datasuit, a Data glove and a headset.

3.2.1 Depth cues

As explained later in chapter 4, depth perception is a must when interacting with objects in a virtual world. When performing a reach motion toward one of these objects, one must be aware of whether we are in front or behind them, or if two entities lying side by side are really at the same distance from us. The human visual system uses several depth cues to distinguish the relative positions of objects in a 3-D scene. A formal classification of various kinds of depth cues was done by David McAllister [29]. He basically classified them into two categories: physiological depth cues and psychological ones. There are four important physiological cues:

Accommodation is the change in focal length of the iris at it focuses on different regions of a 3-D scene.

Convergence is the inward rotation of the eye to focus on an object moving closer to the observer.

Binocular disparity is the difference in the images that are projected on the left and the right eyes when viewing a 3-D scene. The visual system uses this important depth cue to produce the sensation of stereopsis, or depth.

Motion parallax provides differences in views of a scene by moving the scene or the observer. You can determine the depth of two points by observing how much they move relative to each other. As you move your head from left to right or up and down, the points closer to you appear to move more than the points farther away. This is also called the *look-around* capability. Moving your head produces different views of the scene.

There are many psychological depth cues, we will only list here those that we feel are more important and that were useful for the conception of our Virtual Reality.

Linear perspective also known as perspective projection, is a basic property of optics that dictates that the size of an image projected on a display screen or on the retina changes in inverse proportion to the changes in distance between the object and the display screen.

Shading and shadowing are lighting properties in a scene that help in determining the shape and depth relationships of objects by their positions with respect to light sources.

Aerial perspective is the property that causes object that are farther away to appear less distinct, and cloudy.

Interposition (or occlusion) occurs when an object hides or overlaps another. An object hiding or overlapping another object is assumed to be closer. Retinal image size and the knowledge of the world and the size of objects also help in determining the depth of objects. If we perceive the height of an elephant to be the same as that of a mouse, we can assume that the mouse is closer than the elephant.

Texture gradient and colour. The depth can usually be estimated by the amount of detail visible and the brightness of the colors of an object. The more distant the object the darker and more blurred it will be.

Depth cues are usually additive, that is, the more there are the easier it will be to perceive the relative depth between different objects in the scene. Some are obviously more important than others, and some are computationally more costly than others. In designing the Virtual Reality used specifically for the present research work emphasis was placed on using as many of the above cues as possible while retaining low hardware and computation costs. Low hardware costs were important because project requirements requested an inexpensive system. Concerning CPU time, we already mentioned above that features such as shading, shadowing and texture rendering require considerable processing which is not at this time compatible with interactive image generation, at least not without dedicated hardware. Hence while most of the physiological depth cues were used, only psychological cues that complied with the above mentioned constraint were incorporated. The primary techniques that were used were: linear perspective, aerial perspective and interposition. Stereoscopic vision was not used.

3.2.2 Different types of 3-D displays

There are essentially three broad categories of 3-D displays: *holographic, multiplanar and stereo pairs.* The first two are not really widespread and are not used in Virtual Reality systems; thus they will not be discussed. Stereo pairs, on the contrary, are an integral part of most major Virtual Reality systems. In stereo-pair displays, 2-D left and right images are generated and directed to the appropriate eye. Binocular disparity, defined above, will induce the sensation of depth. The displays based on stereo-pairs have a few disadvantages: they require the use of special viewing devices, and some do not have the look-around property (defined above when discussing motion parallax). Also because eye focus is at the plane of the stereo pair, or the viewing screen, accommodation is fixed. This disconnection of accommodation and convergence causes difficulties to some observers to fuse the two 2-D images into a single 3-D image. This is refered to as stereo blindness, a problem which is fairly common [29]. On the other hand, stereo-pair technologies are fairly accessible with prices of about $2000 and since the most popular ones are now making use of liquid crystal display medium-resolution monitors, full advantage of computer graphics techniques can be taken. The most well known of these devices is the EyePhone developed by VLP Research, Redwood City, CA which is a colour stereo display system mounted on the user's head covering both eyes as shown on figure 3.2. A stereo image is displayed by two wide-angle LCD screens. With this system images can be seen from any angle without ghosting. This is a big innovation since the old anaglyph systems that were plagued with ghost images and gave viewers headaches.

When conceiving our Virtual Reality, we decided not to use the technique of stereo-pair display because at that time (1990-1991) the quality of these displays was not adequate for our needs and they were expensive. We decided to use a monoscopic display that gave the effect of looking through a window to the Virtual Reality rather than giving the sensation of total immersion. Furthermore, virtual environments can be experienced from two kinds of viewpoints, egocentric and exocentric. The difference between these viewpoints is best explained by S. R. Ellis in [18], the egocentric viewpoints strategy is one in which the sensory environment

is constructed from the viewpoint actually assumed by the user; in the exocentric viewpoints strategy, the environment is viewed from a position other than that where the user is represented to be. In this case, the user can literally see a representation of himself. Our Virtual Reality is based on the egocentric viewpoints strategy.

Having discussed the origins of Virtual Reality and the tools needed to create and operate it we can now discuss the value of such a tool in robotics and prosthetics research.

3.2.3 Virtual Reality: a valuable research tool

We have discussed at length in the previous chapter the advantages of using a computer simulation over the bench model of an artificial arm. Classical computer simulations are usually programs that contain mathematical models of a phenomenon. The values of precise parameters can be entered and altered at will such as to see how these changes will affect the behavior of the phenomenon. The simulation can then be run, normally producing an output of the form of numerical data, charts or curves. Researchers connected with the research can then interpret the results. With Virtual Reality, we discovered that we could go one step beyond this. Results are not only immediately available but they are offered in a natural way in a form immediately understandable by not only the researcher but also the test subjects. There is no postprocessing required. If the subject is, for example, instructed to move his artificial arm toward the target, he would do it as he would with a natural joint. The results are available to him in real-time. He can, therefore, determine how well he is performing and can make the necessary on-the-fly corrections to get to the target accurately. The subject can simultaneously express his impressions on such items as: the arm geometry, dynamics, and positioning accuracy. Also, useful parameters are, upon request, periodically captured by a system parallel to the one generating the Virtual Reality. All this information naturally leads to a number of conclusions pertinent to the future design and implementation of artificial arms.

Chapter 4

The Computer Simulation of the Artificial Arm and the Three-Dimensional Scene

This chapter discusses one of the important parts of this research work. The guidelines of this work were precisely set specifiying that: an innovative, inexpensive and flexible testing environment be developed to help in assessing the potential use of the principle of extended physiological proprioception in multi-linkage microcomputer based upper limb prostheses. The system was to be developed on a personal computer type workstation with enough flexibility to simulate current and future commercial artificial arms and fast enough to generate interactive three-dimensional (3-D) images. Thus in the light of these contraints, a great deal of effort had to be invested in order to conceive an adequate system with this cost/performance trade-off.

This chapter presents the model used in this research work. It is divided into three main sections. The first section discusses the computer generated image of the artificial arm and the background scene. The preprogrammed coordinated motions called "linkages" are also presented. The second section of this chapter presents the data acquisition and software program used to generate the Virtual Reality. Finally, the basic mathematical model for the arm is described together with the governing differential equations. An analysis of the arm

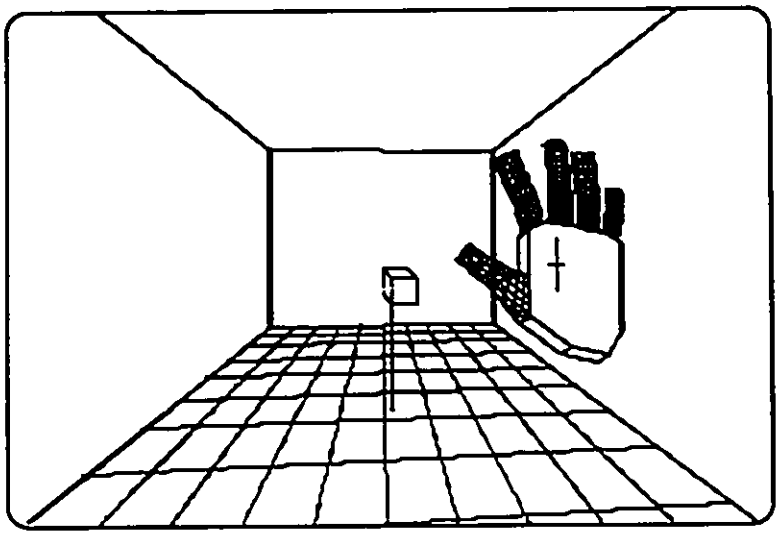

Figure 4.1: Three dimensional Virtual Reality representation of the artificial arm.

dynamics is performed to extract the necessary information that will lead to adequate real-time numerical simulation.

4.1 3-D Simulation of the Artificial Arm

4.1.1 Graphics and Animation

One of the important parts of this study was to implement a 3-D life like image of the artificial arm and display it on the computer monitor exactly as a subject would see his own arm in his natural field of vision when looking at the target and aiming for it. This means that the image on the screen would be a representation of the direct and peripheral vision of the subject as he moves his terminal device toward the target. Figure 4.1 shows what was required and realized.

For the simulation to give a realistic effect, real-time motion of the arm had to be ensured and proper visual perspective had to be incorporated. The above requirements were hard to

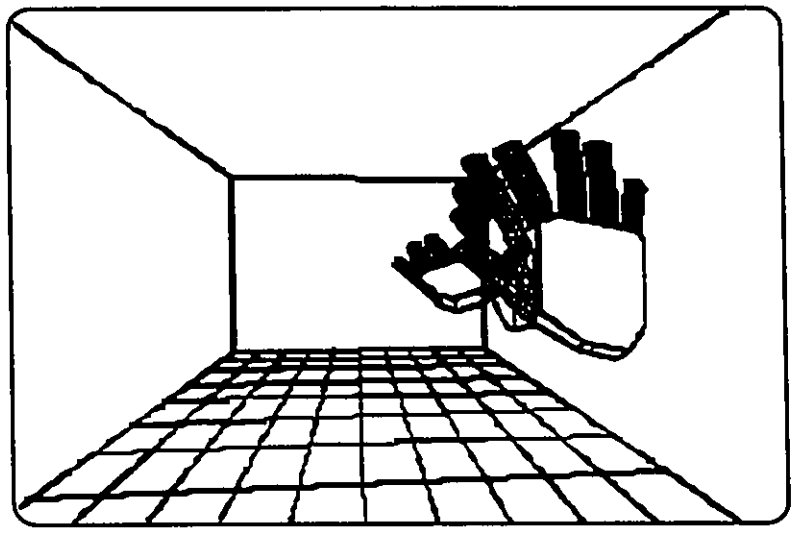

Figure 4.2: The positions of the 3-D hand as a function of input and chosen linkage.

meet, at the time this work was undertaken, using general purpose computer graphics packages. Actually, real-time PC based 3-D animation software were not very common then. For this reason, and others, we decided to develop our own Virtual Reality software. Because of the cost/speed contraints it was not possible to generate interactive photo-realistic computer graphics. Rather, some compromises were used. Based on the fact that our artificial arm uses preprogrammed motions, also called "linkages", the terminal device path, position, and orientation are known at all times. Because of the deterministic nature of the motion of the virtual arm, we can generate off-line all the necessary frames of the terminal device for all the shoulder positions and for all linkages see (figure 4.2). We used a 3-D graphics package called "Design CAD 3D" [14] that produces wireframe shaded-pictures with hidden surfaces removed, to generate the frames of figure 4.2. These frames were stored in memory and could be retreived at high speed. The number of displayable frames per second now is no longer proportional to the complexity of the image or, more precisely, to the number of polygons composing it (as is usually the case) but to the transit time from memory (RAM) to video buffer. The animation

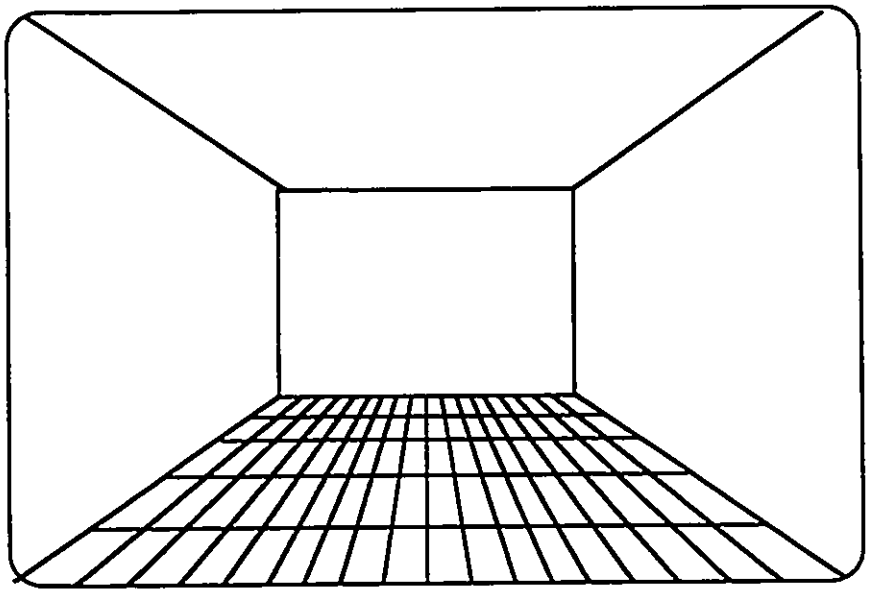

Figure 4.3: The background scene.

effect resulting from this is excellent with, rendering speeds of 40-50 frames per second. For the virtual scenery to be complete, we had to incorporate the depth dimension. A background was generated, composed of a back wall and a chessboard floor with perspective lines originating behind the patient, extending into the Virtual Reality and converging toward an imaginary point at infinity [31] as shown in figure 4.3. Into the above scene, various targets could be displayed depending on the task to be performed. If the subject is required to mimic a motion, a target as shown on figure 4.4 would be displayed. If, on the other hand, the subject is to reach a target, we would then have a more conventional situation as depicted in figure 4.5. In this latter case, we note that the target is anchored to the floor so as to provide the subject with spatial (depth) positioning cues.

Depth cues were discussed earlier in chapter 3. We saw how they provide useful information to work in 3-D space. One of the principal sources of depth perception is steroscopic vision. We could not incorporate binocular vision to our system for various reasons as discussed

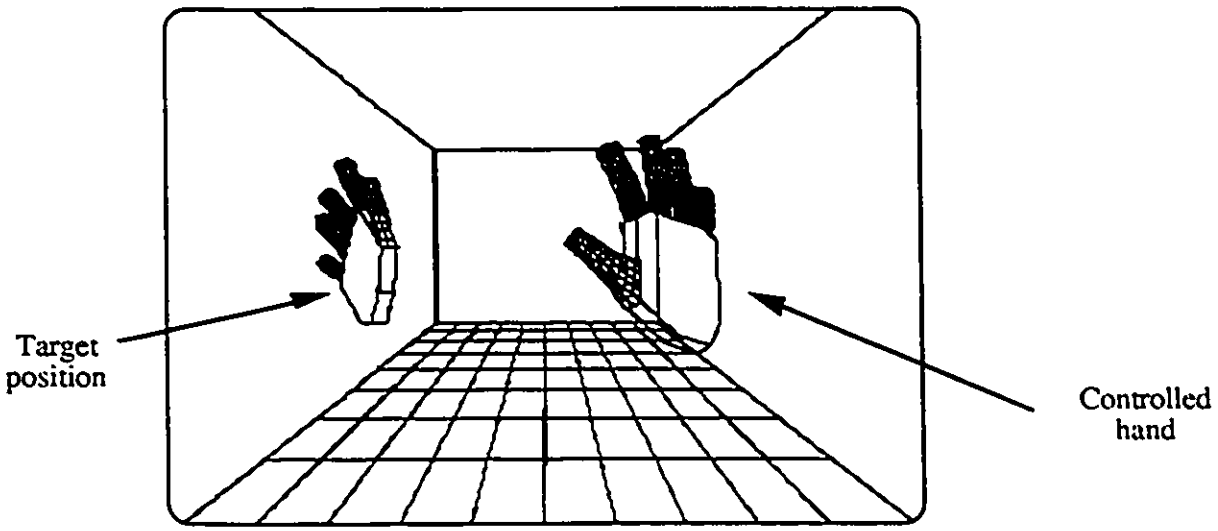

Figure 4.4: A motion-mimic type of target.

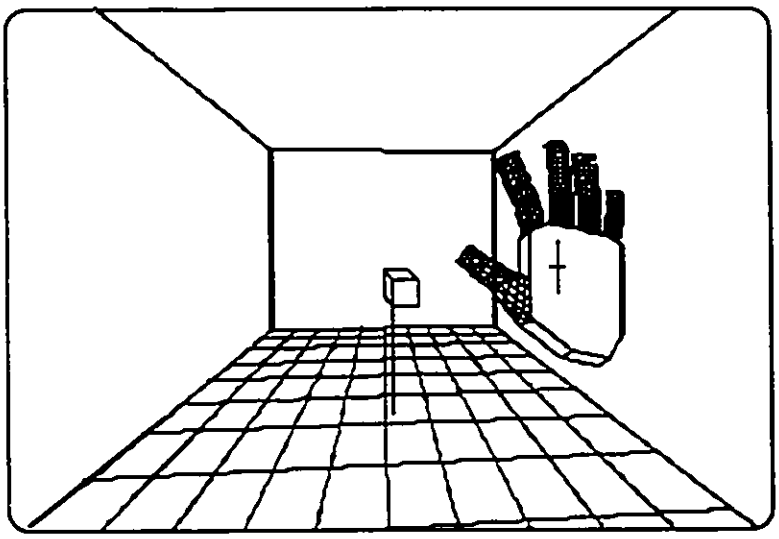

Figure 4.5: Cubic target in the center, the controlled hand on the right (figure 4.1 repeated here for clarity).

in chapter 3. To compensate for this, we decided to use the chessboard floor and the target anchor as our main sources of depth information. The chessboard floor is designed such that the spacing between the horizontal lines diminishes as we go from the viewing screen to the back wall. This accentuates the impresssion of depth as can be seen on figure 4.5. By looking at where the anchor attaches to the floor, the subject can estimate the distance between him and the target. He can then learn to associate his shoulder position to the corresponding target anchor point on the floor, and thus have a depth cue.

The background scene and the targets were generated off-line using a C language program. All possible viewing angles in the vertical and horizontal planes had to be stored in memory. To understand this better, it is necessary to see how the subject interacts with the Virtual Reality. Figure 4.6 is a side view of the subject interacting with the simulation. As explained in chapter 3, there are essentially two ways to participate in a Virtual Reality.

- The subject wears stereo vision goggles embeded in a headset. This is true Virtual Reality since the feeling of immersion is total and the virtual field of view is not restrained. He can turn his head in any direction left, right, up or down as far as he wants, and the corresponding scene image will be generated. The subject is also free to move around as all position sensors are either mounted on his headset, on him [12] or at a distance (ultrasonic tracking).

- The subject looks through a window giving access to the virtual world. In this case, position sensors providing input to the system are not all mounted on the body but usually on the chair where the person sits. When searching for an object outside his field of view, a subject would, in real life, look around by moving his head from side to side (horizontal sweep) and up and down (vertical sweep). When the object is spotted he would reach for it (reach). Horizontal sweep, vertical sweep and reach are events that will induce some changes in the subject's field of vision in a real life context. The same events should also be possible in the Virtual Reality. Horizontal sweep is simulated using chair rotation which will shift the effective view by ± 12 degrees in 0.5 degrees increments. This rotation

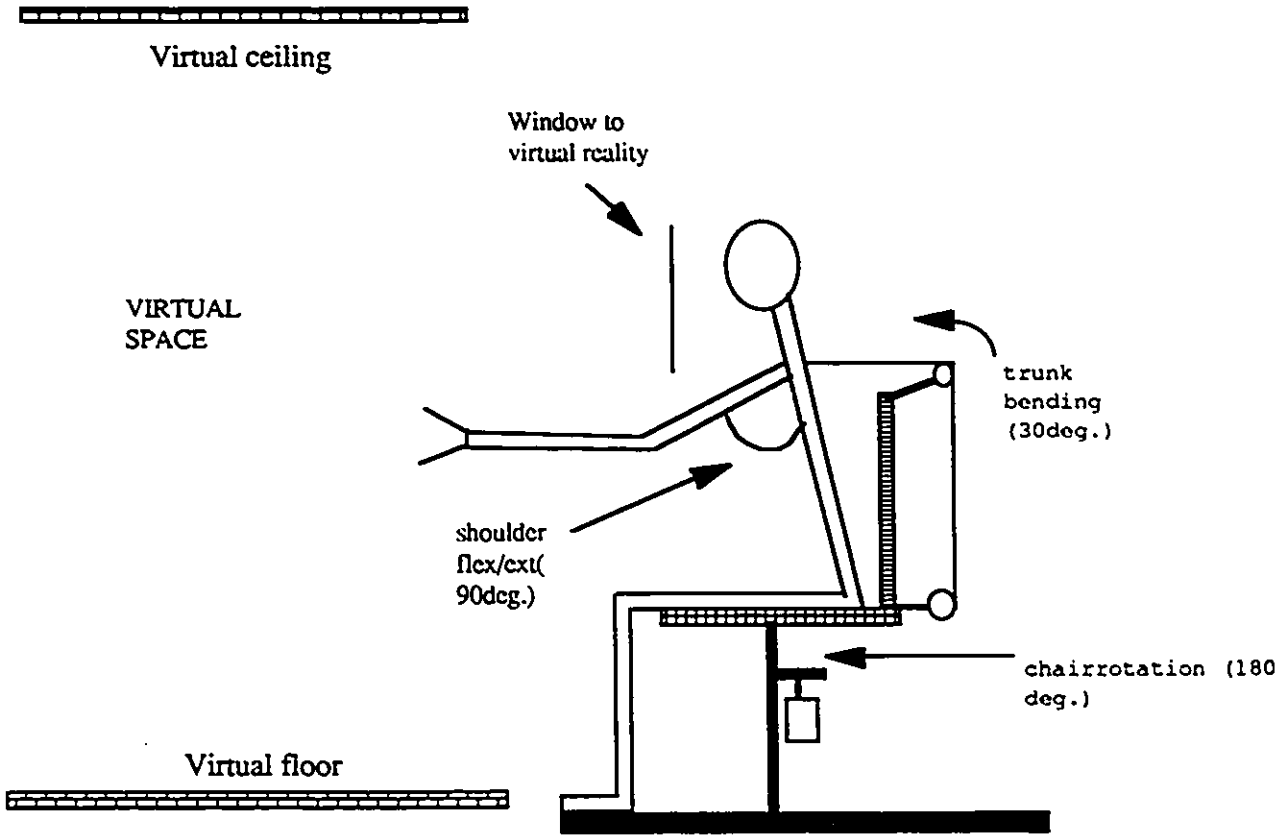

Figure 4.6: The subject looking at the Virtual Reality through a window.

is measured with a single turn potentiometer as show in figure 4.6. Vertical sweep is replicated by using trunk forward bending with a 30 degrees range (see again figure 4.6) measured by a multi-turn potentiometer. Finally, shoulder flexion/extension measured with a goniometer produces the motion of the virtual arm or what we previously refer to as the reach motion. Shoulder maximum excursion is 90 degrees.

Having presented the inputs that allow the user to participate in the Virtual Reality, we can now discuss how the inputs affect the background scene. The rotation of the chair in one direction induces a motion of the background in the other direction. Our setup is such that the window (the computer monitor) giving access to the virtual world, moves with the chair as shown in figure 4.7. A forward trunk bending causes the floor to be drawn perspectively closer to the observer, giving the impression of moving downward. Thus, any action perfomed by the user will be reflected in the Virtual Reality giving him the impression that he is really part of it. Because these inputs are are limited to maximum values, as specified above, all possible combinations could, again, be precalculated and stored in memory for fast access and display. We later found out that most of our algorithms were so efficient (all frame display algorithms were written in Assembler) that we could have generated them at interactive rates.

The signal coming from the two potentiometers and the goniometer are the basic inputs of the workstation. Those specific input motions were selected because of the relative ease with which one can measure their corresponding angles of rotation and also because they allow the subject to reach almost any targets in the 3-D space in front of him from the waist up. Trunk bending is required for fine positioning or for cases where the selected linkage is not exactly appropriate for the task being perfomed. A sketch of the volume accessible to the user is shown in figure 4.8.

All the inputs are fed to the computer via an analog multiplexer. They are then digitized at a sampling rate of $40Hz$ ($\tau = 25$ msec). Such a sampling frequency was chosen from past experience [36][20] and also from work performed by other researchers such as D. S. Childress and

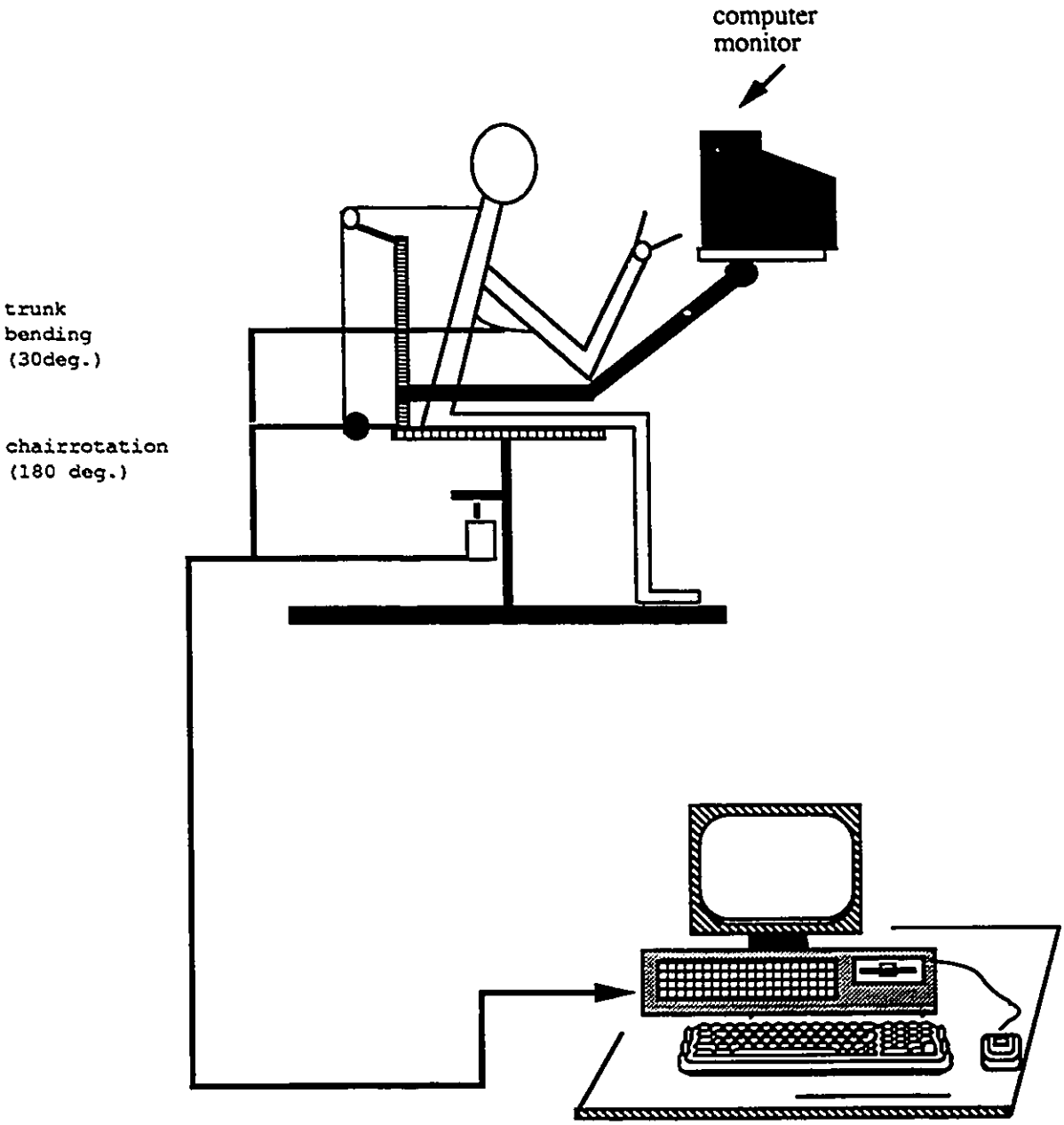

Figure 4.7: The inputs to the Virtual Reality simulator.

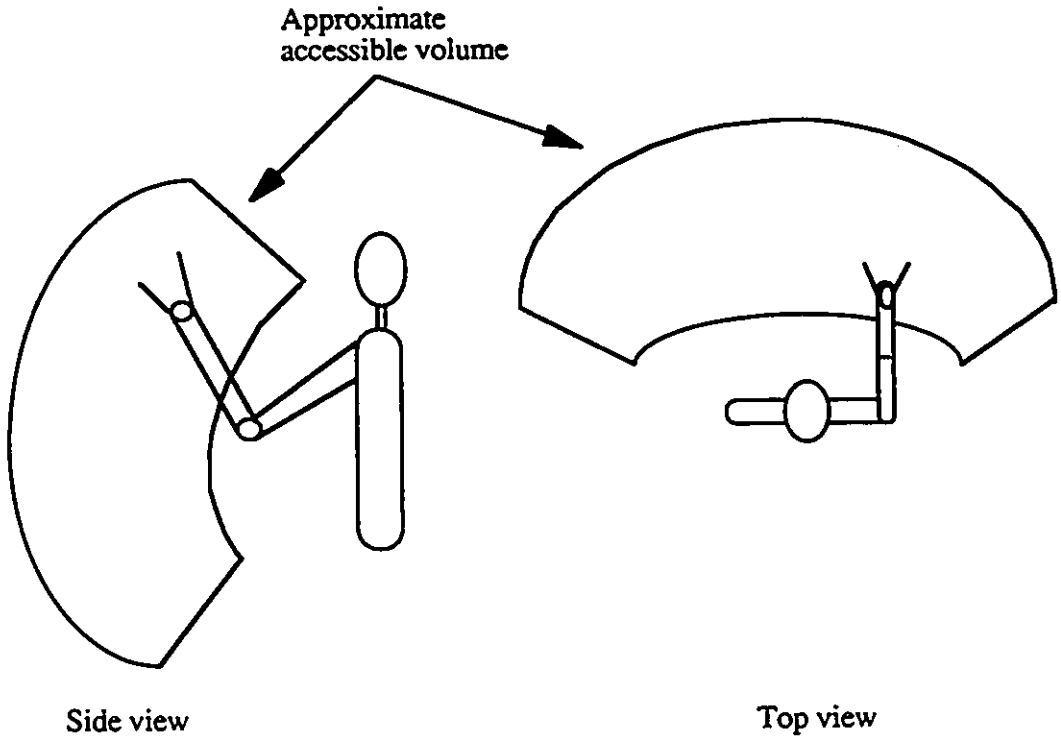

Figure 4.8: Volume accessible by the patient.

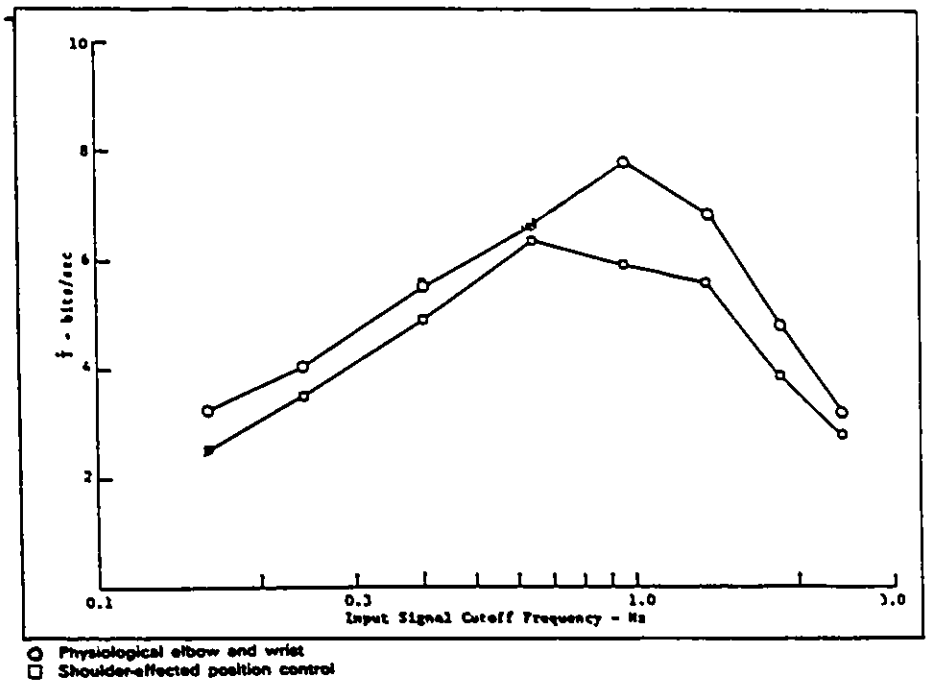

Figure 4.9: Example of information transmission rates for two-dimensional tracking taks performed by the same subject with physiological wrist and shoulder-effected position control using shoulder protraction retraction.

J. A. Doubler [15][14]. Their research was devoted to an investigation of the effectiveness of applying the concept of Extended Physiological Proprioception to the control of upper-extremity prostheses. As part of their work, they investigated the maximum information transmission rates for one and two-dimensional tracking with the physiological elbow, wrist and shoulder. As shown in figure 4.9 they found that for low-frequency input signals, "...the subjects were able to track the targets accurately. There was an approximately linear increase in the information transmission rate with increasing input-signal cutoff frequency". The information transmission rates had a peak for input signals with cutoff frequencies near $1Hz$. Above this, tracking became increasingly difficult as represented by the rapidly diminishing transmission rate. The authors also make an interesting comment: "The inability of human subjects to accurately track random input signals that have significant energy above $1Hz$ is a recurring finding in the literature on manual control". We are not, as these researchers were, investigating the tracking capabilities of e.p.p. controlled artificial arms, because tracking is primarily based on using

visual feedback. We are mostly interested in subconscious control, but we can still use their findings as guidelines. Based on these results, we assumed that an upper bound of $4Hz$ was an over-estimate for the maximum input frequency coming from our input signals which are: shoulder flexion/extension, chair rotation and trunk bending. Each of these signals is filtered to remove excess noise with a passive low-pass filter with a cutoff frequency at $4Hz$. From basic principles of digital communication [40] we know that the minimum sampling frequency should be at least twice the input low-pass filter cutoff frequency. This would correspond to $8Hz$ and we are using $40Hz$. The second reason for using this sampling time τ of 25 milliseconds is to ensure display quality. The peak operating angular velocity of the artificial arm joints is in general in the range of 150 degrees per second [1]. Normal velocities are, however, much less. Hence during one sampling instant, the artificial joints would move by a maximum given by:

$$\text{Maximum incremental rotation} = \tau * \text{maximum velocity} \tag{4.1}$$

$$= 25msec * 150deg/sec \tag{4.2}$$

$$= 3.75deg \tag{4.3}$$

This maximum of 3.75 degrees is just a little less than the animation frame resolution or, in other words, the 3-D terminal device is redrawn on the screen when the incremental change in the input is greater than or equal to 4 degrees. Thus, there is no need to sample at a higher frequency now. The $40Hz$ sampling frequency also allows us to use an identical frame refresh of 40 times/second which give a nonflickering image on the screen. If the sampling rate and frame rate had been different, delays or extra timing routines would have been required for synchronisation. As for the other inputs mentioned above (chair rotation and trunk bending), their rotation velocities are less than 20 degrees/second giving an incremental change of 0.5 degrees per sampling time which is more than adequate for smooth display.

4.1.2 The Preprogrammed Linkages

We have implemented in the simulated environment, various preprogrammed motions or "linkages" taking the virtual arm through different paths and coordinated motions. The choice of which of these linkages is to be used can be keyed into the computer. The primary

input controlling the motion of the virtual arm is the intact shoulder angle moving in a flexion/extension manner as shown on figure 4.7. The corresponding outputs to this specific input are the virtual elbow and wrist joints. In the case of linked motions, the input and outputs have to be uniquely related by a one-to-one relationship. The input/output relationship can be expressed by the following equation:

$$B = F(\theta) \tag{4.4}$$

where θ is the shoulder angle (the input angle) and B is the wrist or elbow angle (output angles). The function F is predefined. It can take, in theory, the shape of any of the curves shown in figure 4.10. However the input/output relationship depicted by curve (b) cannot be used, for the case of an artificial arm, as it might lead to extreme confusion. It can be recognized from curve (b) that more than one output can correspond to a single input. This fact, when translated to our system, means that to one shoulder position (input) could correspond many different artificial arm positions (outputs). The patient using such a linkage would never know exactly where his artificial arm would end up. This, obviously, is not tolerable. That is why in our system, there will always be a one-to-one relationship between input and output. If a different output (motion) is needed, the linkage will have to be changed. We also observed, during our work, that all subjects had more difficulties using nonlinear input-output relationships, as depicted by curve (a) of figure 4.10, than they had using a curve such as (c). From results obtained during testing, it seems that when linkages are learned, the human brain can use and remember linear input/output relationships. Exponential/logarithmic types of relationships were said to be annoying for our subjects, especially when present as a portion of a mostly linear curve as shown by curve (d). A considerable loss of accuracy was noticed during tests containing theses types of nonlinarities[1]. These observations were not really within the scope of this research work but were interesting enough to be included as they could serve as guidelines for future work done in this field. All transducers (potentiometers, joint position encoders, ultrasonic triangulation position detectors) should have their output voltage versus input displacement curve calibrated, at least in the range of utilisation. Possible nonlinearities

[1]The partial nonlinearities were due to a nonlinear potentiometer.

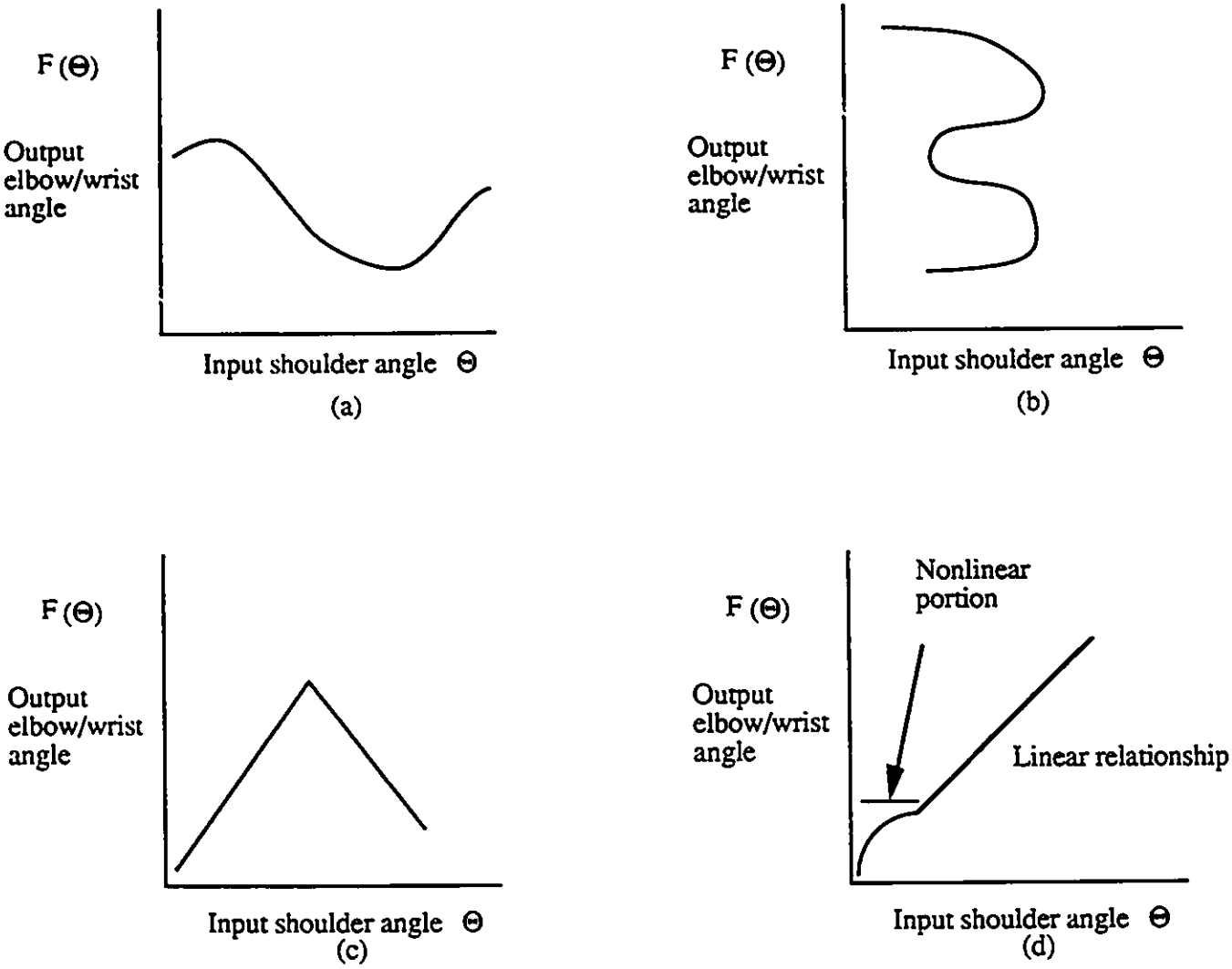

Figure 4.10: Different types of possible input/output curves

can be corrected in hardware or software using linearizing equations.

Modified Extended Physiological Proprioception

As explained in the introductory chapter, we have made use of a modified form of extended physiological proprioception (e.p.p.). In Simpson's original e.p.p. the position of each artificial output joint was determined by the position of one intact joint [44]. However we realized that it is sometimes better to provide the user with a system in which a coordinated motion of the output joints can be obtained by the action of a single input. All tasks chosen to be incorporated in our system, even ones requiring a coordinated motion of many joints, can be executed using just one input, the computer is the one that takes care of coordinating the motion of each joint. Of course, the independent motion of the output joints (elbow and wrist) is not possible without the use of input joint (shoulder).

Example of a linkage

In this section, a linkage is decomposed and explained. The movement that we would like to mimic is that of an individual using the artifial arm to first reach a cup of tea, then pick it up, and finally bring it to his mouth. The subject is seated in front of a table. A few parameters for the arm have to be specified. First the physical dimensions:

1. L1 = 30 cm (12 in) distance between shoulder and elbow joint.
2. L2 = 30 cm (12 in) distance between elbow joint and palm.
3. L3 = 22.5 cm (9 in) distance between shoulder joint and table.
4. H = 5 cm (2 in) height of the handle of the cup from the table.

Figure 4.11 gives a graphical representation of the artificial arm when it has reached the cup. A full decomposition of the motion is given on figure 4.12 (a)-(c). At the start position (a) the palm is facing outward. From (a) to (c) the subject extends his shoulder which causes the elbow to extend and the wrist to rotate in an anticlockwise direction, looking from the top. When the hand reaches the cup in (c), the arm segments are as given by the figure, the shoulder

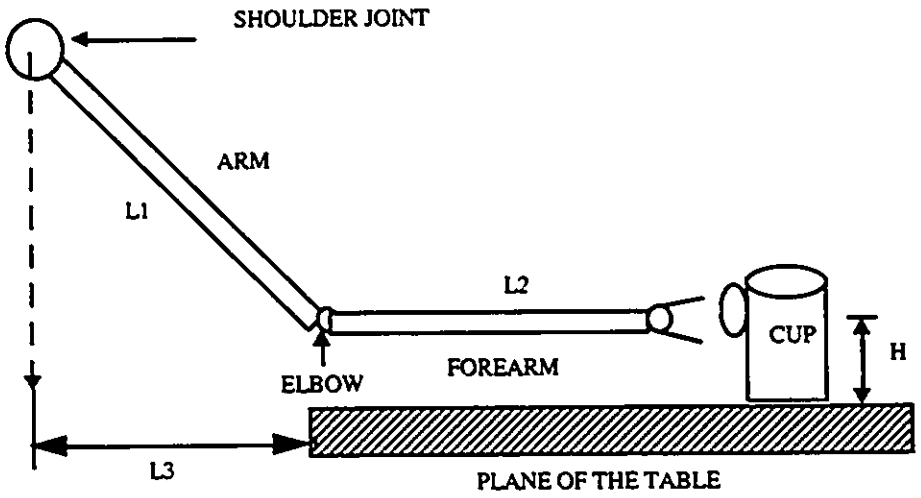

Figure 4.11: The artificial arm grasping a cup.

has extended by 45 degrees, the elbow by 120 degrees and the wrist has rotated by 45 degrees. Fine positioning can be obtained by using the trunk bending motion. When the hand reaches the cup, prehension is performed and the cup is grasped. Further extension of the shoulder joint will, at this point, causes a flexion of the elbow joint. The wrist remains in the same position until the mouth is reached as shown on figure 4.12 (e). The input/output relationship or the function F_{link} for this particular linkage is shown on figure 4.13. The X axis gives the angular displacement of the shoulder (the input) and the Y axis gives the output angles for the elbow and the wrist. This linkage, and all others, were empirically generated by observation of a natural human arm performing the desired motions. Each motion was carefully decomposed such as to provide the information to generate the adequate input/output relationships. The classical forward and inverse kinematic transform was use to go from joint space to cartesien space and vice versa.

It is understood that only anthropomorphic motions are performed. All subjects adapted very easily to the various linkages used as will be discussed in the following chapter. Positioning accuracy and speeds are comparable to those obtained with a natural arm as shown on

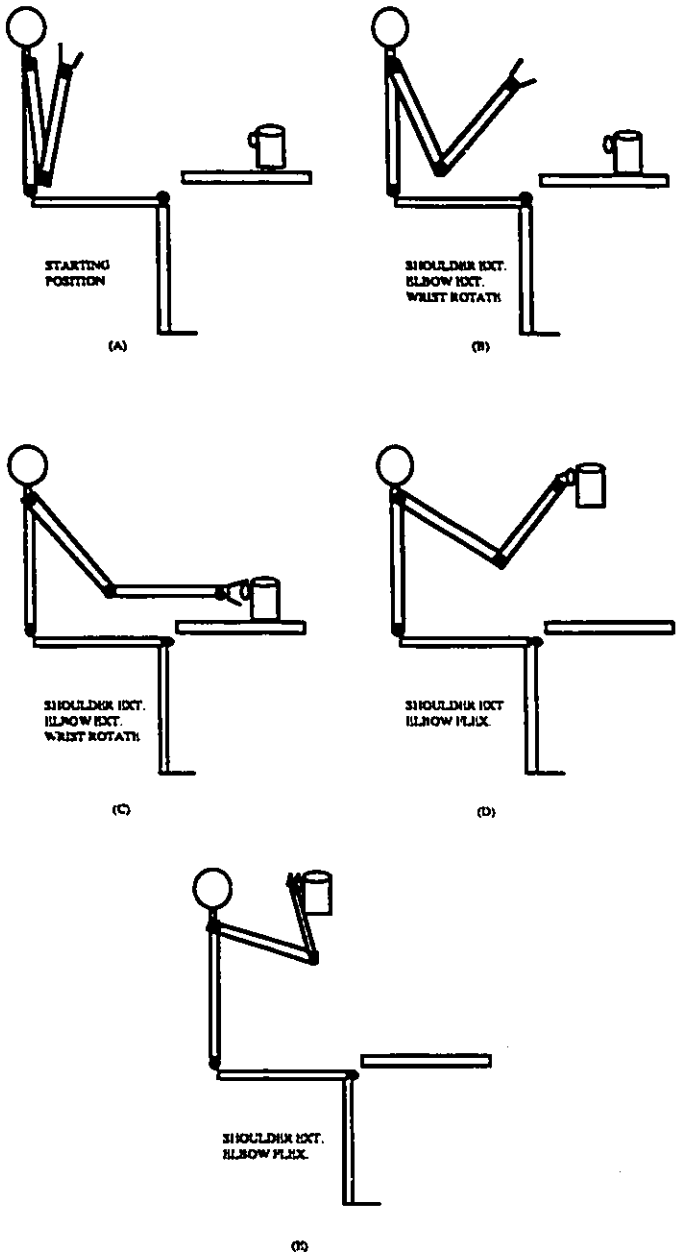

Figure 4.12: The decomposition of a simple linkage.

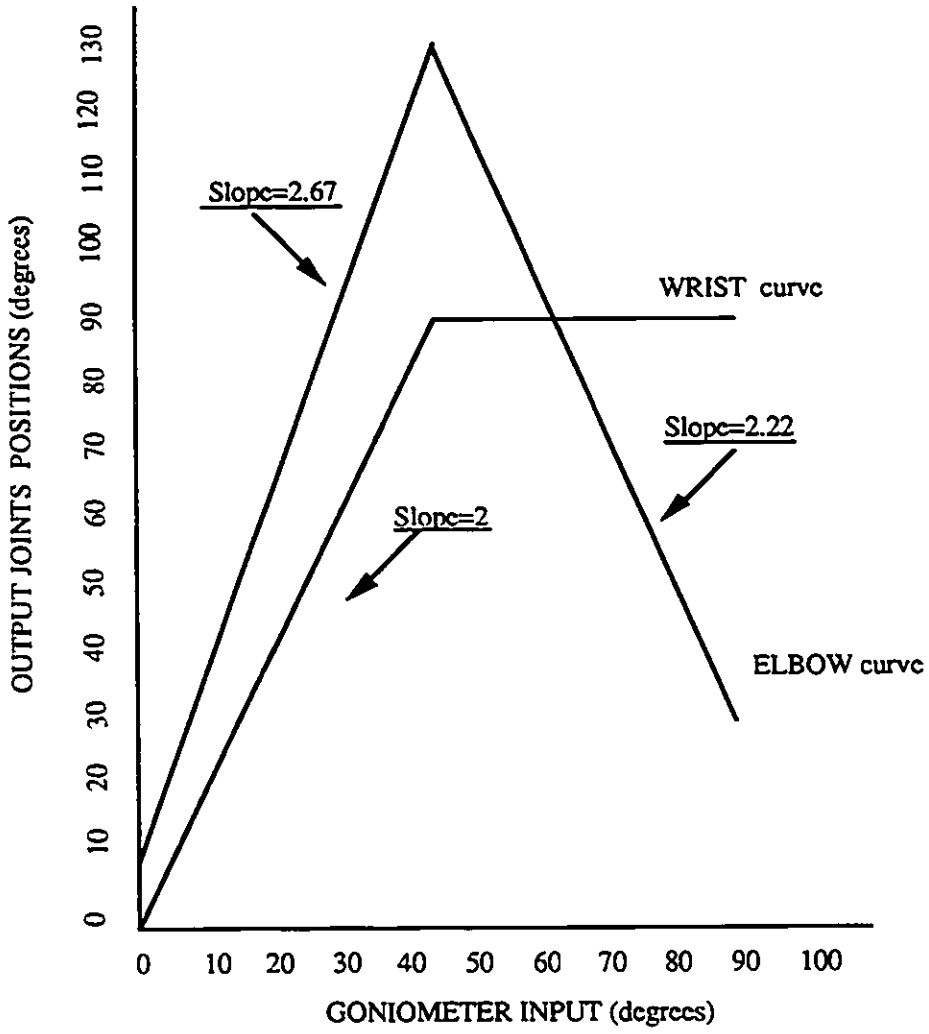

Figure 4.13: Input/ouput relationship for elbow and wrist joint corresponding to the previously decomposed motion.

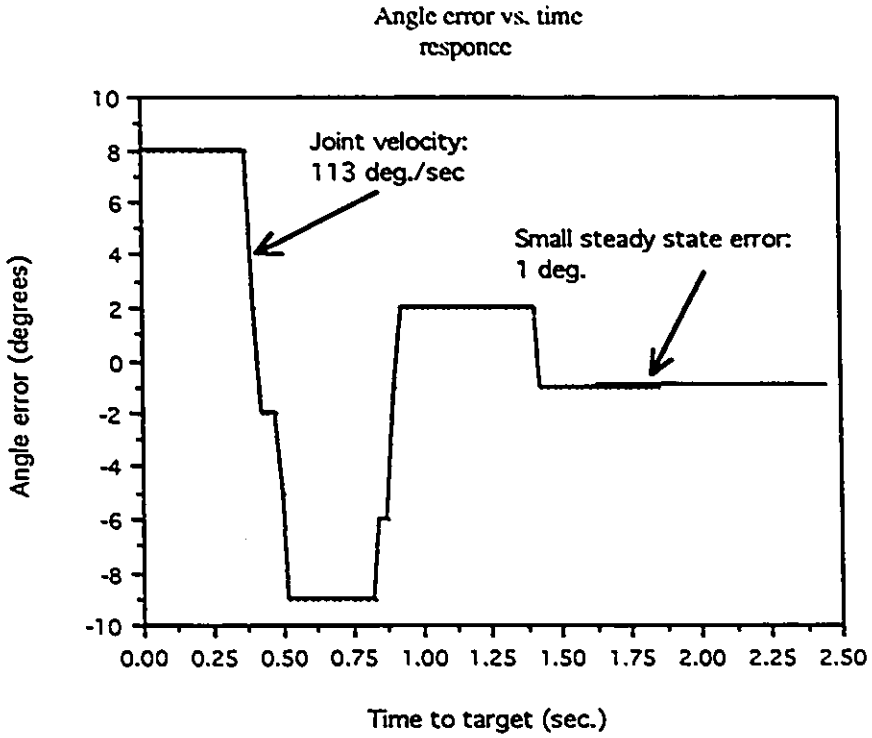

Figure 4.14: Positioning accuracy and speed of the artificial arm executing a motion.

figure 4.14.

4.2 The Simulation Controlling Software

The Virtual Reality simulation is generated and controlled by a main program, with independent modules taking care of specific tasks. The main module algorithm is illustrated, in a flowchart manner, in figure 4.15. The program runs in an infinite loop and the sequence of steps illustrated is always executed in the given order. Here are briefly the actions taken:

1. Do all necessary initialisations:

   - Load all images and targets in memory.

- Provide, through a menu, the choice of linkage, dynamic behavior and operating mode: teach or test.
- Decide whether results are to be recorded or not.

2. Read motion or "linkage" selection.
3. Read goniometer, chair, trunk bending.
4. Verify that the linkage choice is still the same, otherwise take proper actions.
5. Compute the desired positions (i.e. where the next position of the virtual arm should be).
6. Verify that the required motion is within the selected dynamic capabilities of the arm. Otherwise, warn the user and limit the motion to what is permited.
7. The last phase is to update the display by showing the terminal device at its new location.

Each of the steps mentioned above (corresponding to one box of the flowchart of figure 4.15) also contain many other sub-steps executed through external functions making this control program highly modular. Each module was separately written, debuged, tested, and optimized for speed. They were even written as physically independent programs that were later linked through a "project file".

In the next section a mathematical model of the artificial arm is proposed and based on that model, the dynamics equations of the arm are derived. These equations contain the arm parameters that will, according to their settings, dictate the time response.

4.3 The system dynamics

4.3.1 The Model

The system of interest consists of the elbow joint, the forearm, and the terminal device. In order to simulate the dynamics of the system we first have to get a model that approximates

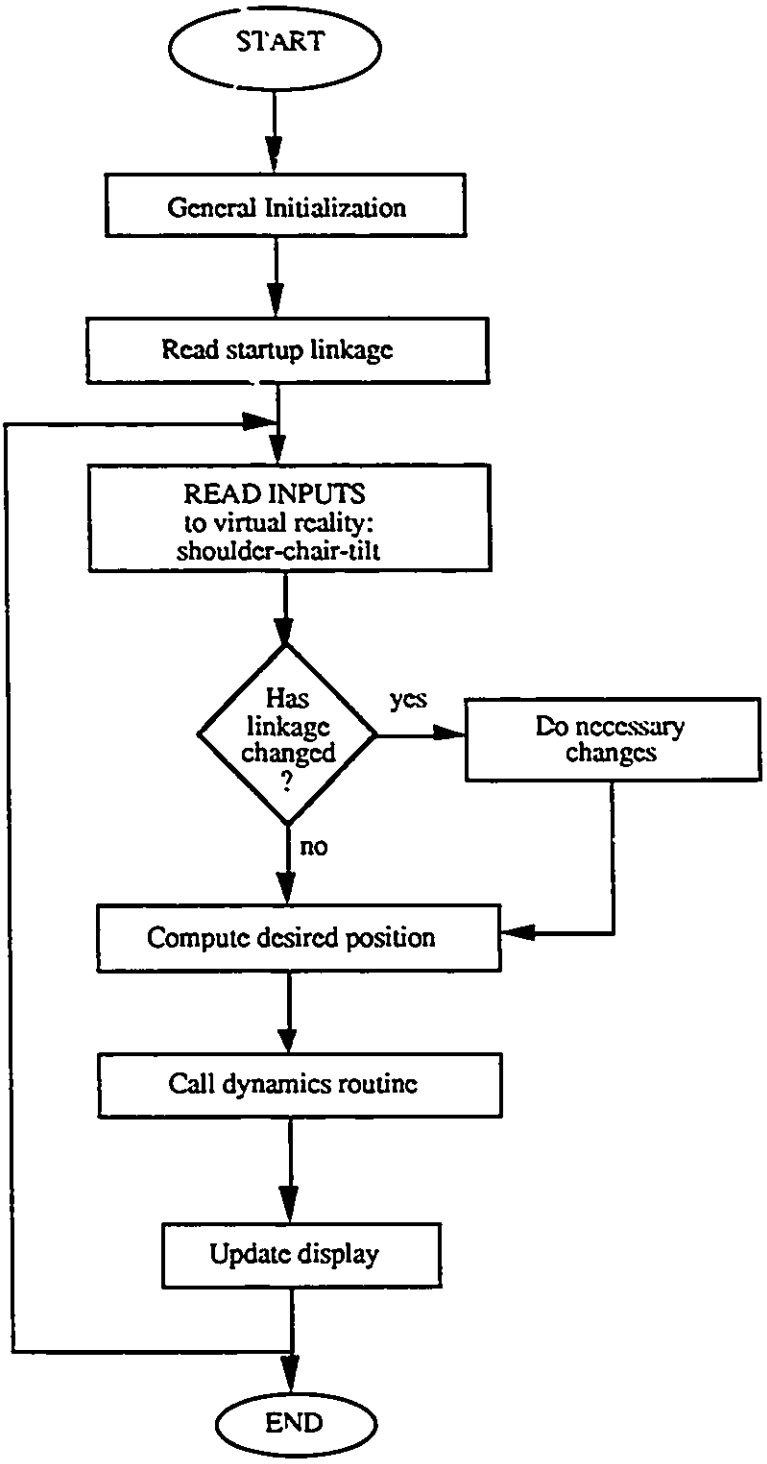

Figure 4.15: Flowchart of the simulation control program.

it adequately. Figure 4.16 is a reasonable model of the artificial arm under consideration, it is assumed that the masses of both links, $m1$ and $m2$, are represented by point masses at the end of the links (this is valid in the case of the Boston elbow and various other elbows since the linking frame is usually made of a light material and most of the weight is due to the joint actuator or the terminal device.)

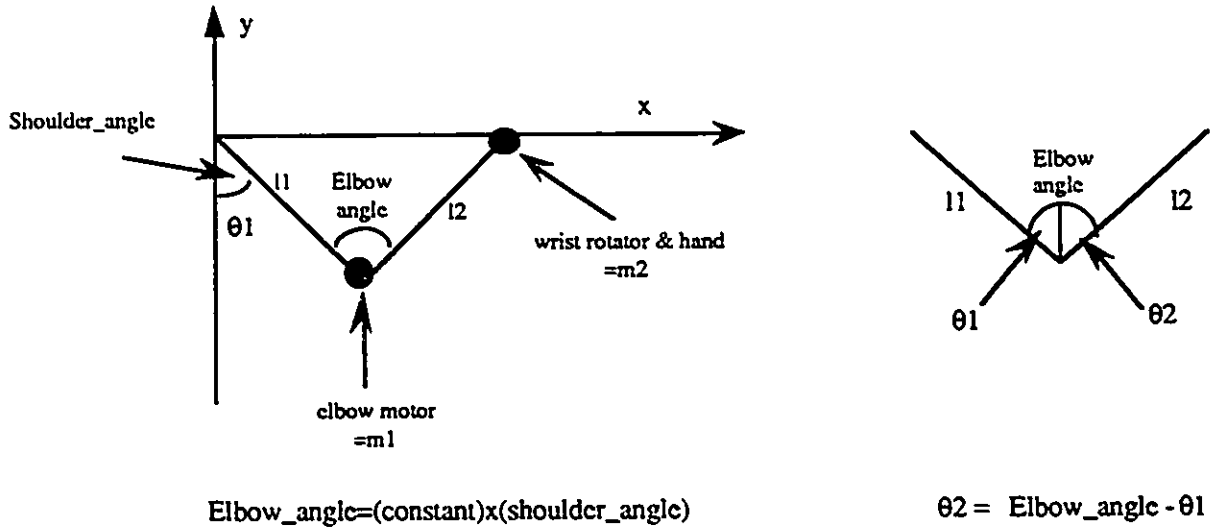

Figure 4.16: A typical two link artificial arm.

We now briefly discuss the steps required to find the dynamics equations of a two link manipulator which closely approximates the one used in this reasearch work. Some guidelines can be found in [35] and in Appendix A. The following analysis is based on the Lagrangian mechanics, but other methods exist to get the dynamics equations. One of them is the Newton-Euler approach. The derivation resulting from the Lagrangian approach or the Newton-Euler approach is equivalent, but the form of the solution is different. Saying that one is computationally more efficient than the other is debatable according to Hollerbach[22]. However, the Lagrangian method is handy in that it provides the dynamics equations for a complex system

in the simplest possible manner [35]. We were also interested in finding a symbolic solution for the arm dynamics such as to have a complete understanding of the control problem. That is why, although numerical approaches are available, we did not use them.

The Lagrangian L is defined as the difference between the kinetic energy K and the potential energy P of the system:

$$L = K - P \tag{4.5}$$

The dynamics equations are obtained as given in [35]

$$F_i = \frac{d}{dt}\frac{\partial L}{\partial \dot{q}_i} - \frac{\partial L}{\partial q_i} \tag{4.6}$$

Where:

F_i is either force or torque (it will be torque in our case).

q_i are the coordinates in which the kinetic and potential energy are expressed.

$\dot{q}$ is the corresponding velocity. Referring to mass m_1, its kinetic energy is:

$$K_1 = \frac{1}{2} m_1 l_1^2 \dot{\theta}_1^2 \tag{4.7}$$

and its potential energy is:

$$P_1 = -m_1 g l_1 \cos(\theta_1) \tag{4.8}$$

Referring to mass m_2 we first need to write expressions for the Cartesian coordinates. Looking at figure 4.16 we have:

$$x_2 = l_1 \sin\theta_1 + l_2 \sin\theta_2 \tag{4.9}$$

$$y_2 = -l_1 \cos\theta_1 + l_2 \cos\theta_2 \tag{4.10}$$

The corresponding cartesien components of the velocity are:

$$\dot{x}_2 = l_1 \cos\theta_1 \dot{\theta}_1 + l_2 \cos\theta_2 \dot{\theta}_2 \tag{4.11}$$

$$\dot{y}_2 = l_1 \sin\theta_1 \dot{\theta}_1 - l_2 \sin\theta_2 \dot{\theta}_2 \tag{4.12}$$

The magnitude of the velocity squared is:

$$V_2^2 = \dot{x}_2^2 + \dot{y}_2^2 \tag{4.13}$$

Substituting the above equations (4.11) and (4.12) in (4.13), expanding the result and simplifying it allows us to write an expression for the kinetic energy K_2:

$$K_2 = \frac{1}{2}m_2 l_1^2 \dot{\theta}_1^2 + \frac{1}{2}m_2 l_2^2 \dot{\theta}_2^2 + m_2 l_1 l_2 \cos(\theta_1 + \theta_2)\dot{\theta}_1 \dot{\theta}_2 \tag{4.14}$$

The height of the mass m_2 is expressed by equation (4.10) so the potential energy is:

$$P_2 = -m_2 g l_1 \cos\theta_1 + m_2 g l_2 \cos\theta_2 \tag{4.15}$$

The Lagragian L is given by:

$$\begin{aligned} L &= \sum K_i - \sum P_i \\ L &= \frac{1}{2}(m_1 + m_2) l_1^2 \dot{\theta}_1^2 + \frac{1}{2}m_2 l_2^2 \dot{\theta}_2^2 + m_2 l_1 l_2 \cos(\theta_1 + \theta_2)\dot{\theta}_1 \dot{\theta}_2 \\ &\quad + (m_1 + m_2) g l_1 \cos\theta_1 - m_2 g l_2 \cos\theta_2 \end{aligned} \tag{4.16}$$

To obtain the dynamics equation for joint i the Lagragian L is differentiated with respect to the i^{th} coordinate as expressed above in equation (4.6), repeated here for clarity:

$$F_i = \frac{d}{dt}\frac{\partial L}{\partial \dot{q}_i} - \frac{\partial L}{\partial q_i} \tag{4.17}$$

We are simulating the motion of an artificial arm attached distally from the shoulder joint in the middle of the upperarm so we do not have control of joint 1. Although we have derived the dynamics equation for that joint in Appendix A, we will just give here the dynamics equation for the joint of interest (i.e. joint 2). To get the torque at joint 2 we proceed by differentiating the Lagrangian L with respect to $\dot{\theta}_2$ and θ_2 as dictated by equation (4.17) and we obtain:

$$T_2 = m_2 l_2^2 \ddot{\theta}_2 + m_2 l_1 l_2 \cos(\theta_1 + \theta_2)\ddot{\theta}_1 - m_2 l_1 l_2 \sin(\theta_1 + \theta_2)\dot{\theta}_1^2 - m_2 g l_2 \sin\theta_2 \tag{4.18}$$

Equation (4.18) discribes the torque at every instant in time, at joint 2. Let us now decompose this torque equation in order to simplify it. T_2 can be written as such:

$$T_2 = D_{12}\ddot{\theta}_1 + D_{22}\ddot{\theta}_2 - D_{211}\dot{\theta}_1^2 - D_2 \tag{4.19}$$

$D_{22} = m_2 l_2^2$ is the effective inertia of joint 2. Acceleration at this joint will cause a torque equal to $m_2 l_2^2 \ddot{\theta}_2$.

$D_{12} = m_2 l_1 l_2 \cos(\theta_1 + \theta_2)$ is the coupling between joint 1 and 2. Acceleration of joint 1 will cause a torque at joint 2 equal to: $m_2 l_1 l_2 \cos(\theta_1 + \theta_2)\ddot{\theta}_1$.

$D_{211} = m_2 l_1 l_2 \sin(\theta_1 + \theta_2)$ is the centripetal acceleration coefficient. Speed at joint 1 will cause a torque at joint 2 equal to: $m_2 l_1 l_2 \sin(\theta_1 + \theta_2)\dot{\theta}_1^2$

$D_2 = m_2 g l_2 \sin\theta_2$ is the gravity torque. This torque varies as a function of the sine of the angle of joint 2 ($\sin\theta_2$).

This total joint torque T_2 gives us a description of how the torque dynamically changes, at joint 2, as a function of arm geometry, gravity, position, speed and acceleration. Thus, T_2 is the load on the D.C. motor of the elbow joint. Hence, in finding an expression for the equation of motion for joint 2, T_2 will play a key role. Before deriving this equation of motion, we would like to further take a look a equation (4.18): substituting typical values for m_2, l_1, l_2, g we get:

$m_2 = 1.5Kg$ for the forearm and terminal device.

$l_1 = l_2 = l = 300mm = 0.3m$

$g = 9.81m/sec^2$

We see that the contribution of the following terms: D_{22}=D_{12}=D_{211}=$m_2 l^2$=$0.135Kg.m^2$ is not significant compared to that of the gravity D_2=$m_2 gl$=$4.41Kg.m^2/sec^2$. Also, considering the fact that joint acceleration will be small[2], D_{12} and D_{22} can be neglected as their effect is more than one order of magnitude below that of gravity. D_{211} will, at most, contribute to a torque of 0.777 N.m at the maximum Boston elbow velocity (2.4 rad/sec, measured). This torque contribution is still neglible compared to the gravity torque. Thus T_2 can now be approximated set as:

$$T_2 \cong -m_2 gl \sin\theta_2 \tag{4.20}$$

[2]Because of the unbeatable servo feature.

The dynamics equation for a D.C. motor can be modelled as (taken from [26]):

$$T_{motor} = J_T\ddot{\theta} + D\dot{\theta} + T_F + T_L \tag{4.21}$$

Where:

J_T = The D.C. motor inertia J_m plus the load inertia J_{load} (reflected through the gears).

D = All the viscous friction torques and other torques proportional to velocity. These quanties will be assumed null as no specifique or typical values can be found for artificial arms like the Boston elbow or the Utha arm. If figures are available, they can be used.

T_{motor} = The dynamic torque required from the motor to generate the motion.

T_F = Constant friction torque in the D.C. motor: Unknown.

T_L = T_2 Above calculated joint 2 torque.

Because of the unknown parameters that we have to assume null, the motor torque T_{motor} can be simplified as follows:

$$\begin{aligned} T_{motor} &= J_T\ddot{\theta} + T_2 \\ T_{motor} &= J_T\ddot{\theta} - m_2 g l \sin\theta_2 \end{aligned} \tag{4.22}$$

Now that we have the dynanic equations for the motor, we need to decide upon a control strategy. Notice that we had to assume that all the friction contributions were null, since no pertinent value could be found in the literature. In order to compensate for the lack of friction, we will make use of a Proportional Derivative (PD) controller in which the gain K_d behaves exactly as a controllable source of friction [49]. The control equation is:

$$\text{Controller torque} = K_c(\theta_d - \theta) - K_d\dot{\theta} \tag{4.23}$$

Now the required motor torque T_{motor} can be made equal to the *Controller* torque as follows:

$$K_c(\theta_d - \theta) - K_d\dot{\theta} = J_T\ddot{\theta} - m_2 g l \sin\theta_2 \tag{4.24}$$

Depending on the linkage chosen, θ_2, as shown in figure 4.16 corresponds to a fraction of the total joint angle $\theta(t)$. We can write:

$$\theta_2 = \alpha\theta(t) \text{ Where } 0 \leq \alpha \leq 0.5 \tag{4.25}$$

Without loss of generality, the desired angle θ_d can be made equal to null and equation (4.24) above can be rearranged to the normal form of a second order nonlinear differential equation:

$$J_T\ddot{\theta}(t) + K_d\dot{\theta}(t) + K_e\theta(t) - m_2gl\sin(\alpha\theta(t)) = 0 \tag{4.26}$$

This equation, when solved, gives the equation of motion that describes the change in the elbow joint angle as a function of time. However, there are two major difficulties associated with using equation (4.26):

1. Because of its nonlinear nature, an analytic solution cannot easily be found in order to obtain the (time) equation of motion. Only numerical methods can be of help to alleviate the problem [R.Vaillancourt[3]].

2. It is not a simple task to model a dynamic system and, furthermore, a system under closed loop control. Normally in such a controlled situation when an external load is added, more torque is supplied automatically to obey loop contraints. It is thus common practice in robotics to assume that there will always be sufficient motor torque to cope with control loop demand. But with the motors of limited size and power which are used in prosthetics, such an assumption is not valid. Frequently, torque requirements go beyond what the joint motor can supply, and a situation is reached where the speed is reduced and the joint position (output) cannot be related to the desired position and velocity (input) through the closed-loop equation. It is a case where the feedback loop is open. This phenomenon happens with the Boston elbow when it is loaded and going up against gravity. Modelling this "system saturation" effect is not really possible with simple dynamics expressions anymore. We have to artificially introduce various limitations on

[3]Dr.R.Vaillantcourt is a professor at the University of Ottawa. He advised us to use numerical method to deal with this problem.

precise parameters such as torque and velocity in order to faithfully model the system under consideration.

In the next section we discuss the mean by which a satisfactory solution can be found.

4.3.2 Real-time modelling of a nonlinear system

Due to the elbow motor torque limitations, equation (4.26) cannot be used to predict joint position with time. A more practical approach was therefore needed to reach that goal. We decided to go in steps to find the equation that would give a real description of the joint motion with time. First, the required torque ($T_{required}$) is computed using the Controller torque equation given by:

$$T_{required} = \text{Controller torque} = K_c(\theta_d - \theta) - K_d\dot{\theta} \tag{4.27}$$

then this value is equated to the motor torque equation T_{motor} given in the previous section, but repeated here for clarity:

$T_{motor} = J_T\ddot{\theta} - m_2gl\sin\theta_2$ we get:

$T_{required} = J_T\ddot{\theta}(t) - m_2gl\sin(\alpha\theta(t))$ with $\theta_2 = \alpha\theta(t)$

The above equation can again be rearranged to the normal form of a second order nonlinear equation:

$$J_T\ddot{\theta}(t) - m_2gl\sin(\alpha\theta(t)) - T_{required} = 0 \tag{4.28}$$

Because of the rotary nature of the joint we are modelling, the effect (incidence) of gravity on the system is modulated by a sine function which is a function, itself, of the angular position of the joint. It is thus difficult to formulate an equation of motion which would give us the position of the joint as a function of time[4]. In order to solve this problem, we turned to numerical methods. The software *MATHEMATICA*™ (see [56]) was used and the behavior of the

[4]It is imperative to remind the reader at this point that we are not controlling a physical system with a computer, but rather we are simulating a system and incorporating its dynamics in the control such as to obtain, as much as possible, a realistic effect.

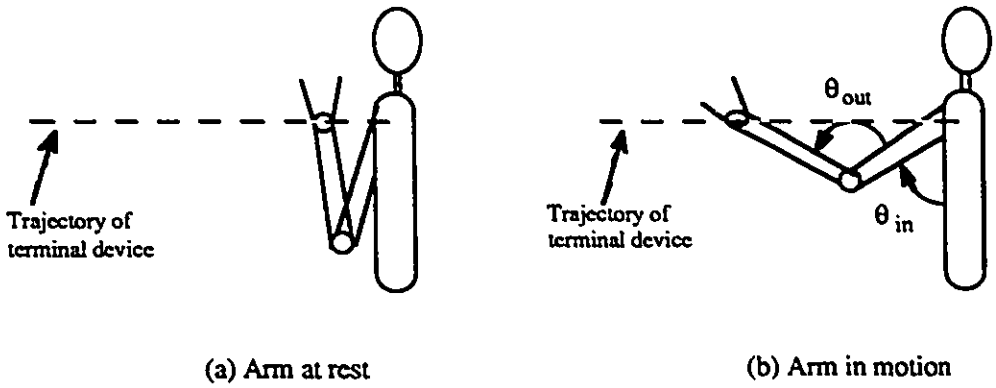

(a) Arm at rest (b) Arm in motion

Figure 4.17: A typical linkage: elbow extends as shoulder is extended.

arm dynamics could be studied. This software proved to be very effective and easy to use. But, the numerical solution of equation (4.28) was done off-line. The solution to this equation is not unique, but it changes as a function of the initial conditions. So, at every sampling instant τ (τ=25 millisec) the arm position is checked. Its velocity is then computed and equation (4.28) has to be evaluted. We did not have the computing power to evaluate that equation within the 25 milliseconds sampling time. As a comparison it took about 60 sec for MATHEMATICA to come out with an interpolating function. So we had to propose an approximation as a piecewise model. All our motions, are of the form given by figure 4.17.(a)-(b), where the forearm extends as the shoulder is extended. Initially, at rest, the arm position is given by figure 4.17.(a). The shoulder angle is zero or near zero and the elbow angle (which is related to the shoulder angle by a direct relation of the form: $\alpha Elbow_{angle}$=$Shoulder_{angle}$) is zero too. By observation and experiments, we saw that for joint angles $\theta(t)$ less than 20 degrees, the gravity term did not have much effect on system dynamics so it can be set it to zero. For $\theta(t)$ greater than 20 degrees, we found the following:

- The artificial arm maximum speeds will be in the range of 140 degrees per second, since the sampling time is $\tau = 25millisec$ the maximum change in one τ is 3.5^0.

- At one instant in time $t_1 = 0$ the elbow angle is found to be θ_{t1}.

- At the next sampling instant $t_1 + \tau$, the maximum displacement will be: $\theta_{t1} \pm 3.5^0$, and the corresponding change in angle between these two sampling time is simply: $\Delta\theta(t) = \pm 3.5^0$. Thus, the change in $\theta_2(t)$ is $\Delta\theta_2(t) = \alpha\Delta\theta(t)$ and, since we always have $\alpha \leq 0.5$ (α was defined by equation 4.25) , the maximum change in $\theta_2(t)$ is $0.5(\pm 3.5^0) = \pm 1.75^0$.

From this, it is clear that the contribution "$m_2 gl \sin(\alpha\theta(t))$" can be assumed constant between two consecutive sampling intervals since $\sin(\alpha\theta(t) + 1.75) \cong \sin(\alpha\theta(t))$. Based on this fact and for small variations around θ_2, the two following differential equations when evaluated at $t = t_1$, $\theta(t_1) = \theta_1$ should give the same results.

$$\text{The exact equation } J_T\ddot{\theta}(t) = T_{required} + m_2 g \sin\alpha\theta(t) \tag{4.29}$$

$$\text{The approximate equation } J_T\ddot{\theta}(t) = T_{required} + m_2 g \sin\alpha\theta_{t1} \tag{4.30}$$

The same initial conditions should be used for both equations:

$$\theta(t_1) = \theta_1, \dot{\theta}(t_1) = \dot{\theta}_1$$

These two equations have been evaluated with as much precision as possible using MATHEMATICA (refer to figure 4.18 and 4.19) and we can see how close the approximation (figure 4.19) is to the exact equation. In all cases, the exact equation and the approximation can be considered identical for small angles. Different senarios of initial positions and initial velocities where tried and the approximation was always valid. Time is on the absica and joint angle $\theta(t)$ is on the ordinate axis. Notice that $\theta(t)$ is given in radians because that is what MATHEMATICA uses for angles.

As we stated before, the solution of the differential equation is an equation of motion $\theta(t)$. Using this equation, we can predict where the joint should be at the end of the present sampling instant and draw it there. Plots given by figures 4.18 and 4.19 show that our linear approximation is valid for angle variations $\Delta\theta(t)$ even greater than 11°. We can now use with confidence the approximation given by (4.30) instead of the exact (nonlinear) equation. But this time we can evaluate the solution of equation (4.30) at every sampling instant since it is a

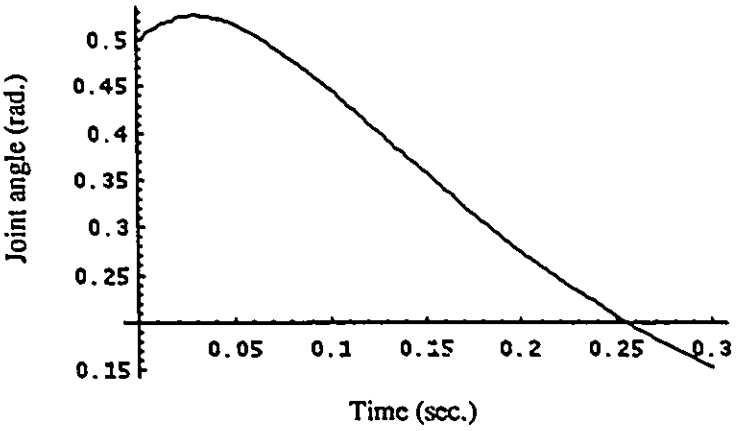

Figure 4.18: The exact nonlinear equation.

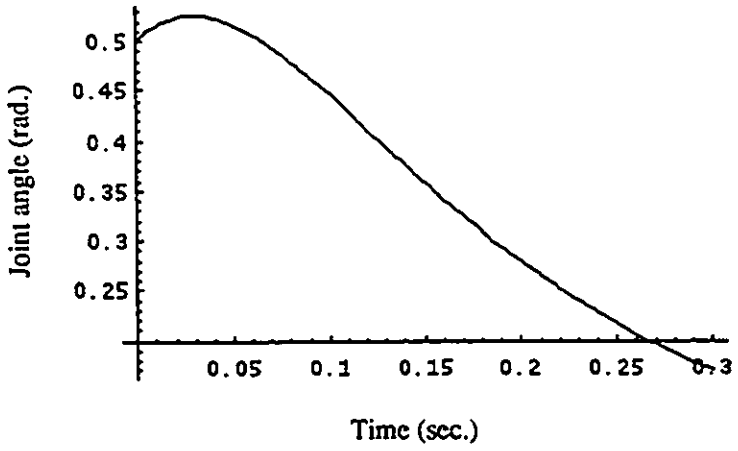

Figure 4.19: The approximation to the nonlinear equation.

simple second order linear differential equation.

Let us now give a brief detail of how the required equation of motion was found from equation (4.30), and how the control loop gains where chosen.

The approximation to the nonlinear differential equation is given by (4.30) and is rewritten below:

$$\begin{aligned} J_T\ddot{\theta}(t) &= T_{required} + m_2 g l \sin \alpha\theta_{t1} \\ \frac{d^2\theta}{dt^2} &= \frac{K}{J_T} \end{aligned} \tag{4.31}$$

$$\text{Where } K = T_{required} + m_2 g l \sin \alpha\theta_{t1} = constant \tag{4.32}$$

Integrating twice with respect to time and using the initial conditions,
$\theta(t_1) = \theta_{t1}$, $\dot{\theta}(t_1) = \dot{\theta}_{t1}$ we get:

$$\theta(t) = \frac{1}{2}\frac{K}{J_T}t^2 + \dot{\theta}_{t1}t + \theta_{t1} \tag{4.33}$$

Replacing $K = T_{required} + m_2 g l \sin(\alpha\theta_{t1})$ in (4.33) we have:

$$\theta(t) = \frac{1}{2}\left[\frac{T_{required} + m_2 g l \sin(\alpha\theta_{t1})}{J_T}\right] t^2 + \dot{\theta}_{t1}t + \theta_{t1} \tag{4.34}$$

This above equation, gives us the position of the joint at every sampling instant τ. The position must be re-computed every τ seconds using the previous position and previous velocity as initial conditions.

It is important to note that equation (4.34) is a function of the required torque $T_{required}$ which is computed using the control equation:

$$\text{Controller torque} = T_{required} = K_c(\theta_d - \theta) - K_d\dot{\theta} \tag{4.35}$$

So $T_{required}$ depends on chosen values of K_c and K_d which in turn will dictate how fast the controlled process will react. Using the assumption made above, that between two consecutive

sampling instants the gravity contribution $m_2gl\sin(\alpha\theta(t))$ can be made constant and equal to: $m_2gl\sin(\alpha\theta_{t1})$, and equating once again motor torque T_{motor} and the required torque $T_{required}$ we get:

$$\ddot{\theta}(t) + \frac{K_d}{J_T}\dot{\theta}(t) + \frac{K_c}{J_T}\theta(t) = \frac{m_2gl}{J_T}\sin(\alpha\theta_{t1}) \tag{4.36}$$

This is a nonhomogenous linear differential equation with $\frac{m_2gl}{J_T}\sin(\alpha\theta_{t1})$ causing the nonhomogeneity. To solve this equation, the right side is set to null and immediatly the characteristic equation can be written to be:

$$\lambda^2 + \frac{K_d}{J_T}\lambda + \frac{K_c}{J_T} = 0 \tag{4.37}$$

The roots of this quadratic equation are:

$$\lambda_{1,2} = \frac{1}{2}(-\frac{K_d}{J_T} \pm \sqrt{\frac{{K_d}^2}{J_T} - \frac{4K_c}{J_T}})$$

$$\text{Choosing } \frac{{K_d}^2}{J_T} - \frac{4K_c}{J_T} = 0 \text{ gives a critically damped response} \tag{4.38}$$

This is all we need to decide upon system parameters K_c and K_d. There are an infinite number of choices for K_c and K_d that will satisfy equation (4.38). To find a unique choice, we placed the constraint that with a null initial velocity, when the difference between the required position and the present one is 4^0, the required torque $T_{required}$ should be the maximum available from the motor we are emulating. The worst case demand on motor torque is when going in one direction and the input abruptly requires the arm to go into the opposite direction at full speed. But we consider this an extreme situation where the unbeatable servo feature would be used. Futher discussion on the unbeatable servo feature can be found in chapter 5.

The following are some of the choices made for various parameters:

We are assuming that the joint 2 (elbow) is actuated by an harmonic drive with a gear reduction factor of 30. We will take the motor inertia J_m to be equal to joint2 (the forearm) inertia after gear reduction [49]. So the total system inertia J_T=J_m+J_{joint2} will be twice joint2 inertia (after gear reduction).

$$J_T = 2\frac{m_2gl^2}{\text{gear ratio}} \text{ with } m_2 = 1.5Kg,\ l = 0.3m.$$

$$
\begin{aligned}
&= 2\frac{0.135}{30} Kg.m^2 \\
&= 9.10^{-3} Kg.m^2 \\
K_c &= 1.518 \text{ chosen} \\
K_d^2 &= 4K_cJ_T \text{ refer to equation (4.38)} \\
K_d &= \sqrt{4K_cJ_T} \\
&= 0.189 \cong 0.2
\end{aligned}
$$

With the parameters as chosen above, the simulated arm moves as expected and mimics the typical responce of a Boston Elbow. Also, the different dynamic behaviour of the Boston Elbow is observed in the Virtual Reality simulation of the arm. When the terminal device is moving towards the subject (i.e. going up) it is slow, and when it is going away from the suject (down) it moves faster. Times to go from fully extended to fully flexed and from fully flexed to fully extended are the same as that of the Boston Elbow. When loaded, the simulation, again, responds like the Boston Elbow. Weight lifting capabilities are also similar. This confirms the adequacy of the chosen dynamics equations and the various assumptions made.

In the next chapter, the different tests performed using the Virtual Reality simulation of the artificial arm will be introduced. The general results will be presented and commented.

Chapter 5

General Testing and Results

5.1 Presentation of tests

5.1.1 Preamble

We have designed our simulation environment such that a variety of tests can be performed in a very straightforward manner and the resulting data can be collected automatically. A description of the basic operation of the system is given below.

1. The simulation is initiated by choosing one among a variety of tests, for example a positioning task.

2. The corresponding linkage is picked, and the system automatically selects a target which is randomly positioned. The target can always be reached by the selected linkage. Figure 5.1 gives an example of what appears in front of the subject.

3. Some time is given for the subject to accommodate to system operation. The subject moves his controlling joint and can see, in the Virtual Reality, the resulting motion of the artificial arm corresponding to the given input. The subject usually needs very little time (less than 5 minutes) to develop a "feel" for the virtual arm he is operating. He is not given any explicit instructions about system dynamics, physical causalities, number of different targets etc.

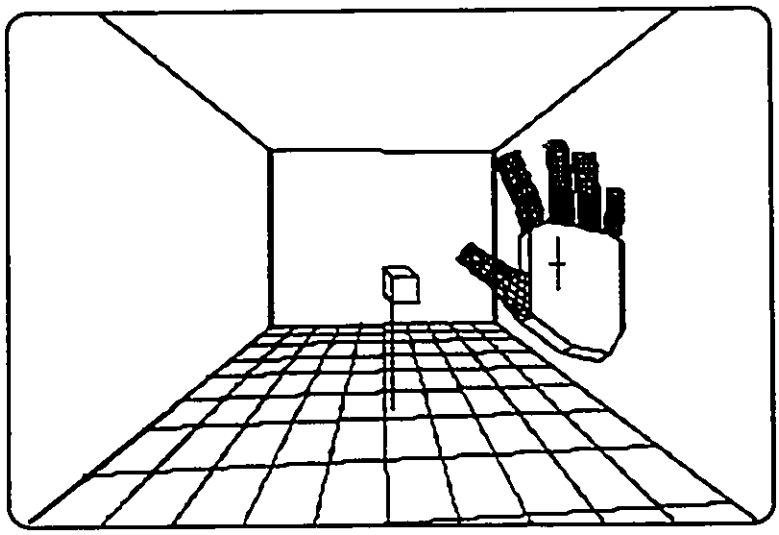

Figure 5.1: 3-dimensional Virtual Reality representation of the artificial arm (figure 4.1 repeated here for clarity).

4. Once ready to be tested, the subject depresses a start key. His first series of tests starts.

In order to ease data collection, the simulation environment incorporated modules especially designed for that purpose. It was also conceived to be user friendly and, at different stages throughout execution, the test subject or researcher supervising operation is prompted for pertinent information. All state variables of the system: linkage, target number, inputs and x,y,z error distances are electronically recorded at every sampling instant. Upon completion of a test session the program writes the information in the subject file in a predefined text format to enable easy export to a database for statistical analysis.

In chapter 2, section 2.1 entitled: Objective and Approach, we outlined precisely the information we wanted to extract from these tests. We thus had to decide upon a testing strategy that would help in highlighting the different aspects of each of the variables under consideration. From this, a variety of tests was devised, after analysis and discussion three

series of tests were retained.

5.1.2 First series of tests

The first series of tests aims at exploring whether an e.p.p. controlled arm can be used efficiently with more than one linkage, and to quantify the loss of accuracy and speed resulting from the addition of new linkages. Some insight into the acquisition of process control skills could also be obtained and contrasted with classical studies such as those by Crossman and Cooke[13].

Note that in all cases a learning phase composed of a number of tests with visual feedback is provided. The subject is instructed to go to the targets as quickly and as comfortably as he or she can. Once a satisfactory level of learning has being achieved, an operational phase consisting of tests with the display of the arm blanked (to remove visual feedback) follows. In the two different testing conditions just discussed, the subject is given a maximum trial time of 50 seconds. The trial can be stopped in different ways: (i) The subject can decide that he is close enough to the target and manually stop the trial; (ii) if he is on target for 2 seconds or more, the trial is automatically stopped; (iii) if on the other hand, he uses up all the allocated time, the test is halted by the computer. (In all instances, the x,y,z distances and test time are recorded and written to the subject's own file.) The arm is then displayed to offer some feedback. Here is in point form the pattern followed for the first series of tests.

1. Learn the first linkage (learning phase) with visual feedback, get a feel for the motion. Perform the test (operational phase).
2. Learn the second linkage with visual feedback, get a feel for the motion. Perform the test.
3. Go back to the first linkage, refresh memory with one trial using visual feedback. Then perform the test.
4. Learn the third linkage with visual feedback, get a feel for the motion. Perform the test.
5. With Linkage 1 and Linkage 2, do as was done in 3 above.

6. Verify if there is any performance degradation due to the learning and operation of these three linkages. If degradation is present check if it is acceptable or not.

We should also mention that, when visual feedback is present (i.e. the learning phase), the subject always gets to the target. Thus the absolute error from hand to target is zero; that is why, the time it takes to get to the target is, in this case, the important measure of learning. When testing is done without visual feedback, the absolute error to the target becomes the determining measure of performance.

The reason for following the sequence outlined above is now explained: Starting with Linkage 1, a preliminary training period consisting of three testing sessions, with visual feedback, should establish whether or not the subject has learned to use the linkage correctly. This is done using the Student t test[1] [3]. By comparing the first and second sets of tests with the third one, we can determine if the populations are not significantly different. If they are, we will have to investigate to see if further improvement is possible or, on the contrary, if the subject is at the tail of the learning curve. If, on the other hand, the third set of tests is significantly different from the first and second set (the populations are different), more practice is given until the Student t test does not show any significant difference and the scoring is adequate. An adequate score is one in which the average time to target is comparable with the average time it would take a non-amputee to perform a similar motion. At the end of this stage, the subject has learned to use the linkage with visual feedback. This is the learning phase. We then move to the operational phase where the same linkage is used but without visual feedback. Again, the same approach as described above is taken. Testing is pursued until satisfactory performance is attained. Pertinent mean and standard deviations of the last test session are computed and are used as a reference for that particular linkage when learning retention is checked later. Also, the step response for each patient is recorded and analysed such that the type of controller emulated by the subject, if significant, is identified.

[1] W.S. Gosset wrote a series of articles describing this test. He used the pen-name "Student". Hence the name of the test.

At this stage, Linkage 2 can be learned. The same procedure as followed for Linkage 1 is used here. Data is gathered, learning is monitored, and performance is measured without visual feedback. Once satisfactory performances are obtained and a reference[2] set for Linkage 2, we can now go back to Linkage 1 and quantify how much has been retained. This is done by performing one test with visual feedback immediately followed by a test without visual feedback. Mean, standard deviation and step response are recorded and compared with the established reference of Linkage 1. The obtained data is analysed to see the extent to which subconcious control is still possible and adequate.

Once again, a third linkage is thoroughly learned and the subject is asked to go back and test with Linkage 1 and 2. The complete results are then studied and performance degradation, if any, is evaluated in order to conclude on the adequacy of providing multiple linkages for an e.p.p. controlled artificial arm.

5.1.3 Second series of tests

This series of tests immediately followed the previous tests because here we are assuming that the subject has learned more than one linkage (whether he has properly retained them or not will be part of the issue of this section). The following testing protocol should provide some data on the possible use of many linkages and, furthermore, it should show the ability of an individual to pick from a set of linkages the one that best fits the task he is about to undertake. Random targets are offered to the subject which require the use of one of the previously learned linkages to reach them. This means that the user has to choose among the set of linkages, the one that will best take him to a target. We have tried to keep the number of variables under consideration to a minimum, such that the task is not unduly difficult for the subject.

[2]The reference will be based on the mean and standard deviation and t test.

5.1.4 Third series of tests

One of the rules established by Simpson [44] was that an "unbeatable servo" feature had to be implemented to maintain the 1:1 linkage and to prevent the input from going too fast or too far for the output to follow. This feature is difficult to implement in hardware and this is why we are trying to study the extent to which this is needed. We believe that because Simpson used pneumatic actuators to move a steel based prosthesis which was quite heavy, the speed of motion was probably slow thus justifying the need for a mechanical unbeatable servo. With a more up-to-date technology for the arm frame, light weight and rigidity can be acheived. The arm can be actuated by electric motors offering more power than pneumatic counterparts. Under these conditions, the artificial arm can probably move as fast as a real arm and thus guarantee the 1:1 relationship between input and output at all times, thus eliminating the need for the cumbersome mechanical unbeatable servo feature. With the direct drive artificial arms conceived and built by Asada's group at Carnegie-Melon University [2], very high speeds of arm operation have been demonstrated using small size high torque motors built around rare earth cobalt magnets. With this fact in mind, it might be possible just to replace the braking system by a warning system. Having the possibility of simulating any arm structure, any weight or any motor power, we will try to specify the limit at which the mechanical unbeatable servo feature is not a necessity and propose a substitute. This third series of tests will be based on perfoming normal tasks with the virtual unbeatable servo feature and see if there are problems associated with using the arm with just this warning feature. Recommendations based on these tests will be made as guidelines for future work done on e.p.p.

5.2 Acceptance of the simulation by the subjects

Before discussing the results, it is interesting to see how the different subjects reacted to this Virtual Reality simulation of an artificial arm. It should be emphasized that the general impression was more than satisfactory. Although the screen resolution was limited to CGA (640x200), for real-time speed contraints, it was good. After a few minutes of use, subjects

found that they were in full control of the arm and they could move it in all possible ways allowed by the system. In fact the 1:1 relationship between the shoulder angle and the terminal device position is so good that some of them thought that they could do any motion with it. Adaptation time in using and positioning the arm via the goniometer, the chair rotation, and trunk bending, was comparable to using a computer mouse. Even depth positioning was acceptable considering the absence of stereoscopic vision and other depth cues. In fact most subjects relied on e.p.p. to evaluate and remember the depth distances of each target. When visual feedback was provided, the subjects all reached the targets in a time comparable to what it would take a non-amputee to perfom a real positioning task similar to the one performed in the simulation. Slightly more time was required when a target was located at mid-range of a specific motion or when two consecutive targets were placed close to each other. In these cases, the absence of some depth cues became obvious and a little bit of hunting was necessary to get the target to light up thus indicating that the hand was on target. Considering that in reality, more than ten different sources of depth cues are commonly available when reaching out for an object [29] we believe that the availability a few more depth cues would have helped to solve these problems. However a desire to have a reliable system with non-fragile components that can be used with disabled subjects drove us away from making use of sophisticated devices such as a head-mounted display providing stereoscopic vision. However we have made in the Conclusion some recommendations for future work, in this field, on how to improve depth perception.

5.3 Results

Introduction

With the system as described above, we have run tests on seven volunteers and have gathered data. From all the results obtained, we have seen that all subjects accommodated quite quickly to the system. To emphasize these general comments, we would like to present the results obtained from three subjects. They were not picked because they were considered good but rather because they exhibited distinct but typical types of behavior to be seen in

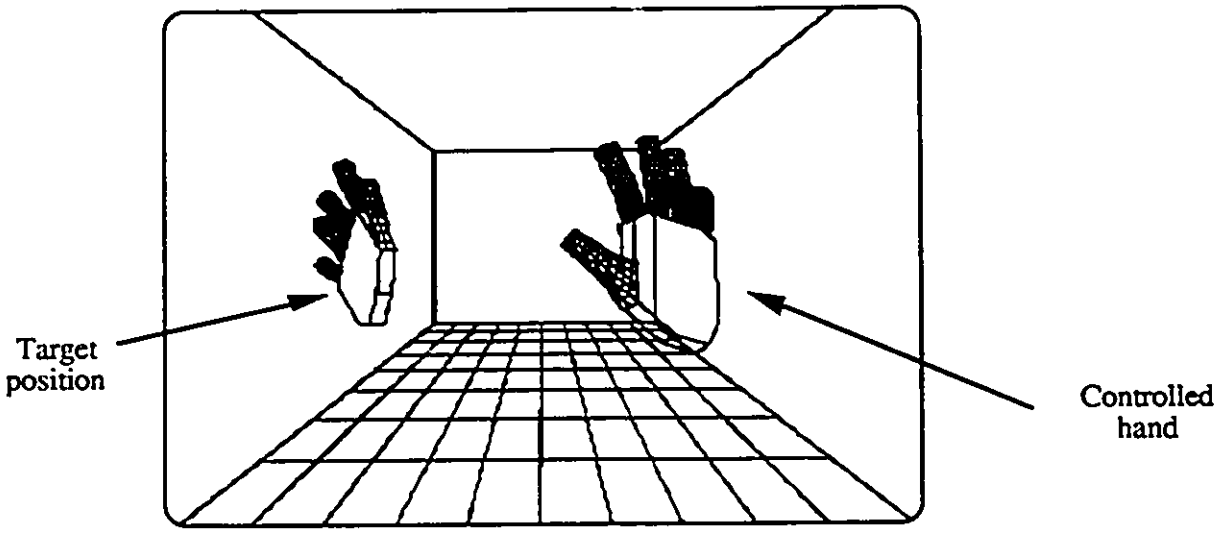

Figure 5.2: Linkage 1, a position replicate type of task.

this type of experiment. For the first test, a linkage was used where the terminal device had to be precisely positioned in space. The task required the subject to replicate the position of the hand as shown in figure 5.2, this we have termed a position replicate type of task. For Linkage 1, in the start position the shoulder angle is zero, the forearm and the hand are straight up, and the back of the hand is facing the subject (The controlled hand in figure 5.2 is exactly in that position). The extension of the shoulder induces a corresponding extension of the elbow and a supination of the hand. At mid-range of the motion, the shoulder angle is 45^0, the elbow angle is 90^0 the palm of the hand is facing to the left of the subject (the target hand in figure 5.2 is in that position). At the end of the motion, when the shoulder angle is 90^0, the elbow angle is 180^0 and the palm of the hand is facing up. In order to perform a test, the system shows the target (which looks like a hand) in a pseudo-randomly chosen position and orientation in space and the subject has to replicate that position with his virtual hand. The positioning accuracy is determined by measuring how close the subject can mimic the position of the target. The subject was given a 4^0 margin within which he would be considered on target.

For the other linkages, a more classical positioning task was performed. The subject had to position the center of his palm, marked with a 3-D cursor, on targets appearing in front of him in the virtual 3-D space. The target was a cube of approximate true physical dimension 2.5cm on each side. Throughout this chapter, when necessary, we will be using the terminology "target unit" to refer to the relative error made by the test subject attempting to reach a target in space. Instead of measuring the error in pixels or in centimeters, we chose the unit as being the size of the target. Hence, we use the terminology that the subject is a number of target distances away from the real target.

For all linkages, when performing a test, there was a common scenario:

- A linkage number was selected.
- There were six different targets specific to that linkage that the system could chose from, and all were reachable with that linkage. The positions of the targets were pseudo-randomly defined.
- Each target appeared ten times throughout the test.
- Each subject performed a total of 60 trials per test session.

At this point in the testing, the linkage selection (before each testing session) was performed by the researcher and could not be altered by the subject.

The t test

Throughout the discussion of the results, some null hypotheses will be stated and the Student t test will be used to see if they can be rejected or not. The t test will essentially be used to establish that a subject has reached a plateau in his learning or in his skill acquisition. We will be dealing, in most cases, with two populations of 10 samples

each. Thus the t test will be based on 18 degrees of freedom. In cases different from the above, the number of degrees of freedom will be specified. The null hypothesis will be that the population of Test(i+1) is not different from the population of Test(i). This means that the subject performing the test has not made any significant progress from Test(i) to Test(i+1). Also, there are adequate grounds (based on [38, 36]) for saying that if a real difference exits it must be because performance was better in Test(i+1) due to increase training level. This narrows the problem in such a way that the one-tail test can be applied. The significance levels used will be $p < 0.025$.

5.3.1 Results for Linkage 1

Summary

Learning Linkage 1 was straight forward. Two targets 2 and 9 are chosen for performance analysis. The learning pattern for each of these two targets is different. Three testing sessions (called First, Second, and Third Test) were perfomed. All subjects did most of the learning during their First Test. This is characterised by an initially long time-to-target averaging 4.65 seconds for Target 2 and 8.0 seconds for Target 9. For all subjects, the saturation in the learning curve came during or after the First Test, or the Second Test. This is characterised by a more constant and shorter time-to-target (2.7 seconds for Target 2 and 4.16 seconds for Target 9) than during the initial learning. Different mean saturation values for the time-to-target are obtained for Targets 2 and 9 and for each subject. The variation in the time-to-target observed between targets is simply due to their distinct location in the virtual space, whereas the difference from subject to subject is due to the fact that every subject has a unique type of behaviour when performing a task. That behaviour is, however, not static and changes with the experience level of each subject. Also global observations suggest that subjects shift from a closed-loop overdamped type of behavior to a critically damped type of behavior.

After observing a saturation in the learning phase, the subjects were instructed to do the

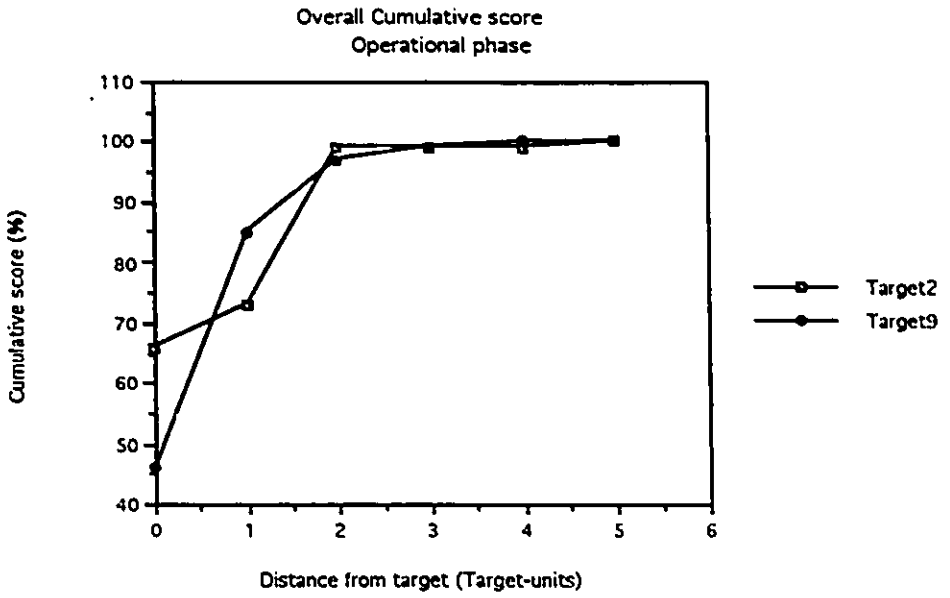

Figure 5.3: Cumulative success rate for Target 2 and 9 for all subjects using Linkage 1.

operational phase tests where they had to reach the same six targets as in the learning phase but with no visual feedback. They had to rely solely on extended physiological proprioception. Recorded scoring rates for reaching the targets are very good for all subjects meaning that the skill to operate Linkage 1 has been well acquired. We have drawn in figure 5.3 the overall cumulative scores (all subjects) for reaching Targets 2 and 9. On abscissa there is the distance from target (in target units) and on the ordinate axis there is the cumulative score in percentage. We can see how rapidly all subjects reach 100% success rate usually around 2 target units.

For Target 2 we obtained an average on-target rate of 66% for all subjects. But this score rapibly climbs to 99% success for a distance of two target units from the target. This mean that all subjects can place their hand within two target units from the target in 99% of the time. For Target 9 (including close misses i.e one extra degree of error) we measured 56% on target. Here again a 100% success is reached around two target units. We could also conclude

from these results and past ones [38] that subjects operating the artificial arm without visual feedback perform in a way comparable to operating their real arm without visual feedback. In both cases error correction is difficult if other sources of feedback (tactile, force) are not used. An open-loop type of behavior prevails. The process of taking the artificial arm and hand to the target is then based on a "mental image" of where the shoulder has to be for the hand to touch the target and a "mental model" of the artificial arm dynamic behavior. The concept of "the mental model" will be elaborated further in latter sections.

5.3.2 In-Depth Study of the Results of Linkage 1

The Learning Phase

The results of a positioning test during the learning phase (with visual feedback) using Linkage 1 are given below in figures 5.4 and 5.5 for three subjects. These curves represent the time it took the subjects to position their terminal devices ten times on Targets 2 and 9. We have also provided in tables 5.1 and 5.2, the various statistical parameters needed for the Student t test[3]. Focusing on Subject 1, we see a rapid familiarisation with the operation of the system. We observe that his first testing session in figure 5.4 shows a typical learning trend where initially the time to reach the target is large and, as the test is repeated more and more the subject learns how to get to the target in a more efficient way. The second testing session shows again initial learning and a rapid saturation. No real improvement is obtained here. Applying the Student t test to these two populations, the null hypothesis that there is no significant improvement from Test1 to Test2 could not be rejected. This implies that there is no evidence that they are significantly different. However, the average time-to-target for Tests 2 of 2.1 seconds is satisfactory as it compares reasonably well to the minimum time required to perform the same task by the author who is an expert in operating the system.

A third test was performed to confirm that the skill acquired does not improve with more practice. Because there is usually an interval of a day between each test, we always observe

[3]The abreviation Not Sig means not significant, and Sig. means Significant difference

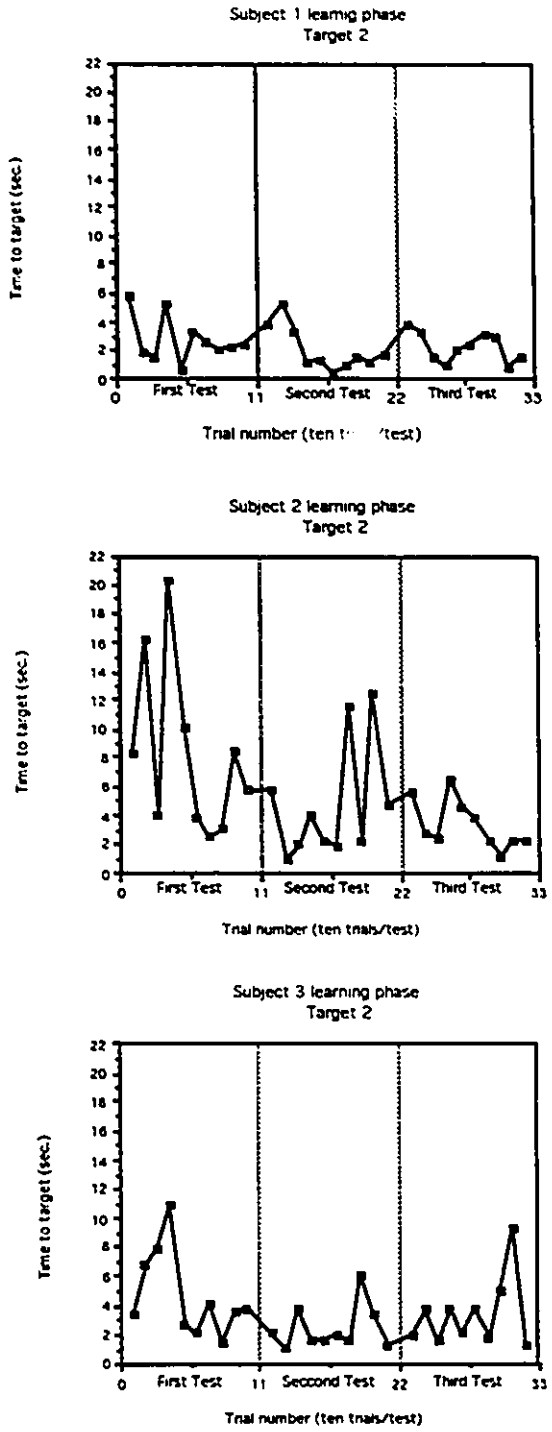

Figure 5.4: Time-to-target vs Trial number for Target 2 for three typical subjects.

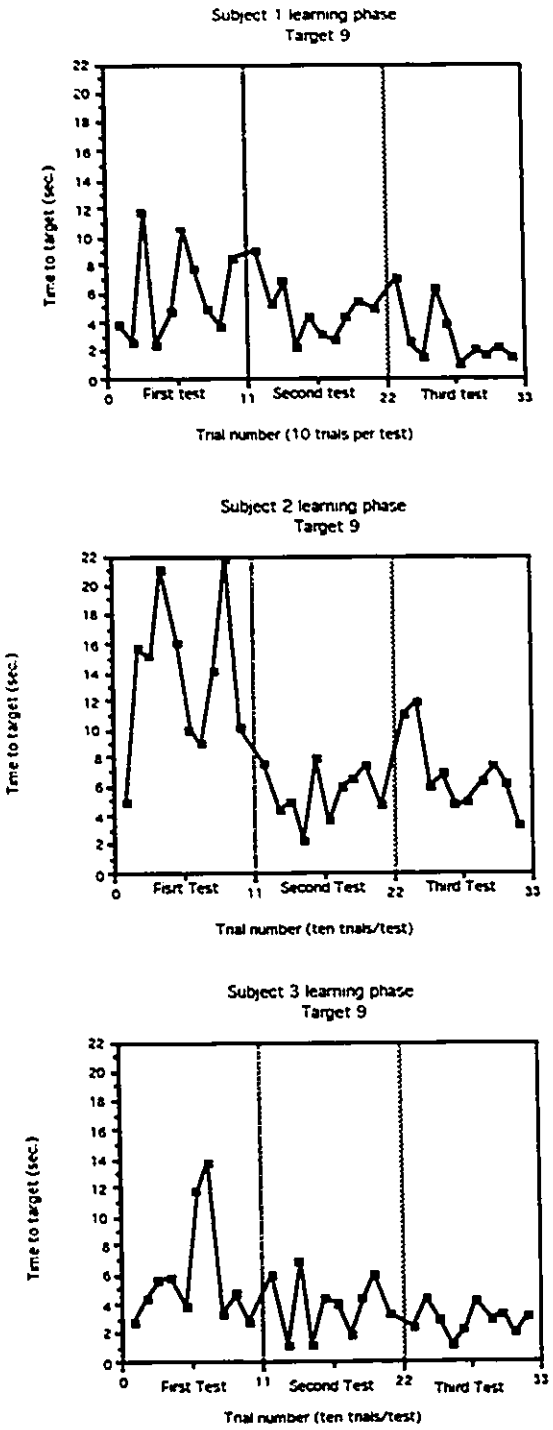

Figure 5.5: Time-to-target vs Trial number for Target 9 for three typical subjects.

	Subject 1		Subject 2		Subject 3	
Target2	Mean	STD	Mean	STD	Mean	STD
Test1	2.719	1.604	8.198	5.94	4.635	2.955
Test2	2.055	1.548	4.745	4.098	2.421	1.579
Test3	2.213	1.411	3.316	1.724	3.39	2.415
Merged	All	All	2-3	2-3	2-3	2-3

Results of the t test

Test1-2	t=0.94	Not Sig	t=1.51	Not Sig	t=2.09	Sig.
Test1-3	t=0.97	Not Sig	t=2.50	Sig.	t=1.03	Not Sig
Test2-3	t=0.11	Not Sig	t=1.02	Not Sig	t=1.06	Not Sig

Table 5.1: Mean, standard deviation and t test of Target 2 for subjects using Linkage 1 with visual feedback

	Subject 1		Subject 2		Subject 3	
Target9	Mean	STD	Mean	STD	Mean	STD
Test1	6.05	3.345	13.714	5.35	5.811	3.805
Test2	4.777	2.026	5.487	1.875	3.89	2.072
Test3	2.947	2.128	6.847	2.733	2.821	0.987
Merged	1-2	1-2	2-3	2-3	2-3	2-3

Results of the t test

Test1-2	t=1.03	Not Sig	t=4.59	Sig.	t=1.40	Not Sig
Test1-3	t=2.47	Sig.	t=3.61	Sig.	t=2.40	Sig.
Test2-3	t=1.97	Sig.	t=1.30	Not Sig	t=1.47	Not Sig

Table 5.2: Mean, standard deviation and t test of Target 9 for subjects using Linkage 1 with visual feedback

some learning at the beginning of each session, however the skill acquired rapidly re-surfaces. This is the case with the Third Test session. Again the t test is applied and no significant difference is found between population 1 & 3 and 2 & 3. We can thus assume that they are from the same population and can merge them into a single group. A new mean and standard deviation can be computed if necessary. A direct conclusion to this observation is that within the span of the First Test this subject efficiently learned to use that linkage. The merged mean and standard deviation of the populations now constitute the reference for this target and, as explained previously, they will be used to evaluate the retention in learning numerous linkages.

The scenarios for Subject 2 and Subject 3, also shown in figure 5.4 and 5.5, is similar. These two subjects simply had a different approach toward learning this linkage especially during the early part of the learning phase (First Test). The first subject confidently went to the target with great speed in an underdamped type behavior, whereas the others used more of an overdamped type control, going slowly and steadily toward the target until it was reached. This of course increased their average time to target. In the latter part of the learning, all subjects were quick and accurate in reaching the target, Subject 2 and Subject 3 reduced their corresponding average time-to-target by 50% or more. It must be emphasized that the average time contained in table 5.1 includes the initial reaction time which varies from person to person between 0.5 to 0.8 second and the voluntary "End Trial", that is perfomed by pressing on a switch, also requiring about 0.5 seconds (measured).

Figure 5.5 shows the results for Target 9 (for the three subjects) that came up during the same testing session. A similar scenario takes place for the three subjects. A fairly erratic behaviour during the First Test and a rapid learning culminating in a drastic reduction in trial time. Analysis of the t test reveals significant differences in population only from Test1 to Test3 but not from Test1 to Test2 and Test2 to Test3. Thus, at that stage, a satisfactory level of saturation in the learning has been reached and further practice did not improve scoring.

The response to a step input for both targets is shown in figures 5.6 and 5.7 respectively

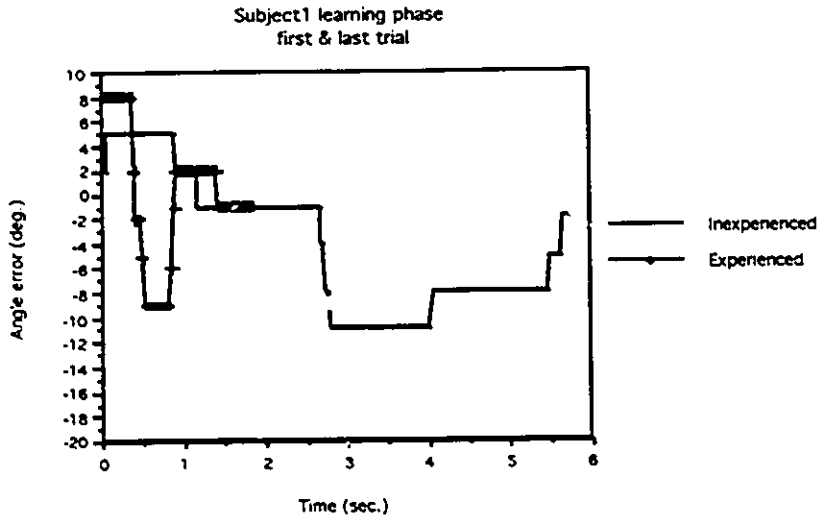

Figure 5.6: Subject 1 Target 2 step response.

for Subject 1. These represent the behaviour of 1) an inexperienced subject, and 2) the same subject but experienced. The oscillations in these curves undoubtedly represent a closed-loop negative feedback control type of behaviour but nonlinearities present for Target 2 (figure 5.6) do not lead to any possible definition of type or order of controller as opposed to what was found by Crossman and Cooke [13]. The step input for Target 9 (figure 5.7) shows, for the inexperienced subject, a typical underdamped response for a second order closed-loop system with rapid rise and ample overshoots. On the other hand, the experienced subject response is almost critically damped, combined with a very short time-to-target, indicating good skill acquisition. The closed-loop nature of the system is also emphasized by the motion-plateau-motion pattern of the final part of the response, demonstrating how incremental error corrections are made using visual feedback.

Moray and Looststeen [30] also showed and confirmed in their reasearch that an operator learning a new skill will, after some time, switch from a damped second order system to a predictive and apparently "open-loop" behavior. We did not observe this phenomenon at this stage

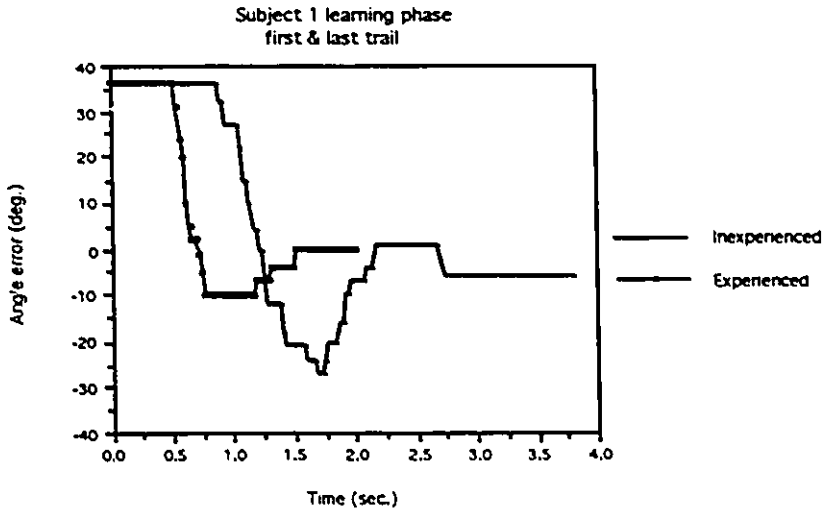

Figure 5.7: Subject 1 Target 9 step response.

(after three testing sessions) as a generalized case among our subjects. Their step responses generaly contained some error corrections, implying closed-loop behaviour. But if the learning phase is extended beyond this stage it is true that apparent signs of predictive control do punctualy emmerge. The operator does behave as if he knows exatly where his terminal device is in space without seeing it; and goes to the target in an unrestrained or open-loop type manner.

The subject response time also goes through a noticable change. As can be seen in figures 5.6 and 5.7, the inexperienced subject takes about one second to react and initiate the motion toward the target. Initially, he is not familiar with the system and he is not confident. Some hesitation is therefore present. The reaction time is reduced by 50% for the experienced subject.

Linkage 1: Operational phase

The second part of this experiment is composed of the operational phase where the subject is asked to perform the same motion using the same linkage as above, but without visual feedback. Spatial positioning of the terminal device is to rely solely on extended physiological proprioception. The same Targets 2 and 9 are considered. In this case, the time-to-target is not critical anymore, but the positioning error is the important parameter. Figures 5.8 and 5.9 show the results for three testing sessions for Target 2 and 9 respectively, and tables 5.3 and 5.4 provide the mean, standard deviation and t test results for these various populations.

Analysis of the data of Target 2 shows that the subjects are operating the linkage very well after three testing sessions. The three subjects exhibit an impressive average scoring rate of 60%, 67% and 73% on-target with no visual feedback. These results are consistent with the results found by Gibbons et al [20] and Philippe-Auguste [37][38] that an e.p.p. controlled artificial arm will provide adequate subconscious control to the user.

The data provided in table 5.3 and table 5.4 allow us to determine when further testing is needed because of major differences between two populations or, on the contrary, when populations can be merged together to form a larger and more accurate representation of the subject performance. Analysis of Target 9 (see figure 5.9 and table 5.4) shows a different subject behavior. Let us look at the case of Subject 1; the first curve, showing the results of his First Test. It displays major swings about the zero axis, meaning that the operator has not yet associated the position of the input with the corresponding target position. The subject is either not far enough or too far to reach the target. During the second day of testing (Second Test) this situation rapidly turns around and after the third trial the subject is systematically on target or very close to it. The third test (Third Test curve) provides evidence that the skill is well acquired. Statistical analysis suggests that from Test1 to Test2 and from Test2 to Test3 the populations are different and there is a major chronological[4] improvement with testing.

[4]We will be using the terminology chronological improvement with testing to emphasize an improvement from one testing day to the next. Punctual improvement from trial to trial will be simply refered to as an

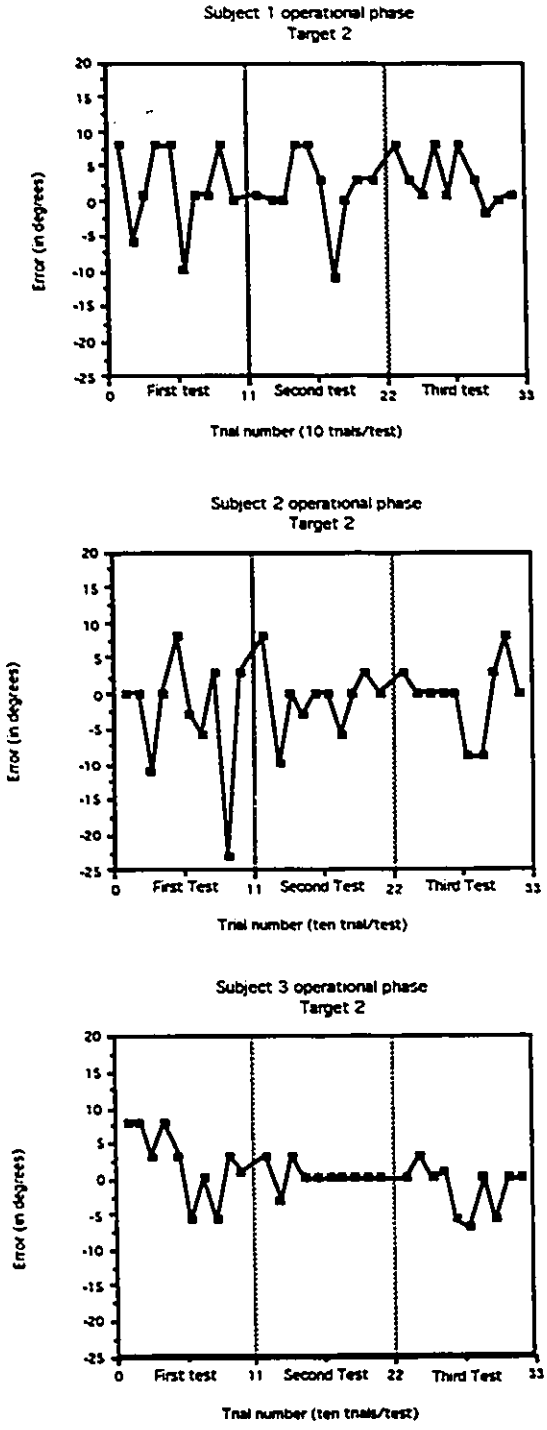

Figure 5.8: Error-to-target vs Trial number for Target 2 for three typical subjects.

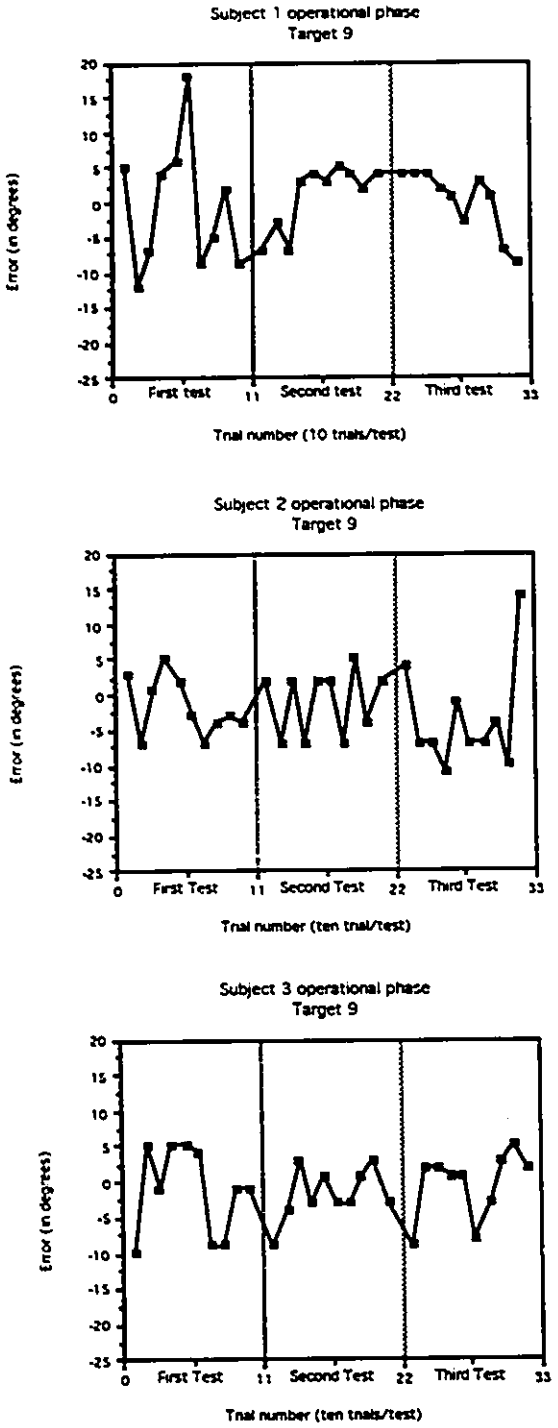

Figure 5.9: Error-to-target vs Trial number for Target 9 for three typical subjects.

	Subject 1		Subject 2		Subject 3	
Target2	Mean	STD	Mean	STD	Mean	STD
Test1	5.1	3.872	5.7	7.087	4.6	3.0
Test2	3.7	3.945	3.0	3.771	0.9	1.44
Test3	3.5	3.24	3.2	3.967	2.3	2.94
Merged	All	All	All	All	2-3	2-3
referen.	4.1	3.6	3.97	5.14	1.6	2.37

Results of the t test

Test1-2	t=0.80	Not Sig	t=1.06	Not Sig	t=3.52	Sig.
Test1-3	t=1.00	Not Sig	t=0.97	Not Sig	t=1.73	Not Sig
Test2-3	t=0.12	Not Sig	t=0.11	Not Sig	t=1.34	Not Sig

Table 5.3: Mean, standard deviation and t test of Target 2 for subjects using Linkage 1 without visual feedback

	Subject 1		Subject 2		Subject 3	
Target9	Mean	STD	Mean	STD	Mean	STD
Test1	7.7	4.62	3.9	1.969	5.0	3.43
Test2	4.2	1.69	4.0	2.31	3.3	2.21
Test3	3.8	2.53	7.2	3.76	3.6	2.84
Merged	2-3	2-3	No	No	2-3	2-3
referen.	4.0	2.10	7.2	3.76	3.45	2.48

Results of the t test

Test1-2	t=2.25	Sig.	t=0.10	Not Sig	t=0.33	Sig.
Test1-3	t=2.34	Sig.	t=2.45	Sig.	t=0.99	Not Sig
Test2-3	t=0.42	Not Sig	t=2.29	Sig.	t=0.95	Not Sig

Table 5.4: Mean, standard deviation and t test of Target 9 for subjects using Linkage 1 without visual feedback

After the last test, the mean error saturates to a level of 3.8^0 and that is within the on-target range. The on-target scoring rate is about the same as for Target 2, however Target 9 was in general a little bit more difficult to attain. The scoring rate for Subject 1 is 33% (or 57% when counting the "close miss" right on the border line). From his cumulative curve given in figure 5.3 we can see, however, how close he gets to a succes rate of 100%.

Subject 3 also constantly improved with time and chronological testing sessions. His error to target went steadily down. He was the one that adapted best to this target. Progress is evident from the time trend but from the t test, the null hypothesis could not be rejected. Thus, merging can take place. This subject displayed an overall scoring rate of 67% (including very close misses) which is impressive.

Subject 2 had problems adjusting to this target and verbally admitted that he was not at ease with it. His initial results during the First Test are better than the following ones (this inconsistency in operating the system will be further analyzed when we look at the concept of the "mental model"). His on-target score is still very good with an average of 53% including close misses.

The error versus time response or step response for the Subject 1 is shown in figures 5.10 and 5.11. This case really corresponds to a worst case situation: visual feedback is absent and the subject has to rely solely on subconscious control. Based on observations done during the course of this research, it was found that error correction could not be made when subconscious control is performed. This means that the subject would have to have a mental image of where his shoulder had to be to get to the target. If this mental image was wrong, there was no way for him to be aware of it and to make the appropriate corrections during the trial.

Consider that when a person is working and gets a call, he does not have to look at the phone on his desk to know where it is in space, he can continue focusing on what he is doing

improvement with time.

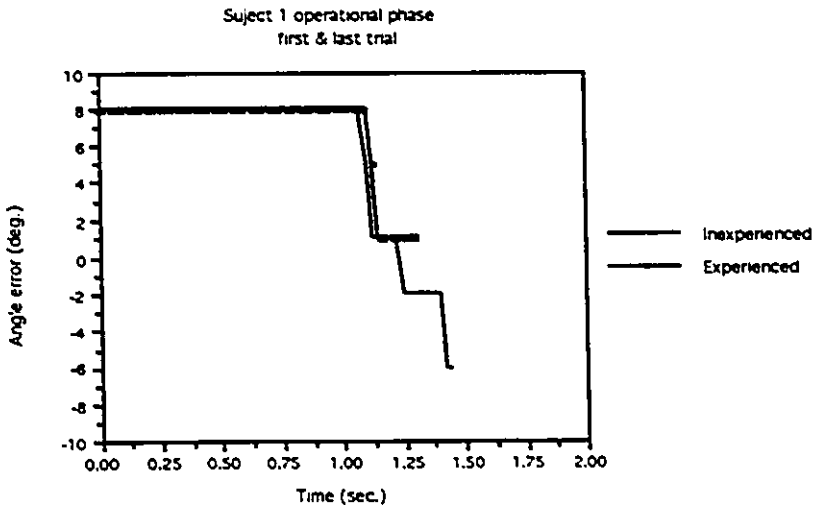

Figure 5.10: Subject1 Target 2 step response without visual feedback.

while reaching for it. If it happens that he misses the handset, the feedback that he is going to get from hitting any surrounding objects (the desk, the phone directory or his cup of coffee) will give him spatial cues to help him get to the phone.

Thus, some form of feedback, visual or not, is needed in this situation even in the presence of the ideal artificial arm i.e. the natural one, our point here being that our artificial arm (rather its simulation) cannot be expected to perform better than the natural arm. In view of these observations, we can very well predict that the step response in this context will be of the open-loop type where the operator goes to the position he thinks is right, and stays there. This is exactly the sort of response that we see in figures 5.10 and 5.11. It is true, however, that with practice the subject can learn to be more and more accurate. These figures show the first trial on that target, when the subject is inexperienced, and the last one when he is experienced. There are 54 other trials in-between involving this target and five other targets.

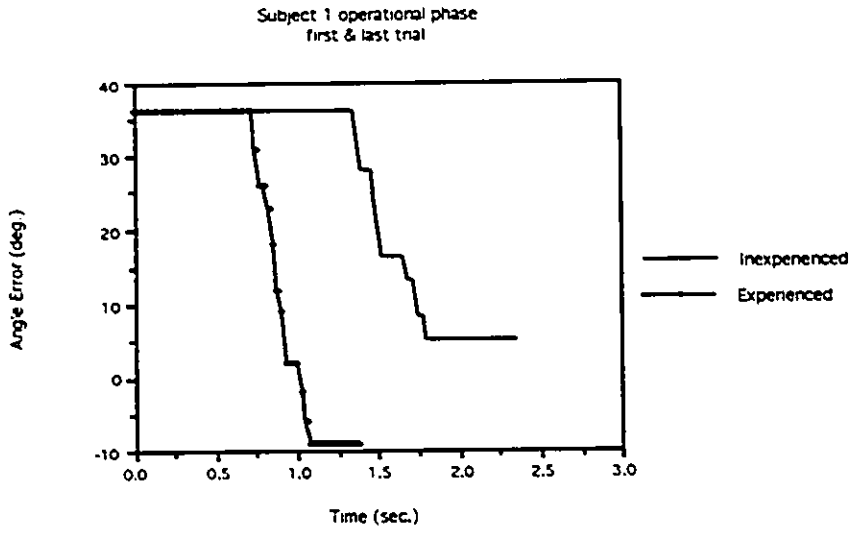

Figure 5.11: Subject1 Target 9 step response without visual feedback.

Conlusion on The First Results

The results obtained with this first linkage are indeed very encouraging. For a casual observer, a success rate between 50 to 73% of reaching a target might not be impressive; It should be restated that the conditions of the experiment were such that:

1. The subject had to reach a target using his artificial hand (also called the terminal device) without visual feedback.

2. The subject could not see his arm or hand; the only thing he could see was the target. Thus, he had to rely solely on physiological feedback (i.e what he could feel from the controlling joint) to reach the target. In order to picture the difficulty of the task, we can ask ourselves how often do we reach for an object without looking at it and manage to place our hand at once, without groping over the object, to pick it up.

The results presented in the cumulative score curves of figure 5.3 definitly show that subjects are always on-target or in a vicinity 2 target units from the target more than 90% of the

time.

To put the results that we have obtained here in proper perspective, it might be interesting to look at another control strategy which we have discussed at the beginning of this paper: electromyographic (EMG) control. We will refer to a paper published by Philipson and Sörbye [39]. These researchers were, like us, trying to see the extent to which different artificial arm motions could be controlled. To be more precise: how many different motions could be performed, and with what accuracy. Notice that although their work is similar to ours, it is at another level. The work done by these researchers is still at the level where they are trying to quantize the percentage of success of whether or not the desired motion was the one executed by the artificial arm. Hence, when they talk about X% of success this means that in (100-X)% of the cases the prosthesis is not performing the desired motion. With our control strategy, this problem does not exist. 100% of the time, the artificial arm performs the desired motion. The variable being here the accuracy with which it is performed.

Without getting into the details of the work done by Philipson and Sörbye we can just say that they were using a dual-site 9-state EMG system to control the motion of the artificial arm. Two antagonist muscles (biceps and triceps) where used. The level of contraction of these two muscles would determine which of the 8 different motions would be executed as shown in figure 5.12. Note that the muscle at rest is considered as one state. Philipson and Sörbye call each of these states a target and through a set of tests determined with what percentage of success these targets can be reached. The average success rate in their group of test subjects in trying to execute 8 different motions is 53.3% whereas ours is always 100%.

Our research work is definitely one step ahead of this group. To illustrate this, we could categorize on a pyramid form (see figure 5.13) the various aspects that can be studied in the initiation and performance of a motion. We would be, at this stage, on the fourth to fifth major levels of the pyramid starting from the base.

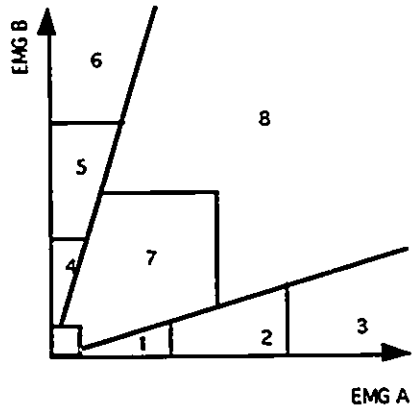

Figure 5.12: Each one of these 8 regions represents a motion (taken from [39]).

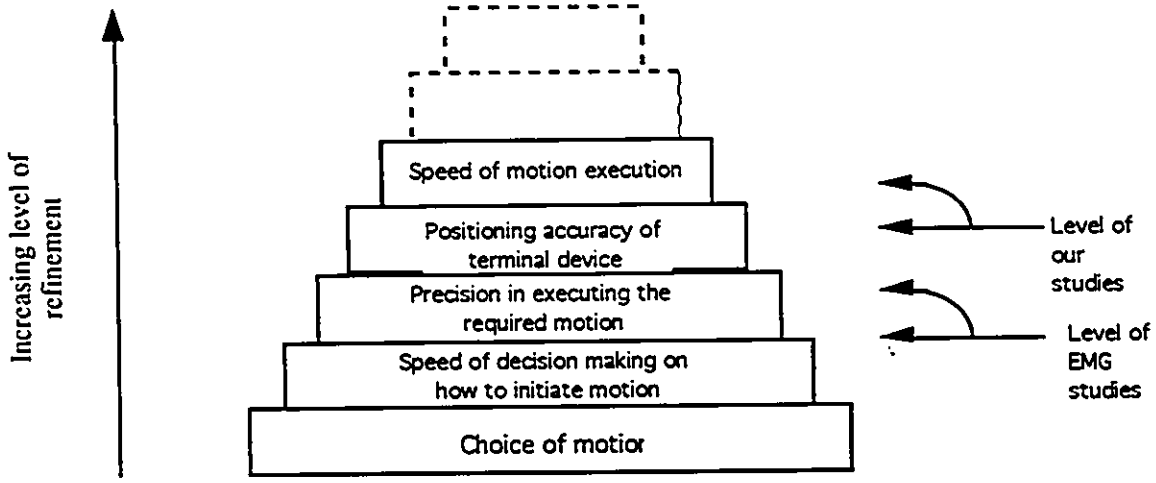

Figure 5.13: The various levels encountered in the initiation and performance of a motion.

With the system as it is now, we have established that our 3-D Virtual Reality simulation is an efficient artificial arm emulater. We have shown that a normal subject controlling an e.p.p. artificial arm can position the terminal device accurately using only subconscious control.

5.3.3 Results for Linkage 2

Summary

The operation of Linkage 1 required only the motion of the e.p.p. joint (the shoulder). Thus the level of difficulty was uniquely associated with controlling one part of the system or one subsystem. In a desire to investigate the response of subjects to controlling more than one subsystem during the course of one test session, a second linkage was designed that required both the motion of the shoulder (the e.p.p. joint) and the chair. The motion emulated was the traditional reach to a target task. The subject had to position the center of his palm in the center of the target as shown in figure 5.14. One could argue about the benefits of having subjects control other subsystems besides the e.p.p. joint, but we felt that it was necessary to simulate a realistic situation as much as possible. When positioning his hand in space, a person needs to access a volume as large as possible. Besides moving his shoulder and elbow, he might have to rotate the chair he is sitting in or walk closer or to the left or to the right of the object he is aiming at. All of these extra motions are not directly related to the shoulder and arm motions, but are still essential in providing the necessary fine adjustments. They can be simulated by having the subjects operate these subsystems. Thus, the subsystems will be the inputs required to get the terminal device to the desired point. We recall that these are: shoulder flexion/extension, trunk bending and chair rotation.

As could be expected, the operation of this linkage was a little more involved than the previous one. All subjects managed to adapt to and learn Linkage 2 within the three test sessions. The analysis is based on two targets: Target 15 and Target 17. In the early stage of the learning phase, the time-to-target varies greatly from trial to trial. This reflects in the standard deviation that is fairly high (1.64 seconds, overall average). Also, the coordinated

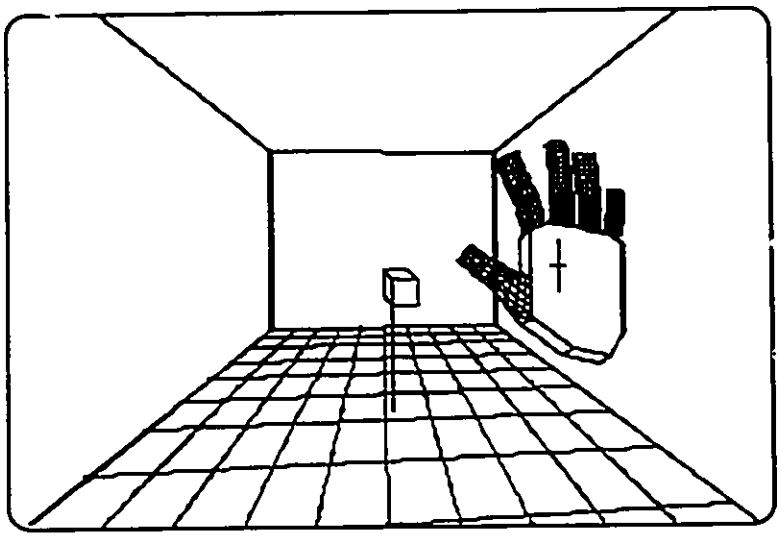

Figure 5.14: Typical reach to a target type of task (figure 1 repeated here for clarity).

operation of the shoulder and chair is not optimal, subjects prefer to move one subsystem at the time. Many corrections are necessary to get to the target, which suggest a closed-loop underdamped type of control. This induces an overall[5] average time to target of 3.52 seconds. As familiarization with the linkage improves, a more optimal (simulataneous) utilization of the subsystems takes place, giving rise to a much steadier (standard deviation is reduced by 50%) and shorter time-to-target (2.6 seconds). The performance of experienced subjects also shows a minimum number of corrections to get to the target, indicating a migration from closed-loop to open loop control.

General observations made for the operational phase for Linkage 2 are very similar to those made for Linkage 1. As can be seen in figure 5.15 all subjects managed to place their hand 97.5% of the time in a vicinity of one target-unit from the target (for both Target 15 and 17). Thus when subjects are not exactly on-target, they are usually very close to it. On-target scoring rates averages 46% for Target 15 and 64% for Target 17 for all subjects. This results,

[5]For all seven subjects.

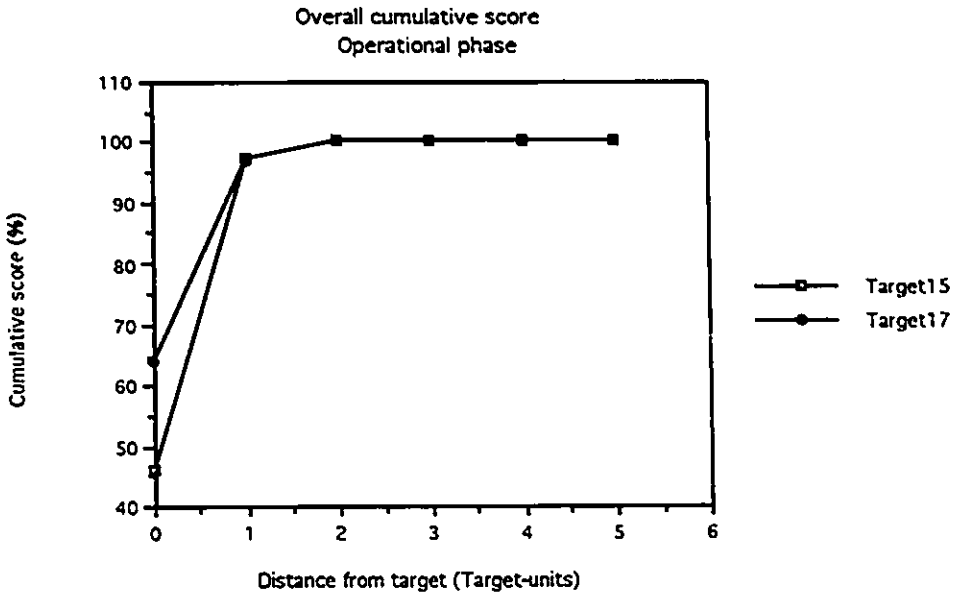

Figure 5.15: Cumulative success rate for Target 15 and 17 for all subjects using Linkage 2.

once again, demonstrates the strength of e.p.p. Without any visual cue one can still, via the e.p.p. joint, know where the artificial arm is in space with very good precision. Thus one can trustfully rely on subconscious control to execute some routine movements, just like one does with the natural arm. Once the terminal device is in close vicinity to the object, conscious control using visual feedback can be used to fine position the terminal device and perform the desired action. The importance of subconscious control can again be stressed. If an amputee is to use his artificial arm, most of his attention should be devoted to the task he is performing. He should not have the burden of constantly visually monitoring the position of his artificial arm in space in order to know where it is.

5.3.4 In-Depth Study of the Results of Linkage 2

The Learning Phase

The results of tests for the learning phase (with visual feedback) are given below in figure 5.16 for Target 15 and in figure 5.17 for Target 17. These are the two chosen targets (among six different ones) for this linkage. Again as for Linkage 1, different subjects develop different feels for the system and this induces variations in the learning patterns. For consistency, we had to use the same scale for each subject under test. Because of this, it might not be possible to see some of the details. We have included for the three subjects for Target 15, more accurate time versus trial number curves in Appendix B. Looking once again at Subject 1, we notice that most of the learning is done during the First and Second Test for Target 15 and 17. The t test reveals that the population of Test1 is significantly different from that of Test2 and Test3 (see tables 5.5 and 5.6). Also for Target 15, Test2 and Test3 are from different populations but the average error on Test3 is greater than Test2, indicating no significant improvement in the learning. In the case of Test2 and Test3, for Target 17, our null hypothesis cannot be rejected, hence the two populations can be considered the same. We can conclude that there is a learning plateau after Test2.

On the contrary, Subject 2 did most of his learning for Target 15 during his Third Test.

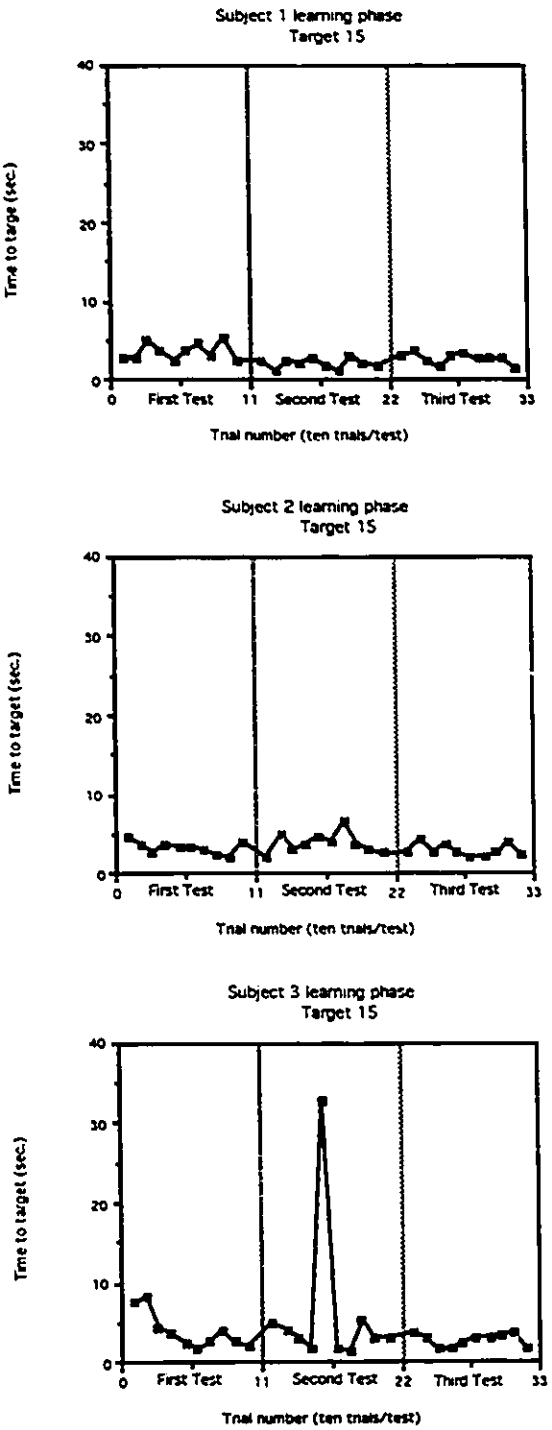

Figure 5.16: Time-to-target vs Trial number for Target 15 for three typical subjects.

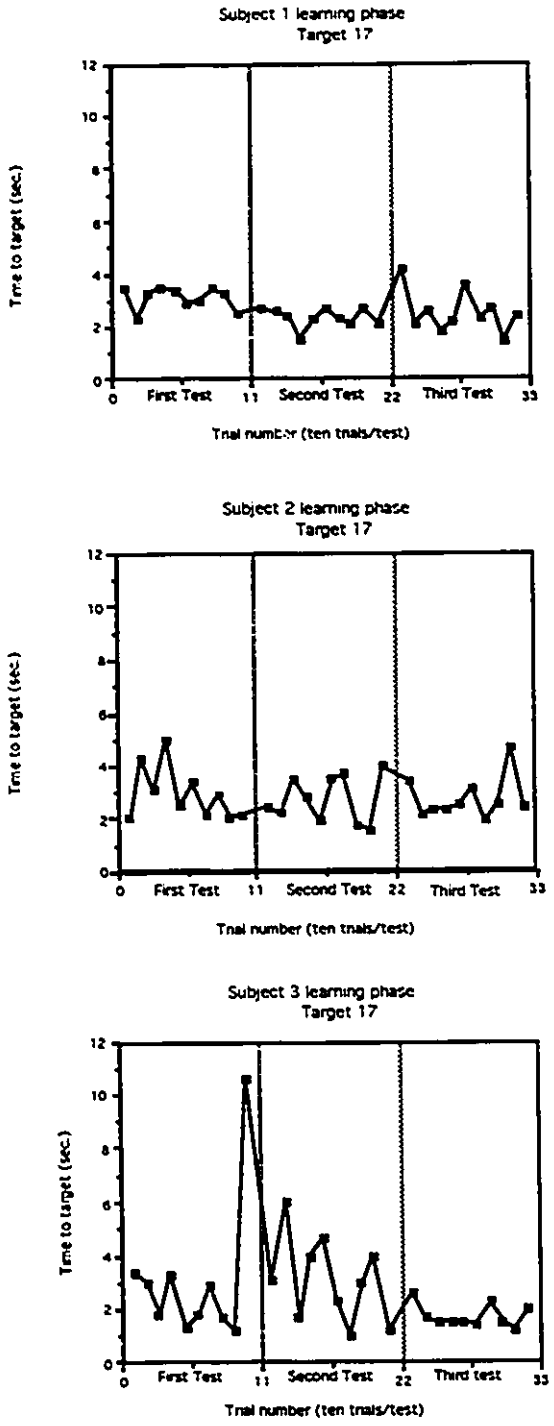

Figure 5.17: Time-to-target vs Trial number for Target 17 for three typical subjects.

	Subject 1		Subject 2		Subject 3	
Target15	Mean	STD	Mean	STD	Mean	STD
Test1	3.54	1.080	3.28	0.779	3.90	2.249
Test2	2.05	0.629	3.86	1.310	6.04	9.427
Test3	2.61	0.698	2.86	0.843	2.69	0.83
Merged	None	None	None	None	All	All

Results of the t-test

Test1-2	t=3.75	Sig.	t=1.18	Not Sig	t=0.70	Not Sig
Test1-3	t=2.28	Sig.	t=1.16	Not Sig	t=1.58	Not Sig
Test2-3	t=1.87	Sig.	t=2.02	Sig.	t=1.12	Not Sig

Table 5.5: Mean, standard deviation and t test of Target 15 for subjects using Linkage 2 with visual feedback.

	Subject 1		Subject 2		Subject 3	
Target17	Mean	STD	Mean	STD	Mean	STD
Test1	3.07	0.423	2.92	1.019	3.08	2.75
Test2	2.30	0.362	2.68	0.888	3.07	1.60
Test3	2.49	0.818	2.71	0.796	1.69	0.43
Merged	2-3	2-3	All	All	1-2	1-2

Results of the t-test

Test1-2	t= 4.38	Sig.	t=0.55	Not Sig	t=0.00	Not Sig
Test1-3	t= 1.99	Sig.	t=0.50	Not Sig	t=1.58	Not Sig
Test2-3	t= 0.68	Not Sig	t=0.07	Not Sig	t=2.64	Sig.

Table 5.6: Mean, standard deviation and t test of Target 17 for subjects using Linkage 2 with visual feedback.

In his First Test and Second Test, his average time was high and individual time samples were very different, indicating an adaptation phenomenon. In his last test, his testing time steadily went down together with the standard deviation marking a more constant and stable time to target. For Target 17, mean time to target is observed to decrease steadily from First Test to Third Test. The decrease is not significant enough to generate different populations. Thus, we can say that after Test1 the subject has completed learning.

Subject 3 is, in this case, the slowest. He has, for both targets, the slowest time-to-target. Nonetheless, he manages to reach his learning plateau during the First Test, for Target 15, and no significant learning takes place after that. For Target 17, a classical learning curve is observed between Test2 and Test3 and saturation is marked at the end of Test3.

A typical phenomenon that takes place in the early phase of the learning process is that just one subsystem (either the shoulder or the chair) is moved at the time. Our observations and analysis of the data lead us to acknowledge the following scenario: The inexperienced subject normally moves the chair first until facing the target. He then reach out to it with his virtual arm. He moves in discrete steps and generally overshoots when reaching the desired point in space as shown in figure 5.18. These curves were taken from the third trial of the First Test. As he becomes more and more accustomed to system operation, he moves with great confidence the two susbsystems at the same time and with a mimimun number of corrections reaches the required point as given in figure 5.19. These figures were taken from the third trial of the Third Test. The subject at that point is experienced.

In figure 5.18, it seems as if there is a change in both subsystems at the same time, this is simply due to the fact that chair rotation inherently induces a change in the distance from the terminal device to the target.

Figure 5.18 shows a considerable amount of closed-loop activities, whereas in figure 5.19 the tendency toward simplified open-loop control is obvious. Identical observations are made

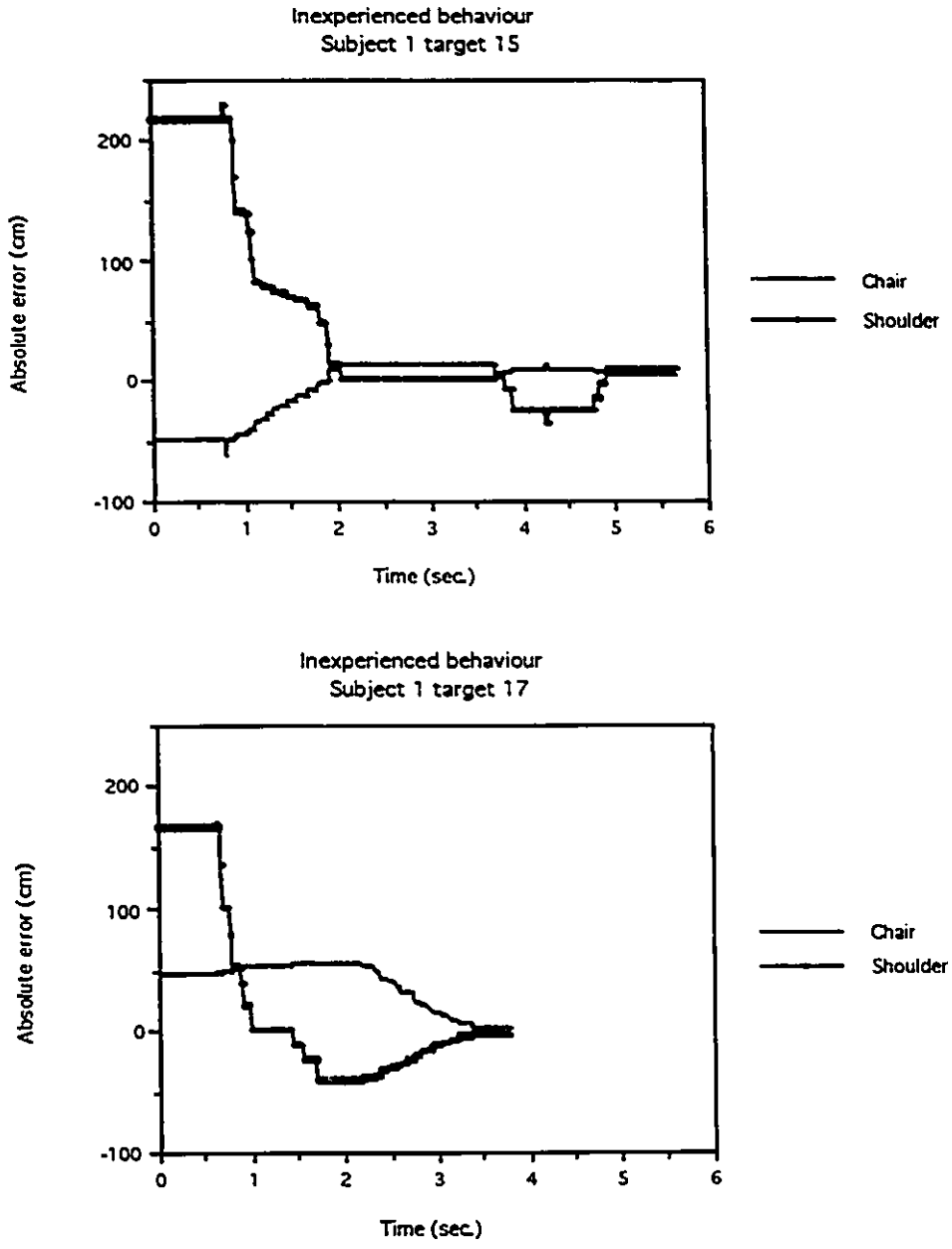

Figure 5.18: Inexperienced subject operating the two subsystems one after the other.

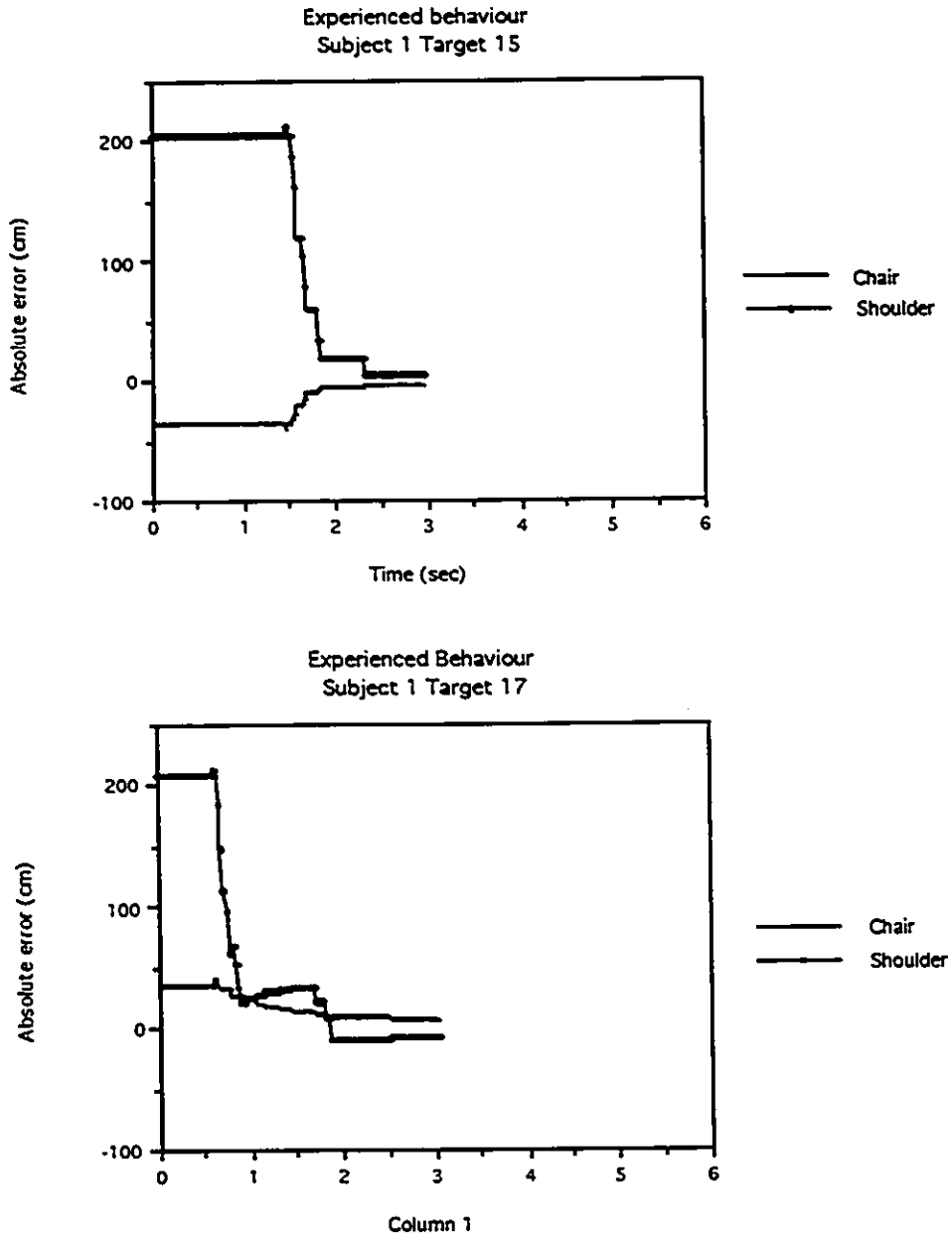

Figure 5.19: Experienced subject operating the two subsystems at the same time.

	Subject 1		Subject 2		Subject 3	
Target15	Mean	STD	Mean	STD	Mean	STD
Test1	29.42	19.97	16.17	8.917	34.49	18.34
Test2	25.07	9.122	27.5	17.03	32.57	24.88
Test3	19.96	9.439	24.36	5.875	22.45	13.6
Merged	All	All	2-3	2-3	All	All
Referen.	24.82	13.88	25.93	12.50	29.84	19.56

Results of the t-test

Test1-2	t= 0.63	Not Sig	t=1.86	Not Sig	t=0.20	Not Sig
Test1-3	t= 1.35	Not Sig	t=2.42	Sig.	t=1.67	Not Sig
Test2-3	t= 1.23	Not Sig	t=0.55	Not Sig	t=1.13	Not Sig

Table 5.7: Mean, standard deviation and t test of Target 15 for subjects using Linkage 2 with no visual feedback.

for different targets and different subjects. These observations confirm those of Moray et al. [30] and provide a validation for using this Virtual Reality simulation as a test bed for acquisition and retention of process control skills.

Linkage 2: Operational phase

We now look at various results obtained using Linkage 2 without visual feedback. A thorough analysis of the curves here will not be really necessary as the behavior observed for the first linkage is also valid in this case. The point here is to identify reference populations for later checks of skill retention after learning the next linkage (Linkage 3). We can however comment on these results by saying that all subjects did very well during the learning phase, such that as they went on into the operational phase, little learning, if any, was noticed. Any learning that did occur was not significant to the point of forming different populations as can be seen from the cuves of figures 5.20 and 5.21 and from tables 5.7 and 5.8.

Thus for Target 15, Subjects 1 and 3 can have their three tests merged into single indi-

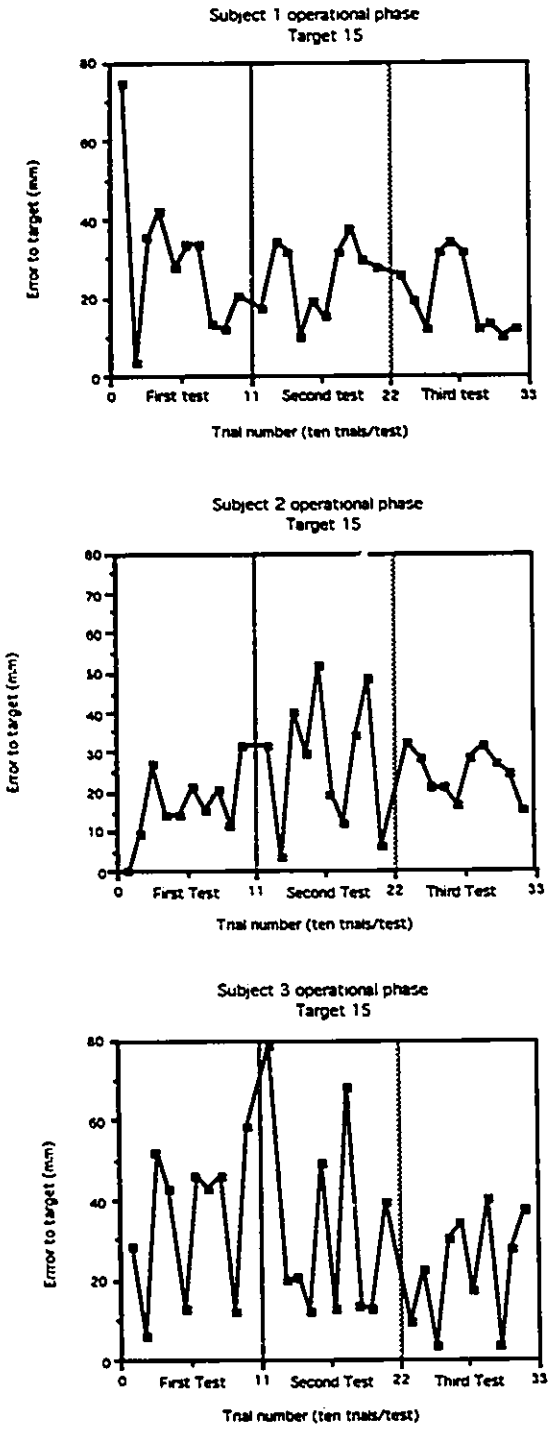

Figure 5.20: Error-to-target vs Trial number for Target 15 for three typical subjects.

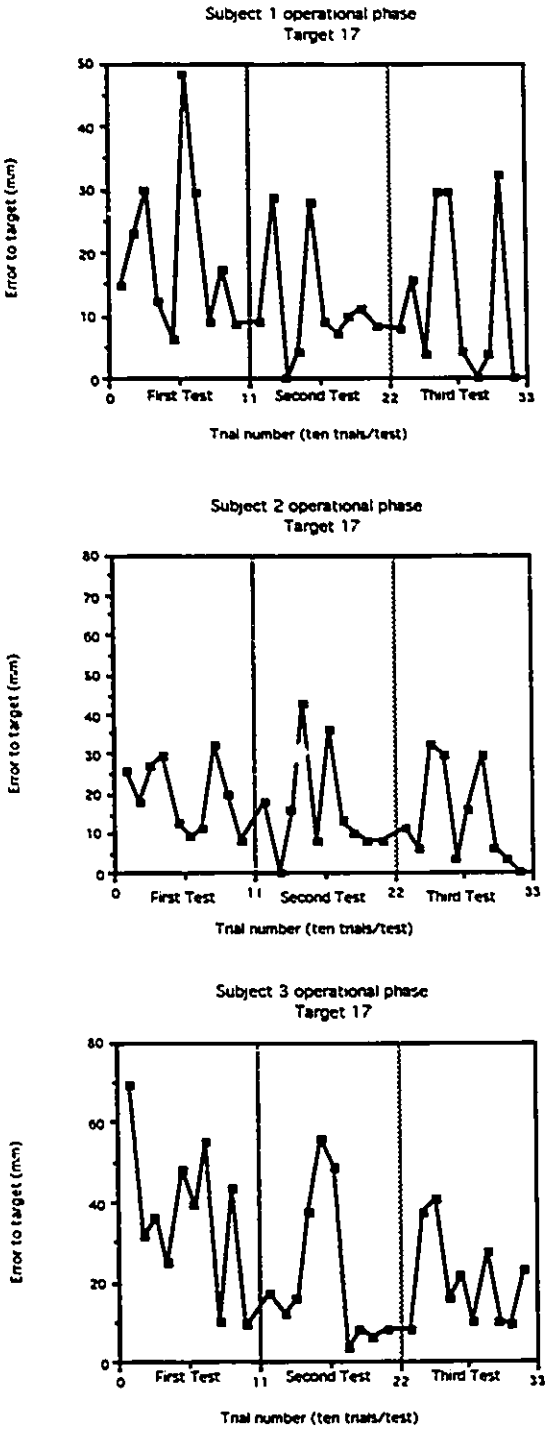

Figure 5.21: Error-to-target vs Trial number for Target 17 for three typical subjects.

	Subject 1		Subject 2		Subject 3	
Target17	Mean	STD	Mean	STD	Mean	STD
Test1	19.82	12.982	19.22	8.89	36.55	18.9
Test2	11.49	9.32	15.80	13.41	21.16	18.91
Test3	12.63	13.09	13.77	12.31	20.28	11.84
Merged	All	All	All	All	2-3	2-3
Referen.	14.65	12.10	16.26	11.49	20.72	15.36

Results of the t-test

Test1-2	t=1.65	Not Sig	t=0.67	Not Sig	t=1.82	Sig.
Test1-3	t=1.23	Not Sig	t=1.13	Not Sig	t=2.31	Sig.
Test2-3	t=0.22	Not Sig	t=0.35	Not Sig	t=0.12	Not Sig

Table 5.8: Mean, standard deviation and t test of Target 17 for subjects using Linkage 2 with no visual feedback.

vidual populations and the Second Test and Third Test of Subject 2 can be merged. On-target scoring rates averaged 46% for all subjects and all have a mean error within "one target unit" of the target. In the case of Target 17, Subjects 1 and 2 can have all their three tests merged whereas we can only merge Tests 2 and 3 of Subject 3. Subjects adapted better to Target 17 than to Target 15. The average on-target rate was this time 64% (Subject 1 had 70%).

5.3.5 Results for Linkage 3

Summary

In the third stage of this experiment the subjects were required to learn a linkage involving the action of three subsystems. The motion of the shoulder, the chair rotation and the trunk bending are used in conjunction, to position the virtual hand in the simulated environent. The reasons for using three subsystems to position the 3-D virtual hand is as explained earlier. In this case, the complete volume situated in front of the subject is now reachable. The subject is again offered a target geometrically identical to the one found in Linkage 2, but the possible target locations are different and in greater number. Also the motion generated by the linkage

is totally different.

As expected, the increased complexity of this linkage, brought about a corresponding increase in the time-to-target. The study of the learning phase, reveals that Linkage 3 amplifies the different types of control behaviour each subject uses in controlling the artificial arm. The direct consequence of this is a time-to-target that is very different from subject to subject. Another observation is that all subjects benefitted greatly from having learned other linkages before learning this one. They immediately felt at ease and instinctively understood the kinematics of Linkage 3. Thus, no real classical learning trend could be observed from the time-to-target curves. But some adaptation to the linkage was still necessary as explained in the next subsection.

Since three subsystems had to be controlled, initially the inexperienced subjects tried to separately operate each of them independantly to get to the target. Once the kinematics of the linkage, the chair rotation and trunk foward bending were mastered, the experienced subjects started moving them at the same time with good coordination.

In the operational phase, the visual feedback avenue is removed, the operation of this third linkage is rather involved, three subsystems have to be subconciously operated. We thus had some concern about the results. It is suprising enough how extended physiological proprioception can be efficient in providing an internal feedback path from machine to man via the e.p.p. joint. We remind the reader that the target is a cube of approximate true physical dimension of 2.5 cm on the side.

With the minimum amount of training given to the subjects in the learning phase, it was generally difficult for most of them to be exactly on-target when performing the motion without visual feedback. Some skilled subjects manage to reach scores as high as 70% on-target but the group average is around 22.5% for Target 8 and 10% for Target 12. Suprisingly enough when we look at the score obtained for getting within two-target-distance from the target, as

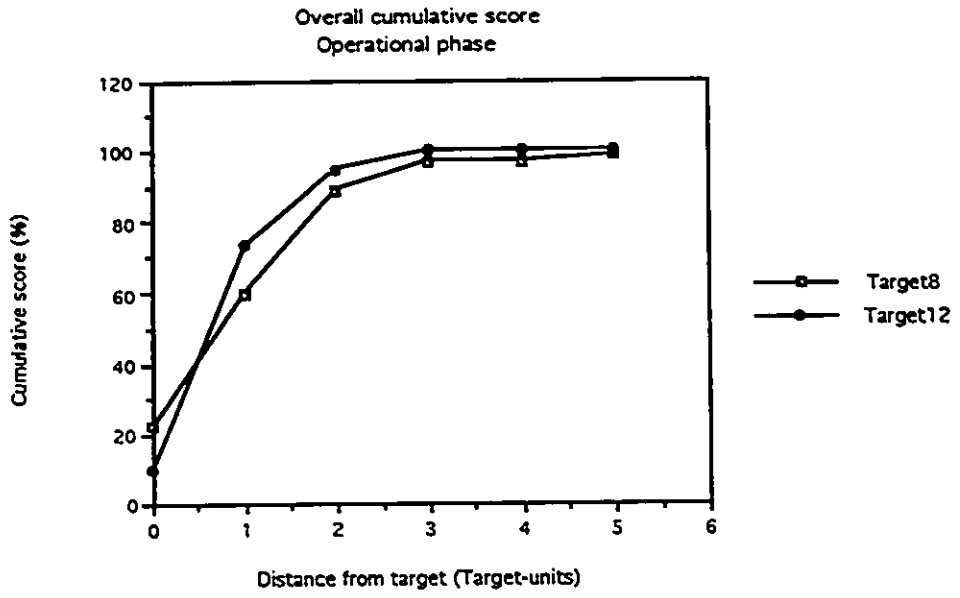

Figure 5.22: Cumulative success rate for Target 8 and 12 for all subjects using Linkage 3.

given in figure 5.22, we get an overall average above 95% for all subjects for both Targets 8 and 12. This result suggests that subjects were generally in a close vicinity of the target. They certainly had a good subconscious feel of where their hand was, and either more training or additional forms of feedback (e.g. tactile) would have allowed them to precisely reach it. (In the past, our rescach group conducted some tests to quantify how subjects using their intact arm could precisely position their hand in space on a target identical to the one used in the simulation. The results were published in [38] and they suggest that they could position their hand in a volume comprised within one-target-distance of the target in 78% of the cases. There is thus, a close similarity between these results and the one found with the simulation.)

It was also observed that, sometimes, a systematic and constant error in positioning the hand on the target was made. The error was usually within one target-distance of the target. This phenomenon also directly contributed to reducing the averaged on-target rate

discussed above. In a following section allocated to the in-depth study of the operational phase of Linkage 3 we will explain the nature of this constant error and also suggest a modification in the testing protocol of the operational phase in order to avoid it.

5.3.6 In-Depth Study of the Results of Linkage 3

The Learning Phase

On the average, it took Subject 1 3.5 seconds to get to the targets with Linkage 1 (just one subsystem) whereas it took him 5.3 seconds to get to the targets of Linkage 3. Subject 1 was the one that had the fastest time-to-target. Subject 1 and Subject 3 would always move rapidly and confidently to the target in a constant search to improve their performance trial after trial. Subject 2 had a more conservative approachs towards these tests as it reflects in his time-to-target in figures 5.23 and 5.24. He would move slowly and carefully, in a more overdamped manner, making sure that the target is reached precisely without overshoot. We believe that these behaviors are dictated by the character of each individual and are not in any way related to the type of tests under consideration. Similar observations were made by our research group in the past [38] when performing positioning tests with the physiological arm and a bench model. This is one of the reasons why we did not try to compare the populations between subjects.

For this linkage, the analysis is based on Target 8 and Target 9. Looking at figures 5.23 and 5.24 we can see how the time scale is different from Subject 1 to Subject 2. In four out of a total of six test sessions, subjects had no problem adapting to this linkage. In fact, it seems that the skills acquired in using the virtual arm when learning the first two linkages have reinforced the subject's confidence. Hence when now faced with learning this new linkage (Linkage 3) no learning trend (or very little) could be observed with chonological testing (although Linkage 1, 2 and 3 are kinematically very different). This is the case for the examples of Subject 1: Target 8 and Target 12; of Subject 2: Target 8; and also of Subject 3: Target 12. Subject 2 had problems in the case of Target 8 to use the depth cues provided to him. The direct effects

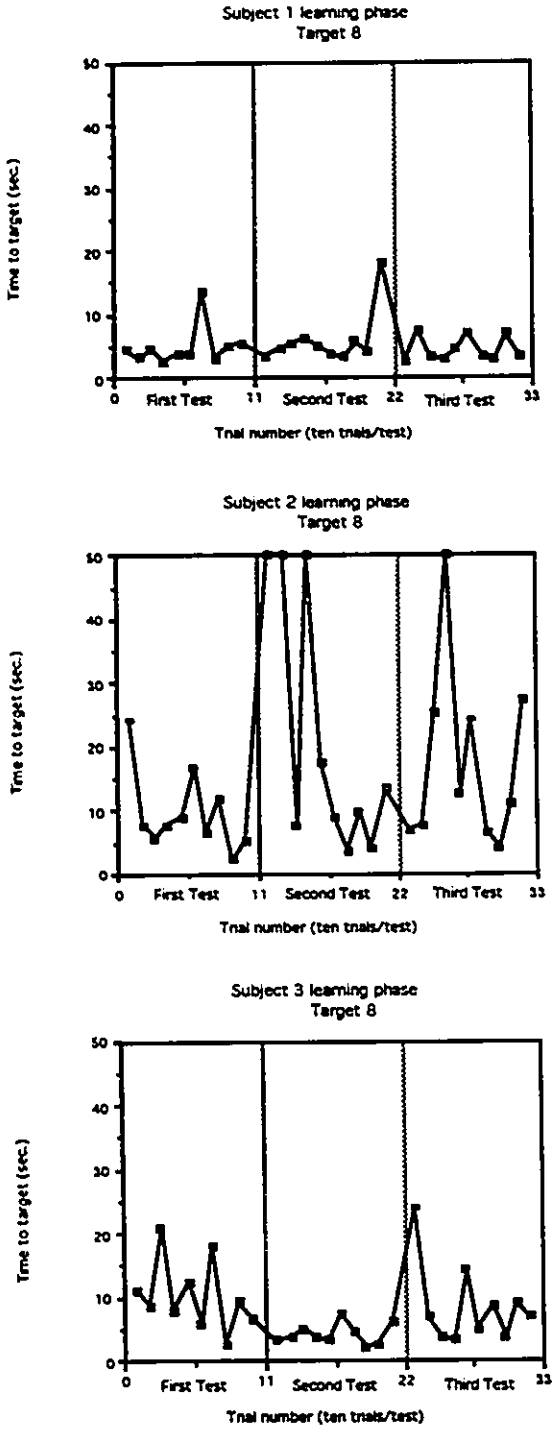

Figure 5.23: Time-to-target vs Trial number for Target 8 for three typical subjects.

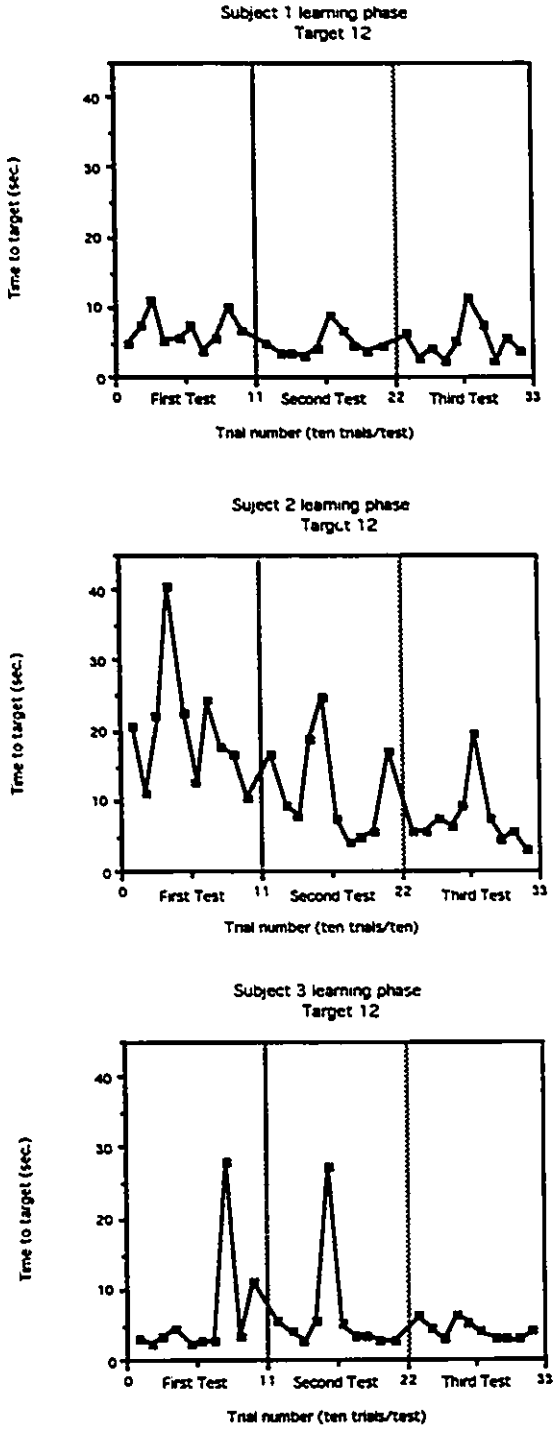

Figure 5.24: Time-to-target vs Trial number for Target 12 for three typical subjects.

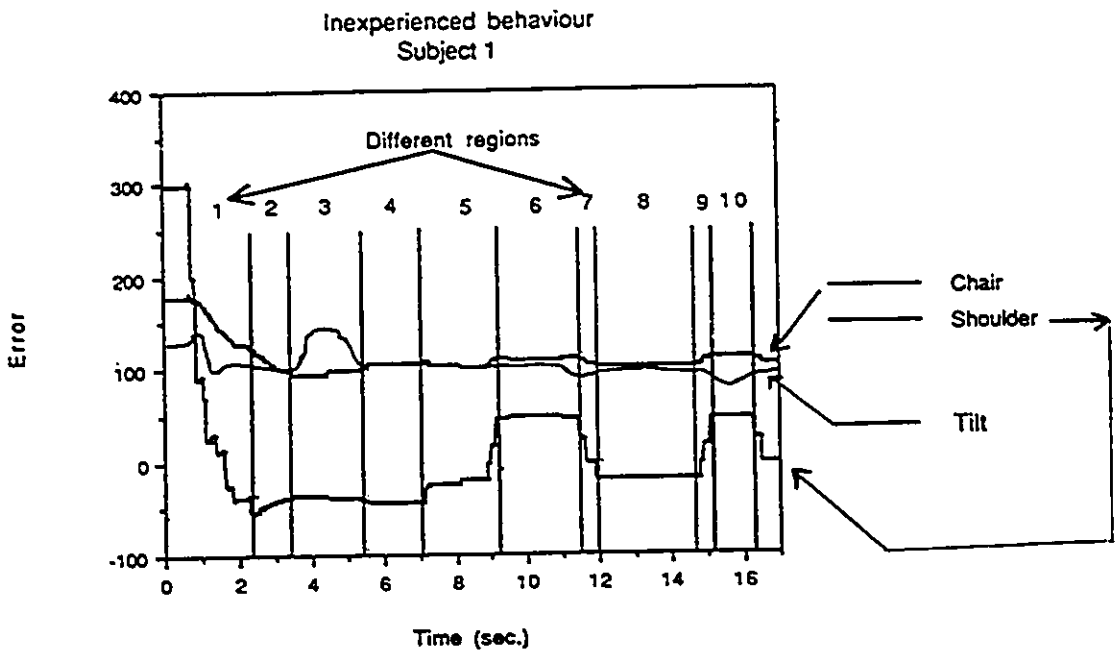

Figure 5.25: Inexperienced subject operating the three subsystems one after the other.

of this can be seen in his "time versus trial number" curve (figure 5.23) that contains three peaks indicating hunting. This is partly due to the fact that he uses prescription glasses and has slight depth perception problems in daily life. The learning and accurate operation of this linkage, however, required the use these depth cues. His average time to target is more than the others, but not unreasonably long considering the size of target, his overdamped control type behavior, and the number of subsystems to operate. Also, we used time as a relative measure of learning but we did not release this information to the subjects. They were only instructed to go as comfortably as precisely and as quickly as possible to the target, with no emphasis placed on any of the above underlined adjectives.

Even if no drastic learning trend was observed, some adaptation to this linkage was necessary. This is emphasised by looking at the time response of the first trial and the very last one. The same phenomenon observed for Linkage 2 is present here. The inexperienced Subject 1 moved one subsystem at a time as shown in figure 5.25. There was a typical pattern for this linkage, since all inexperienced subjects followed it. They first moved the chair to face the tar-

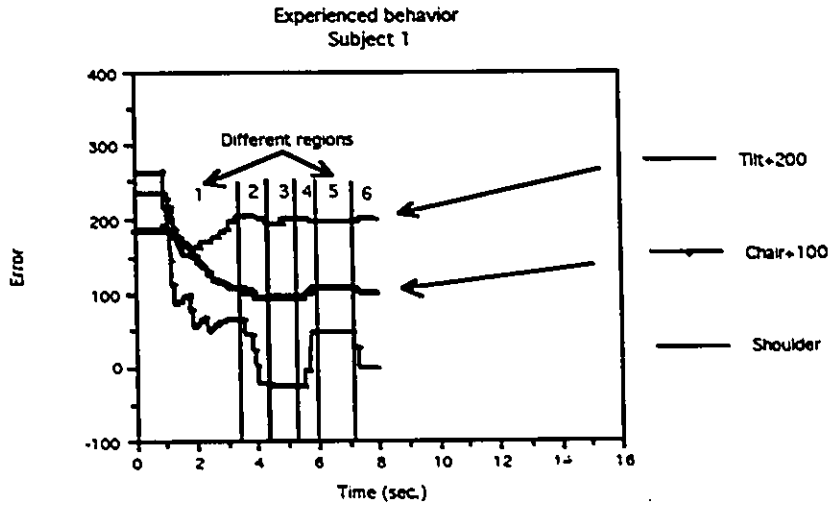

Figure 5.26: Experienced subject operating the three subsystems together (Tilt and chair errors were shifted up by 100 and 200 for better viewing).

get, then they moved their shoulder foward and finally bent their trunk to complete the motion. This is very similar to what takes place in performing a similar motion with a natural arm. Figure 5.25 has been split into different regions labelled 1 to 10 to best follow the sequential utilisation of the subsystems. In region 1, the chair is moved. Because chair error computation and shoulder error computation are cross coupled, some changes are also observed in shoulder error but the shoulder joint is steady. Some small variations on the trunk bending error are also noticed, these are simply due to parasitic motions of the trunk during chair rotation. In region 2 the shoulder is moved in an attempt to reach the target, but the vertical position of the terminal device is not correct. That is why in region 3 the trunk bending motion is used to correct for that mater. In region 4 the inexperienced subject realized that he is still not on target so he paused and in succeeding regions (5-10) he will search for the fine adjustements in each subsystem that will take him to the target.

The experienced subject not only reduced his trial time by 50%, but he now moves the 3

subsystems at the same time as shown in region 1 of figure 5.26. In region 2, the shoulder is moved again and in the appropriate direction but it has overshot. The subject realized that he overshot (in region 3) and moved his shoulder (region 4) in the opposite direction. He noticed that he overshot once again, so he corrected for that in 6. All these adjustments are done rapidly and most of the dead time is reaction time due to the fact that the subject got within a close vicinity of the target but not quite on it, so he had to react and move again.

Linkage 3: Operational phase

Again, for the analysis of this phase, the same two targets 8 and 9 were chosen. The results obtained for Target 8 are very good for Subject 1 and Subject 2, especially for the second and third sets of tests as shown in figure 5.27. Subject 1 is systematically on-target whereas Subject 2 is 100% of the time within two or less target units from the target. For Target 12, Subjects 1 and 2 are within one target unit from the target 92% of the time and all subjects are within two target units 94% of the time (see figure 5.28).

Subject 3 had poorer results than the others. This is in partly due to professional constraints preventing him from testing on consecutive days (only in the case of Linkage 3). Thus, some of his learning phase tests and some of his operational phase tests were spaced by a few days. This inconsistency is reflected in his results. However, we wanted to include this situation as part of the results in order to see how intermittent learning and testing had affected the general linkage learning process. In the learning phase discussed above, there was no noticable difference with other subjects, but the difference is obvious in the operational phase for both targets. Computing the mean and standard deviation for each population and applying the t test, using the usual null hypothesis[6], we can again identify the same populations, group them together to form larger and more representative sample sets for each target. Tables 5.9 and 5.10 provides us with the necessary summary for the operational phase of Linkage 3. For all subjects, no significant difference is found between the populations of the First Test and Second Test. However, the null hypothesis could be rejected when comparing the First Test

[6] "The population of Test(i+1) is not different from the population of Test(i)".

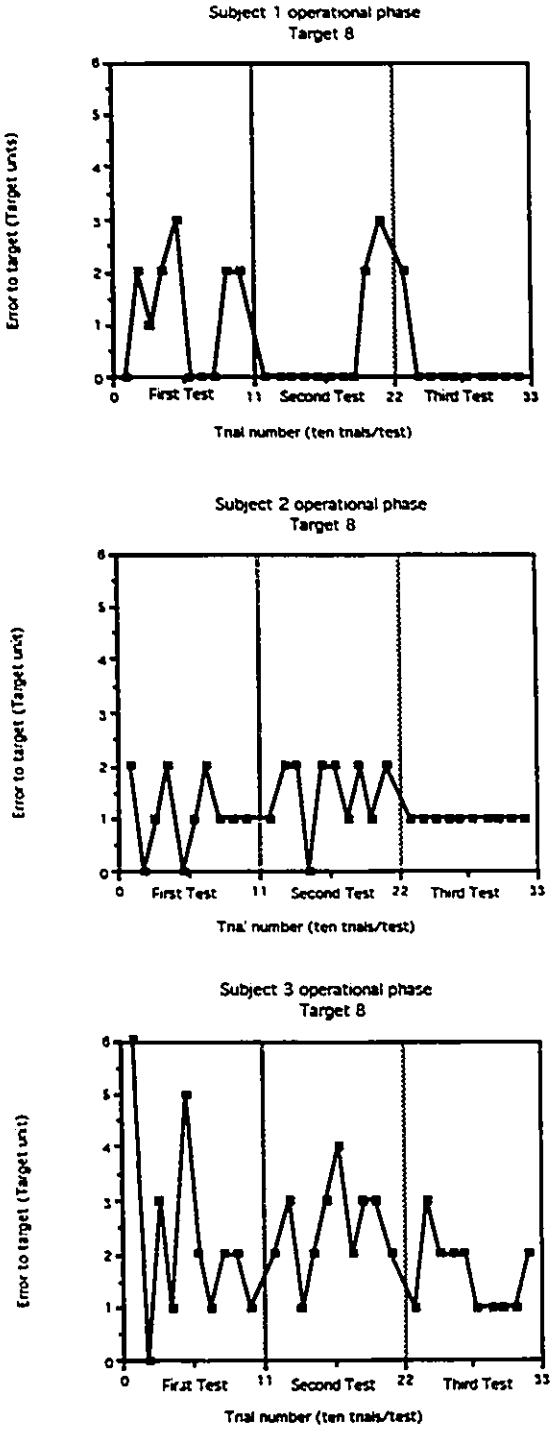

Figure 5.27: Error-to-target (in target units) vs Trial number for Target 8 for three typical subjects.

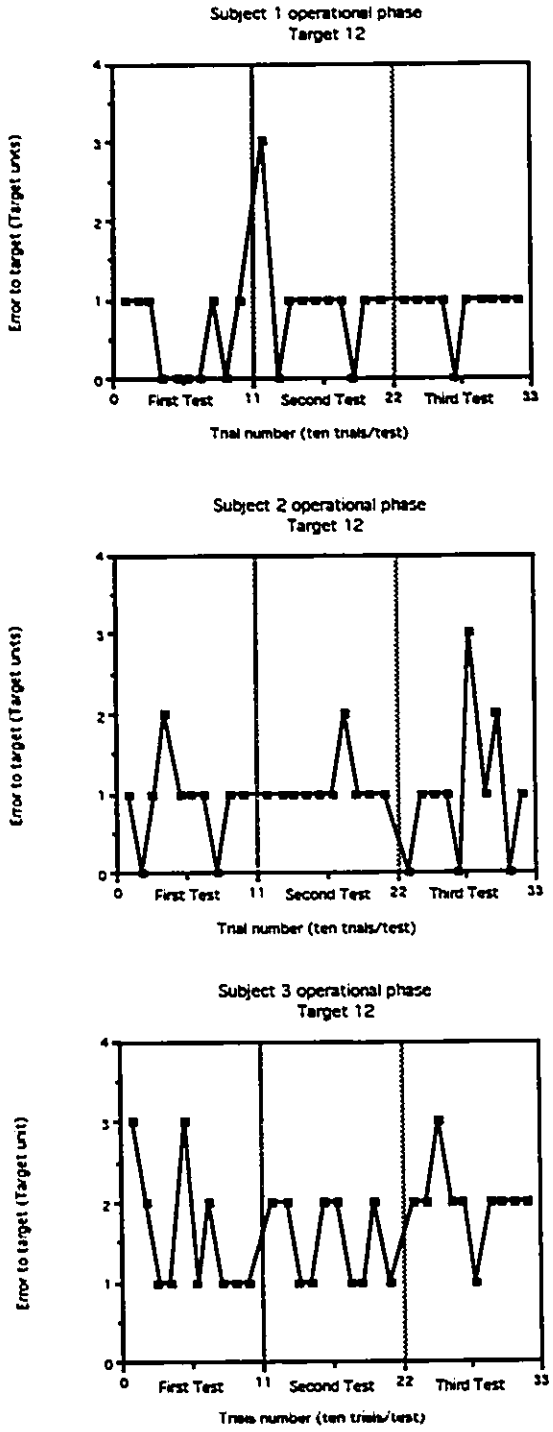

Figure 5.28: Error-to-target (in target units) vs Trial number for Target 12 for three typical subjects.

	Subject 1		Subject 2		Subject 3	
Target8	Mean	STD	Mean	STD	Mean	STD
Test1	1.2	1.135	1.1	0.738	2.3	1.889
Test2	0.5	1.08	1.5	0.707	2.5	0.849
Test3	0.2	0.632	1.0	0.0	1.6	0.70
Merged	2-3	2-3	None	None	None	None
referen.	0.35	0.875	1.0	0.0	1.6	0.70

Results of the t-test

Test1-2	t=1.42	Not Sig	t=1.24	Not Sig	t=0.30	Not Sig
Test1-3	t=2.42	Sig.	t=0.43	Not Sig	t=1.09	Not Sig
Test2-3	t=0.76	Not Sig	t=2.24	Sig.	t=2.59	Sig.

Table 5.9: Mean, standard deviation and t test of Target 8 for subjects using Linkage 3 with no visual feedback.

	Subject 1		Subject 2		Subject 3	
Target12	Mean	STD	Mean	STD	Mean	STD
Test1	0.5	0.527	0.9	0.568	1.6	0.843
Test2	1.0	0.816	1.1	0.317	1.5	0.527
Test3	0.9	0.316	1.0	0.943	2.0	0.471
Merged	2-3	2-3	All	All	None	None
referen.	0.45	0.65	1.0	0.643	2.0	0.471

Results of the t-test

Test1-2	t=1.63	Not Sig	t=0.97	Not Sig	t=0.32	Not Sig
Test1-3	t=2.06	Sig.	t=0.29	Not Sig	t=1.31	Not Sig
Test2-3	t=0.36	Not Sig	t=0.32	Not Sig	t=2.23	Sig.

Table 5.10: Mean, standard deviation and t test of Target 12 for subjects using Linkage 3 with no visual feedback.

and Third Test or Second Test and Third Test meaning that these population are significantly different. In most cases the Third Test is better and the error goes down. However, in two cases the mean error was observed to go up. By no means can these slight increases in the average error be taken as a form of negative learning, the explanation is best explained looking at a specific case. As shown in figure 5.28 the First Test, Second Test and Third Test of Subject 1 display an almost systematic error of one target-unit. This means that he is always in the same vicinity around the target but not on it. Thus the feedback he is getting from his e.p.p. joint is taking him back, trial after trial, to about the same point, not anywhere else. But since we do not allow the patient to momentarily switch from the operational phase back to the learning phase, he could not "readjust his shot". This observation brings about two interesting comments: The first one is just a confirmation that extended physiological proprioception really provides subconscious control as a subject can without any usual source of feedback (visual, tactile) reach the same point in space on demand while performing a non-repetitive task. The second point is important since it shows that verbal and intermittent visual feedback (between each trial) are not enough to re-adjust an e.p.p. set point. When performing the test without visual feedback, the subjects were shown, after each trial, their virtual hands and the target so that they could see the error they had made. They were also told what was wrong so that next time around they could correct for it. In light of the above observations, we can now conclude that better performance could be obtained by allowing the subjects to physically reajust or recalibrate the e.p.p. joint as the operational phase progresses.

Following the plan outlined in subsection 5.1.2 of this chapter, seven subjects were taught one linkage (learning phase) and had to use it only relying on extended physiological proprioception (operational phase). Once a saturation was observed in their progress, they had to learn a new linkage and go through the same process. After experimenting with the second and third linkage, a check was done to verify how much was retained from the previously learned linkage. The experiment was done for three linkages. In the next section we will discuss some of the important aspects to consider when providing an amputee with an artificial arm possessing multiple linkages.

5.4 Learning Retention

5.4.1 Discussion

In everyday life, we perform numerous motions with arms and hands. All these motions, are usually done with great dexterity and we do not have to look at our joints or even think when executing these motions. That is why we say that we are able to perform subconscious motions. Our ultimate aim would be to provide amputees with an artificial arm that can perform many different motions with high precision and, as the natural arm, require as little concentration as possible. We have shown in the past [38] that a single-linkage e.p.p.-controlled artificial arm provides both precision in motion execution and subconcious control. We would like to now show that this is also valid for an artificial arm possessing numerous linkages.

Seven subjects were trained to use three different linkages through a first stage called learning phase where the learning took place, and a second stage called operational phase where subjects had to use the virtual arm without visual feedback. Subjects' performances were monitored and reference populations established. We will now present the results obtained when verifying learning retention and contrast the statistical results with the reference ones.

Checking Retention of Linkage 1

After learning Linkage 2 we checked retention of Linkage 1 and after learning Linkage 3 we checked the retention of Linkage 1 and that of Linkage 2. Thus two checks (labeled check#1 and check#2) were made for Linkage 1 as can be seen in figure 5.29 and 5.30. We have, for consistency selected Targets 2 and 9 of Linkage 1, as in the previous section.

Because the time elapsed between the initial learning of a particular linkage and the retention check#1 of that same linkage is between 10 to 15 days we were expecting to see a somewhat erratic behaviour at least in the early stage of the retention checks. Moreover, some confusion between the kinematics of Linkage 1 and Linkage 2 was also expected. It can be

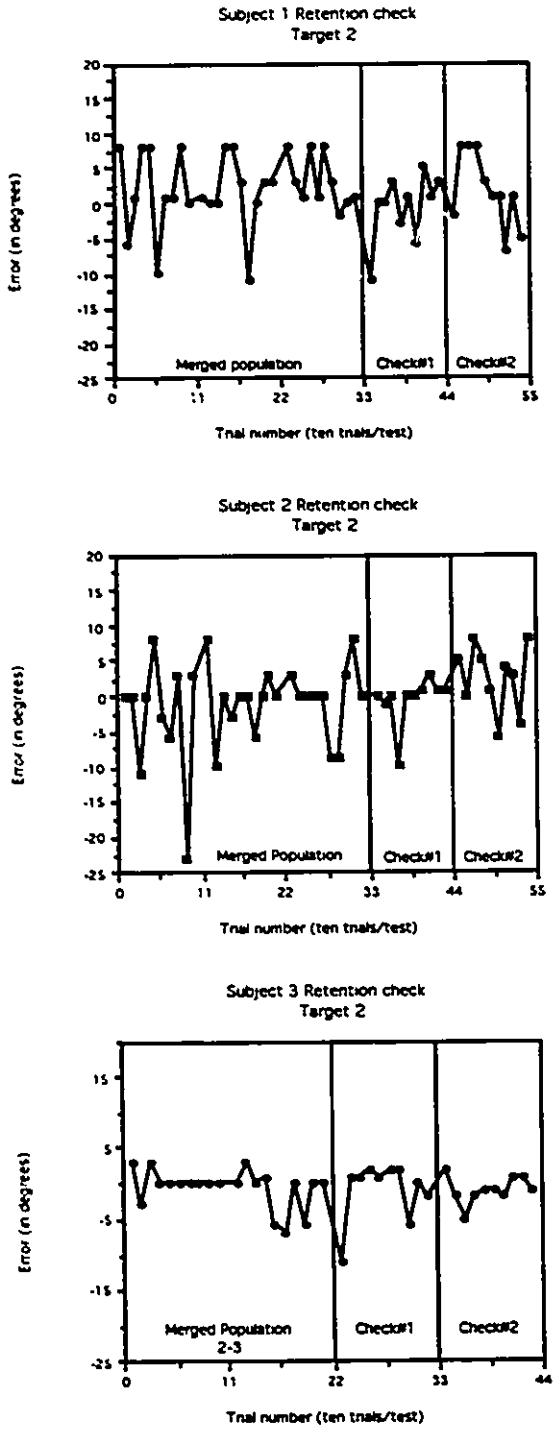

Figure 5.29: Comparison of reference population and new population for Target 2 for three typical subjects after they learned three linkages.

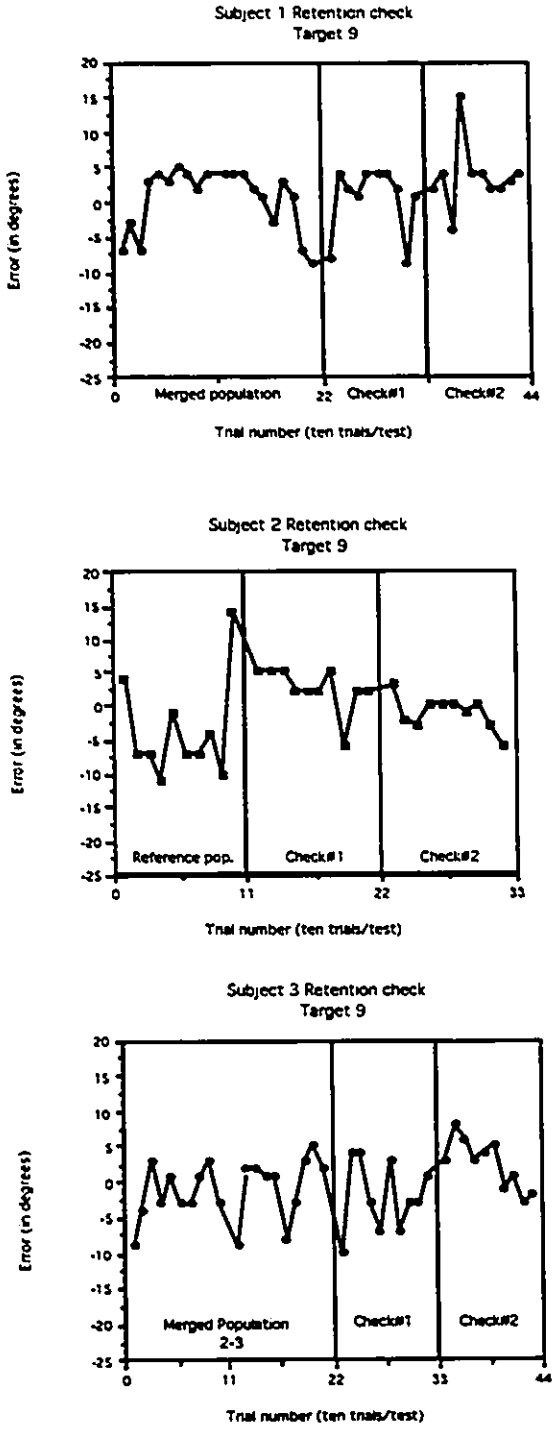

Figure 5.30: Comparison of reference population and new population for Target 9 for three typical subjects after they learned three linkages.

seen by looking at theses curves (figures 5.29 and 5.30) that this was not the case. All subjects returned to use Linkage 1 as if they had never stopped using it. Applying the t test between the reference population and the new one (check#1), the null hypothesis could not be rejected. This suggest that no significant difference was found between the reference population and the new one for all subjects for both targets as is shown in tables 5.11 and 5.12. The mean error and standard deviation are lower in almost all cases for the population of check#1 than they are in the reference population. This means that the subjects not only recall the linkage but they are improving their ability to use it. The main reason suggested here is that using linkages that are kinematically different allows the subject to get a better feel and acquintance with the system.

At this stage, on the grounds of these findings, it has been established that a person can learn efficiently and use without visual feedback an e.p.p. controlled artificial arm with two linkages without lost of spatial accuracy and with no observed confusion what-so-ever between the two.

After learning a third linkage, i.e. Linkage 3, again we verified to see if there was a noticable change in operating Linkage 1. At that point, a period of time between 16 to 21 days had past since Linkage 1 had been learned. During that time, it had been used only once for the retention check#1. When performing the learning retention tests, we were quite impressed by the ease with which all subjects performed the tests. The curves called check#2 in figures 5.29 and 5.30 again do not reveal any significant difference between the initial reference populations and the new ones. Applying the t test to these two populations only confirms the visual observations as shown in tables 5.11 and 5.12. Extremely low values of t are found implying the statistical similarity of the two populations. It is interesting to look a little closer at tables 5.11 and 5.12.

- There are no significant differences between the reference population and the new (check#2) population for all subjects except Subject 2 Target 9. This subject not only displayed good learning retention but he drastically improved his performance. This means that

	Subject 1		Subject 2		Subject 3	
Reference Mean and Standard Deviation						
Target2	Mean	STD	Mean	STD	Mean	STD
Referen.	4.1	3.6	3.97	5.14	1.6	2.37
New values of Mean and Standard Deviation						
Check#1	3.3	3.36	1.7	3.06	2.8	3.33
Check#2	4.4	3.13	4.4	2.63	1.8	1.23
Results of the t test between reference						
population and new population of retention check 1 and 2						
Test1-1	t=0.62	Not Sig	t=1.31	Not Sig	t=-0.11	Not Sig
Test1-2	t=-0.23	Not Sig	t=-0.25	Not Sig	t=-0.25	Not Sig

Table 5.11: Comparison of Means, Standard Deviations and t tests of Target 2 for subjects using Linkage 1 without visual feedback before and after learning two and three linkages.

	Subject 1		Subject 2		Subject 3	
Reference Mean and Standard Deviation						
Target9	Mean	STD	Mean	STD	Mean	STD
Referen.	4.0	2.10	7.2	3.76	3.45	2.48
New values of Mean and Standard Deviation						
Check#1	3.9	2.73	3.6	1.71	4.5	2.68
Check#2	4.4	3.8	1.8	1.99	3.6	2.22
Results of the t test between reference						
population and new population of retention check 1 and 2						
Test1-1	t=0.111	Not Sig	t=2.75	Sig.	t=-1.07	Not Sig
Test1-2	t=-0.37	Not Sig	t=4.01	Sig.	t=-0.16	Not Sig

Table 5.12: Comparison of Means, Standard Deviations and t tests of Target 9 for subjects using Linkage 1 without visual feedback before and after learning two and three linkages.

learning other linkages was not a source of confusion for him but on the contrary enhanced his ability to operate the artificial arm.

- For Subject1 and Subject 3 the error to target increased a little bit after learning the third linkage by an average of 0.26° which is not significant.

- The average standard deviation of the reference populations for all three subjects is 3.24° whereas it is 2.5° for the retention check#2. This faithfully reflects the reality during testing and confirms what was previously mentioned above that as more linkages are learned the subjects master more and more the system and, as a direct consequence to this, positioning becomes more precise and "favors" the process of making the artificial arm a natural extension of the body [48] in a similar way that a tennis racquet or a golf club becomes a natural extension of a person using it.

Checking Retention of Linkage 2

At this point each subject has learned Linkages 1, 2 and 3. The learning retention of Linkage 1 was verified above after learning Linkage 2, and after learning Linkage 2 and 3. We now expose how the subjects retained operation of Linkage 2 after learning Linkage 3.

General results are no different from what was obtained for Linkage 1. The ability of subjects to use efficiently Linkage 2 does not seem to be affected by the fact that other linkages have been learned and used. No "cross-talk" seems to take place between the utilisation of one linkage to the next or the previous. Comparisons between Reference populations and Retention check populations, as shown in figures 5.31 and 5.32, do not lead to any apparent differences. In all cases, the subjects kept going to the target with similar mean errors and standard deviations. No initial readaptation time can be identified from these curves. When using the t test to statistically compare Reference populations and Retention check populations the null hypothesis could not be rejected for Target 15 for all subjects as given by table 5.13. For Target 17, Subject 1 improved his error-to-target score, whereas for Subjects 2 and 3 no difference was found as can be seen in Table 5.14. Again for all subjects for Target 15, the

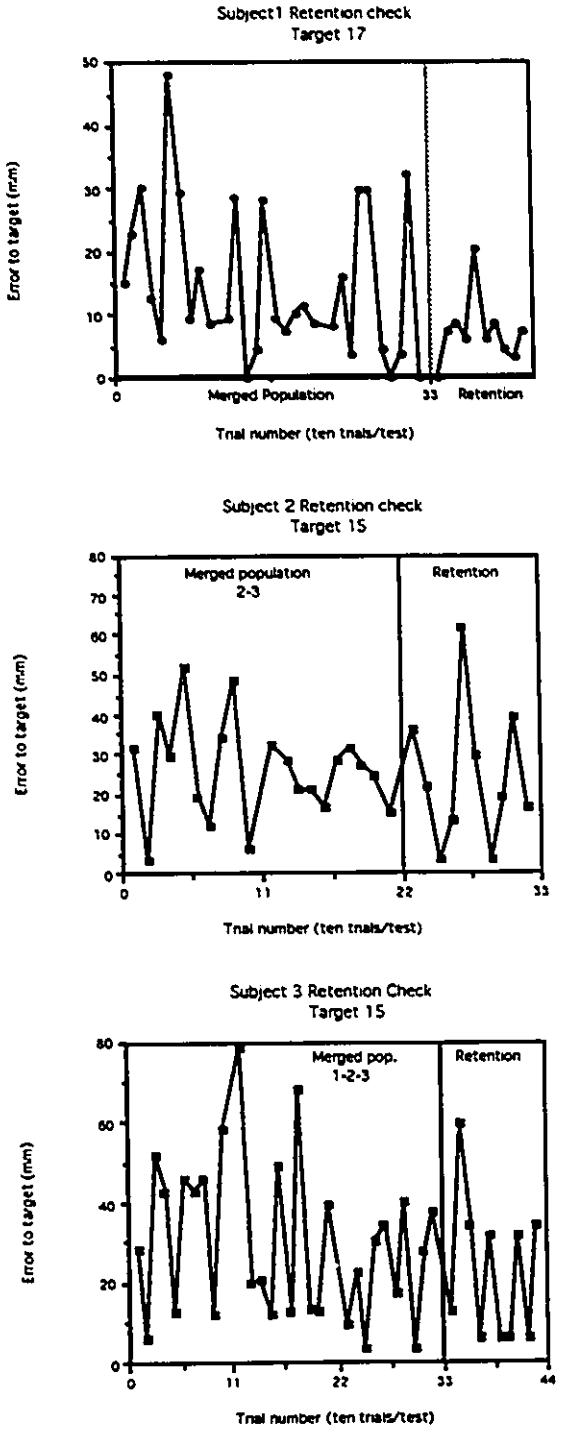

Figure 5.31: Comparison of reference population and new population for Target 15 for three typical subjects after they learned three linkages.

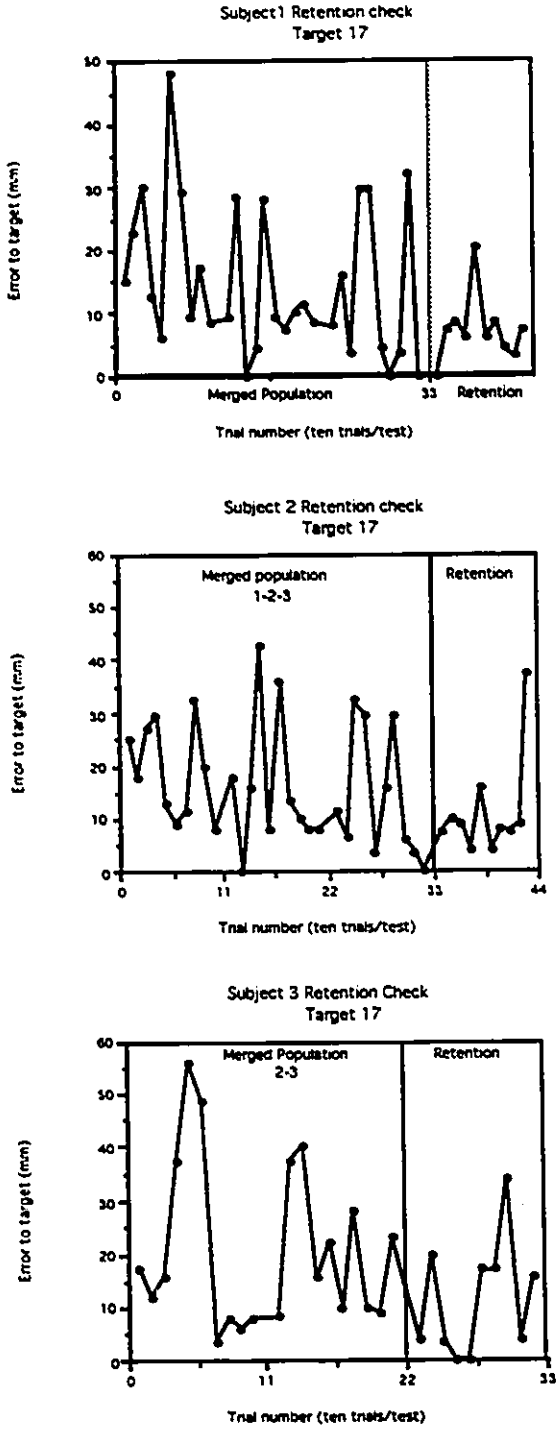

Figure 5.32: Comparison of reference population and new population for Target 17 for three typical subjects after they learned three linkages.

	Subject 1		Subject 2		Subject 3	
Reference Mean and Standard Deviation						
Target15	Mean	STD	Mean	STD	Mean	STD
Referen.	24.42	13.88	25.93	12.50	29.84	19.56
New values of Mean and Standard Deviation						
Check#1	19.34	13.21	24.41	17.91	22.71	18.0
Results of the t test between reference						
population and new population of retention check 1						
Test1-1	t=1.09	Not Sig	t=0.27	Not Sig	t=1.0	Not Sig

Table 5.13: Comparison of Means, Standard Deviations and t tests of Target 15 for subjects using Linkage 2 without visual feedback before and after learning three linkages.

	Subject 1		Subject 2		Subject 3	
Reference Mean and Standard Deviation						
Target17	Mean	STD	Mean	STD	Mean	STD
Referen.	14.65	12.01	16.26	11.49	20.72	15.36
New values of Mean and Standard Deviation						
Check#1	7.03	5.24	11.16	9.65	11.56	11.0
Results of the t-test between reference						
population and new population of retention check 1						
t-test	t=1.92	Sig.5%	t=1.26	Not Sig	t=1.67	Not Sig

Table 5.14: Comparison of Means, Standard Deviations and t tests of Target 17 for subjects using Linkage 2 without visual feedback before and after learning three linkages.

average error has gone down from 2.67 cm for the Reference population to 2.0 cm for the Retention check population. For Target 17, the average reduction in error-to-target went from 1.72 cm to 1.0 cm. Thus, in all cases there was an improvement in subject performances.

5.4.2 Conclusion

One of the goals of this research work was to study how different subjects operating a multiple-linkage artificial arm would learn, use, remember and descriminate between these linkages. The linkages programmed into the system were kinematically different, some were, according to the subjects, easy to learn, others were difficult. All replicated common anthropomorphic movements. There was an interval of several days (10-15 days) between the initial learning of a linkage and its re-utilisation to perform the learning retention check that took place after a different linkage had been learned.

The Mental Model

From the results previously presented, it is apparent that subjects using a multiple-linkage artificial arm can remember and efficiently use the different linkages that are made available to them. On the basis of these experiments, we believe that if the linkages are reasonably different[7], subjects can and will develop a natural feel for them. Another direct conclusion of this research is that an e.p.p.-controlled artificial arm, like natural extremities or tools, will be used more and more efficiently by the subject as more practice is gained and also as he learns to use it in a variety of ways. This should be even more so with a physical artificial arm (as opposed to a simulation) that has a certain weight and geometry. The subject, via the e.p.p. connection between stump and arm, will learn to adapt and develop a feel for the artificial arm dynamics. When this is done and the subject can skillfully use the arm, Moray et al. [30] suggest that a "mental model" of the process dynamics has been acquired. The

[7] We are aware that the terminology "reasonably different" is vague but the goal in providing multiple linkages to amputees is not to try to give them all the possible motions available in a natural arm but rather some linkages that will allow them to perform specific daily tasks with, of course, some built-in flexibility.

ability to operate the artificial arm without visual feedback and precisely position it in space at different pseudo-randomly requested locations using an open-loop type of behavior is one piece of evidence confirming these allegations.

A second interesting observation is made in the learning process. Subjects familiarized themselves with the system's operation during the learning phase. They did learn to use the artificial arm, but the process of generating the "mental model" does not take place until the subjects are challenged, that is when they get to the operational phase where the visual feedback avenue is removed. In a majority of cases, the first trial on a specific target without visual feedback is not good. Then, mentally, some corrections are made to adjust for the observed error and it is those corrections that will force the use of the feedback path from artificial arm to stump and to the brain, provided by extended physiological proprioception. That is why, if during a trial a particular target is reached, all succeding trials would take the arm to the same location with the precision demonstrated in previous sections. If, on the contrary, the "mental model" is not yet adequate, succeding trials will refine it until satisfaction is obtained, provided that adequate intermittent visual cues are given. If a subject makes a consistant error on a target, an alternation between the operational phase and the learning phase should solve the problem.

Monitoring of the subject's behaviour when using the simulation of the artificial arm has led us to the conclusion that, if a subject has to go from a START point to an END point as shown in figure 5.33 when visual feedback is present, the subject essentially does incremental control. He provides control from one discrete point on the path to the next until the END point is reached. He only has to remember where he was during the last "conscious" point (e.g. P2), he then drives the arm to the next point (P3). When at P3 he does not care about P0, P1, or even P2 anymore, his only concern is where he is (P3) and where he is aiming at (P4). Fine adjusments will be done on the fly to get him at the END point. On the contrary, when visual feedback is absent, local points like P1, P2 or P6 are not important any more but the START and END points are now the important paremeters. The mental model will provide

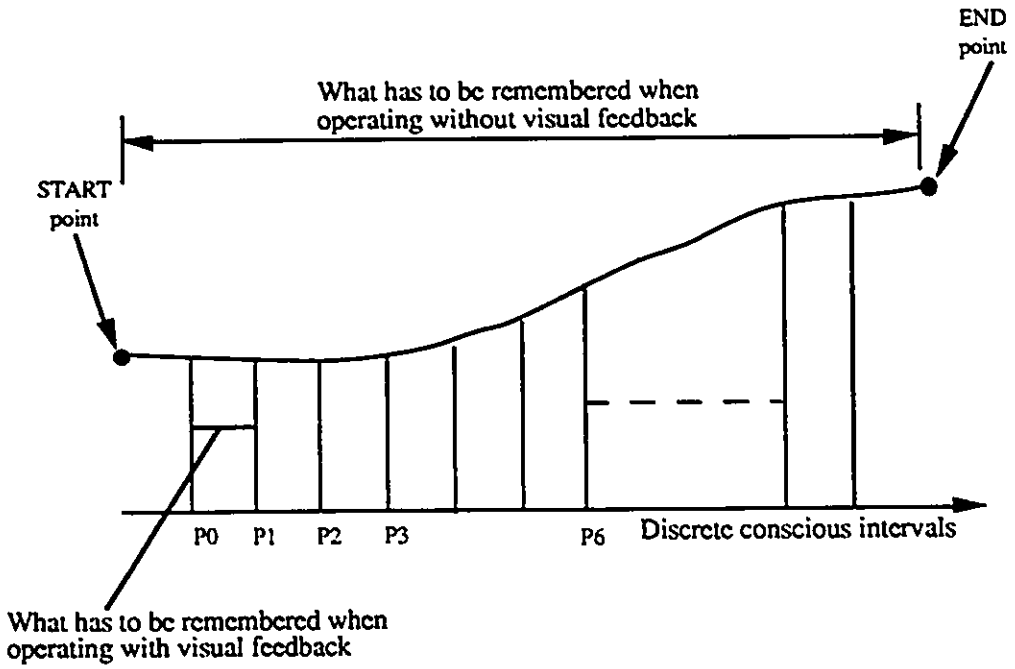

Figure 5.33: Different approach when going to a target with and without visual feedback.

instinctive drive to get the arm from START to END.

Recommendations

These observations led to the following recommendations:

- When a subject is fitted with an e.p.p.-controlled artificial arm, part of his training towards adapting to the arm should consist of performing subconsious tasks such that a proper "mental model" is developed.
- The artificial arm should incorporate a variety of kinematically different linkages that will help the subject in developing a better acquintance with the operation of the arm.

5.5 Discussion on the Ability of Subjects to Pick the Correct Linkage for a Given Task

Having shown that subjects operating an e.p.p.- controlled artificial arm possessing multiple linkages can learn to efficiently use and remember the operation of these linkages, the next logical step was to assess the ability of subjects to pick from a set of linkages the one that best fits the task they are about to undertake.

The test that the seven subjects had to take this time is now explained:

- Each of the two targets associated with Linkage 1 (Targets 2 and 9), Linkage 2 (Targets 15 and 17), and Linkage 3 (Targets 8 and 12) are grouped into a new set.
- During each test the six targets are offered three times in a pseudo-random order to the subjects. Reaching each target requires the selection of one of the previously learned linkages.
- This means that the user has to choose among the repertoire of linkages, the one that will reach the target.
- The accuracy or the speed with which the target is reached is not an issue this time. Choosing the right linkage is.
- Each subject takes the test three times.

When running this second series of tests, a scoring protocol had to be established. At the beginning of each trial the target appears in front of the subject. He selects a linkage. The following could happen:

1. Right choice. No penalty, he scores "0". Trial is ended with subject going to target. Total score: 0.
2. Wrong choice. One penalty point "-1" because subject gets cue for the next step.

- The subject can realize immediately that his choice is wrong and switch to the right linkage without suffering any more penalties. Trial is ended with subject going to target. Total score:-1
- The subject does not realize his wrong choice. He uses the linkage in vain in trying to reach the target. He gets another penalty point "-1" for that. The subject must then choose another linkage. This choice will take him to the situation depicted in 1. or 2. above. Penalty points will accumulate until he reaches the target.

An example is now taken to illustrate the various possiblities. Assuming that a target is offered to the subject, that requires the use of Linkage 1. The initial linkage in the system is also Linkage 1. Figure 5.34 represents the state diagram of this situation. The possible state transitions are as shown in figure 5.34. The gains on the branches represent the penalty points. It can be seen that for case a) in figure 5.34 the no penalty path is to stay at Linkage 1 until target is reached. The most costly path with no state revisited twice is: Go to Linkage 2, loop at 2, then go to Linkage 3, loop at 3, and finally go to Linkage 1. This is a four penalty point path. Of course longer paths exist but some states will be revisited.

Similar state diagrams can be drawn for cases when Linkage 2 or Linkage 3 are the correct linkages to reach the target and the system starts up with either the correct linkages or with one of the other ones.

The Results

The testing protocol was such that, a test was composed of six targets offered three times in a pseudo-random order. Each subject took the test three times.

Having done the test with our subjects, the results can be summarized in point form:

1. There was never more than one penalty point given in one trial. This simply means that

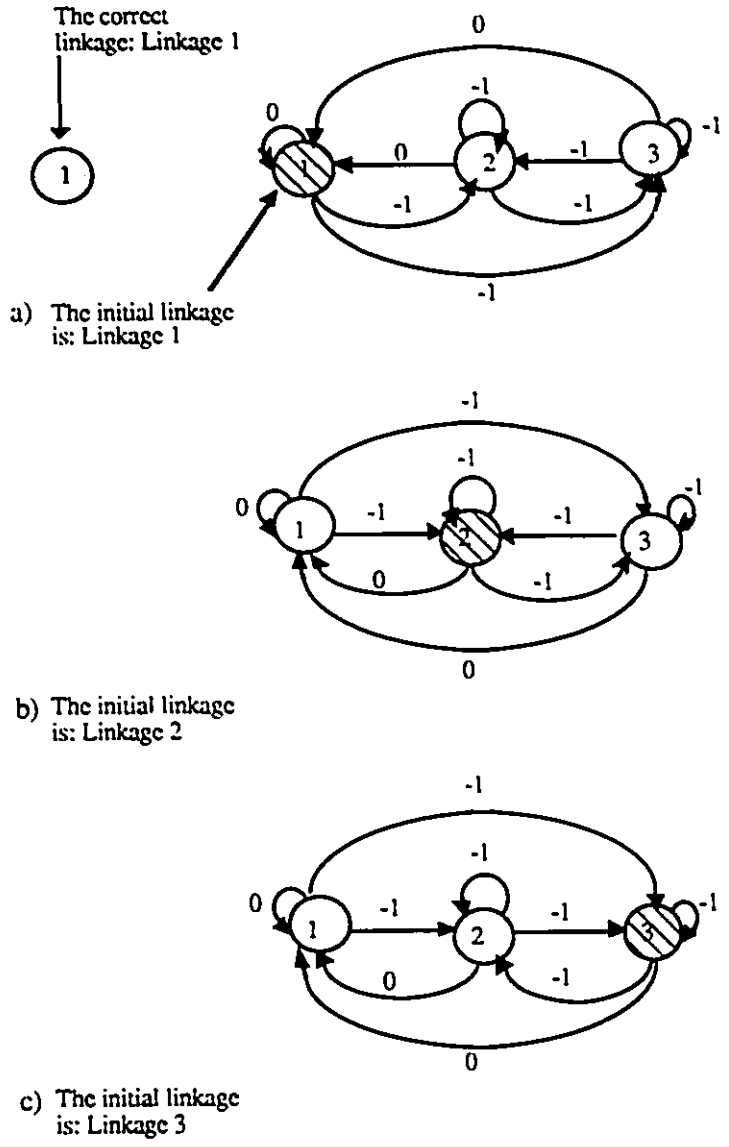

Figure 5.34: The state diagrams for all possible initial conditions in the system.

when an incorrect linkage was selected, it was never even used. The subject immediately recognized his error and picked the correct linkage. Thus errors in selecting the linkage were much more attributable to inattention than confusion.

2. Overall, subjects selected the wrong linkage, as explained above, in 2.47% of the cases.

3. All errors, if any, in selecting the correct linkage, happened during the first two tests. None of the subjects selected an incorrect linkage during the last test.

4. A unaminous comment from the subjects was that there was no confusion whatsoever in their mind in associating the correct linkage to a specific task.

Conclusion

These tests aiming at proving that subjects operating an artificial arm possessing multiple linkages can chose without confusion the correct linkage to perform a given task are indeed very conclusive. These tests took place 45 to 90 days after the ones where the subjects had to learn and operate each linkage separately. During this elapsed time, the subjects were not allowed to use the simulation. They were just allowed a quick refresh of ten trials using each linkage before starting these tests. Most of the subjects did not even feel the need for such a refresh, but they took it anyway. The few errors made in choosing the right linkage were done by those that had not used the artificial arm for more than 75 days. No inadvertent movements were done when switching from one linkage to another one as subjects instinctively stayed at the reset position during the transition.

In conclusion we can note that when an incorrect linkage was selected, it was never used. The subject always recognized his error immediately and corrected for that in the next step. Thus, these errors can be attributed to familiarization with the testing protocol and the stress generated by the decision making process rather than by real confusion. There was never any hunting for the correct linkage which definitely rules out the hypothesis of possible confusion. After the second test a 100% success rate was attained and maintained thereafter.

5.6 Discussion on the Unbeatable Servo Feature

In this section we will discuss one of the important features of e.p.p.- controlled artificial arms, the unbeatable servo. This mechanical principle was essential in properly operating the arm. Let us now see why it plays a key role and if it can be substituted by a simpler system.

In the original e.p.p. system conceived by Simpson [46], there was a 1:1 relationship between the position of the e.p.p. controlling joint (the shoulder) and the position in space of the artificial arm and thus the terminal device. This enabled the subject to know where the terminal device was in space without looking at it. To ensure that the input signal never exceeded the output capabilities of the system, a mechanical system connected to the artificial arm output continually monitored the input. If at some point the input moved too fast or too far, this system slowed down or stopped the input joint. Simpson called this system an "unbeatable servo" [46].

The unbeatable servo principle was effective in Simpson's carbon dioxide powered prostheses. These prostheses were designed for patients with upper limb amelia (congenital absence of the limb). They replaced the shoulder, the upper-arm, the forearm and the hand. Thus space was available for emplementing the mechanical "unbeatable servo" principle. Our research group worked on an above-elbow artificial arm which, because it occupies a lesser volume than Simpson's artificial arm, did not provide adequate room to incorporate a mechanical "unbeatable servo" principle. We decided then to see the extent to which this mechanical system could be replaced by an audio or a vibrational feedback feature. We first expose the conditions under which the "unbeatable servo" principle would enter in action, discuss how we accounted for that in the simulation, and finally give general recommendations. We did not discuss the cases where the subject picks up an unexpectedly high load or when the artificial arm is blocked as these are very specific cases. We, however, accounted for these situations by having the simulation's warning system to be set off in the event that they occur. Modelling of these special cases is also possible with the simulation.

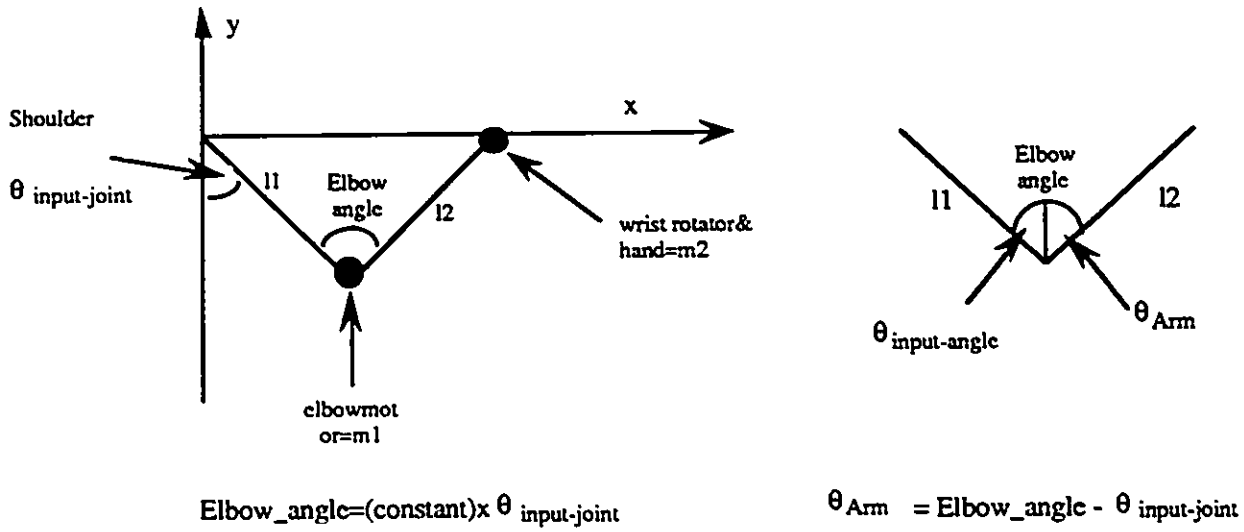

Figure 5.35: Model of the artificial arm.

The unbeatable servo enters into action when the torque required to move the arm plus external loads is not available. There could be two main reasons for that: Firstly the controller gains K_e and K_d from the required torque equation 5.1 are not appropriately chosen.

$$\text{Required torque} = K_e(\theta_d - \theta_p) - K_d\dot{\theta} \tag{5.1}$$

Solving this is easy, the value of K_e, and consequently K_d, is simply increased until the controller torque equation provides sufficient torque for the worst case situation. Secondly the artificial arm's motor cannot supply the required torque. To understand this case we must identify the worst case torque requirements. Looking at the graphical model of the arm (for a particular linkage) as shown in figure 5.35, there are again two broad scenarios that can be taken as worst case.

- The arm is extending at full speed (the terminal device is moving to right in figure 5.35) and the subject suddenly decides to retract the arm (move the terminal device to the left). In the required torque equation 5.1 we can see that the velocity term will add

to the position term giving a maximum torque. The occurence of such a situation is highly unlikely, because we rarely, in everyday life, need to do such abrupt changes in the direction of motion of our joints. An exception is, for instance, when we are reaching for an iron and expect to grab it by the steel base instead of the handle and, when close enough to it, we suddenly feel that it is hot. If that hot sensation is triggered by air surrounding the iron we would be in a reflex situation of abruptly reversing direction of motion. This situation will not be used as the typical worst case torque requirement.

- The other case is much more common and involves being in a situation retracting the arm at full speed and having the arm in a geometrical position where the gravity effect is at its maximum. This would correspond to having the arm fully extended in figure 5.35. We can also assume that there is no initial velocity (the arm is at rest) to help overcome inertia.

Having identified a likely worst case torque situation,for this specific linkage, we can now see how this will relate to the unbeatable servo feature. Let us call this torque T_{max}. Equation 5.1 above will give us the value of that torque. θ_d is the desired position and is imposed by the e.p.p. joint i.e. the input. The maximum change in θ_d is obtained by multipliying the shoulder (the e.p.p. joint) maximum start velocity ($500^0/sec.$ or 9 rad/sec[8][1]) with the sampling time τ. θ_p is the present position of the artificial arm elbow. In our worst case situation, the factor $\theta_d - \theta_p$ will give the maximum difference between present position and desired position.

The maximum resulting artificial arm displacement due to this maximum torque T_{max} is given by the following equation derived in chater 4:

$$\theta(t)_{Arm} = \frac{1}{2}\left[\frac{T_{max} + m_2 g l \sin(\alpha\theta_{elbow})}{J_T}\right] t^2 + \dot{\theta}_p t + \theta_p \qquad (5.2)$$

The θ_{elbow} is the output joint angle and α is defined by the linkage used.

[8]The arm maximum velocity is given to be $1000^0/sec.$ but it is not possible to attain that speed at start so we took an the average between null velocity and full velocity as the maximum start velocity.

The change in $\theta(t)_{Arm}$ in one sampling instant τ and assuming a null initial (not start) velocity $\dot{\theta}_p$ and a maximum effect of gravity i.e. $\alpha\theta_{elbow} = 90^0$ equation 5.2 can be rewitten as:

$$\Delta\theta(\tau)_{Arm} = \frac{1}{2}\left[\frac{T_{max} + m_2 gl\sin(90)}{J_T}\right]\tau^2 \tag{5.3}$$

Because of the 1:1 relationship required between input joint ($\theta_{input-joint}$) and output joint, it follows that the change in the output joint given by equation 5.3 should be directly proportional to the change in the input joint; let us call it: $\Delta\theta_{input-joint}$, and the proportionality constant relating them is: β (a constant=$\theta_2 \div \theta_{input-joint}$). Thus we have:

$$\begin{aligned}\Delta\theta(t)_{Arm} &= \frac{1}{2}\left[\frac{T_{max} + m_2 gl\sin(90)}{J_T}\right]\tau^2 \\ &= \beta\Delta\theta_{input-joint}\end{aligned}$$

The change in the input joint can also be expressed as the product of the input joint velocity and the sampling time τ as such: $\dot{\theta}_{input-joint}.\tau$. Incoporating this in the above equation and rearranging it in a way to isolate the maximum torque T_{max} we get:

$$T_{max} \geq \frac{\frac{\beta\dot{\theta}_{input-joint}}{J_T} + 0.5m_2 gl\sin(90)\tau}{0.5\tau} \tag{5.4}$$

From the above equation 5.4 we can conclude that knowing the maximum torque T_{max} that the motor can provide, we can adjust the rest of the parameters such that the above inequality is respected. If it is, the servo will not be beaten. Most of the parameters like artificial arm inertia, weight or gravity (J_T, m_2, g) cannot be controlled or are difficult to control. We can however select a motor with adequate torque, adjust the sampling time and finally teach the subject to avoid as much as possible violent changes in position or direction.

Recommendations

During the course of these tests we found that when emulating the Boston elbow, that has a maximum torque of $6.1N.m$, the servo was often beaten; so, based on equation 5.4, we found that for proper operation of our system with the assumptions made on friction and inertia, the bare minimum torque corresponded to about $10N.m$ without any external loads.

With this amount of torque, the servo was never beaten during tests. We do not believe that this amount of torque is excessive. Now or in the near future, light-weight, small size motor should be available for this purpose. If that can be found, a mechanical unbeatable servo is not indispensable. There is a possibility that an amputee wearing an e.p.p. controlled prosthesis after a period of time gets accustomed to it to the point of operating it to the limit. In this case, to preserve the 1:1 relationship, it would be sound to equip it with just a discrete warning system that would indicate to the user to slow down.

Chapter 6

Conclusion

6.1 Summary of the Research

This research presents a novel system developed to aid in the understanding, design and evaluation of a specific class of assitive devices. The system is to be used to improve artificial assitive arms for above-elbow amputees. It is based on a Virtual Reality simulation of an artificial arm using the control strategy called Extended Physiological Proprioception. The system was designed to be a software simulation mostly for flexibility reasons. A broad range of characteristics could be tested experimentally with each variable controlled individually. The intact arm is a complex system, and some of its functions are not even completely understood. That is why the requirements of a prosthesis are never completely specified. Thus, a designer always includes in the artificial arm what he feels will benefit the user. The designer can then test these features using the simulation to see if they are implementable and useful. Another advantage of the computer simulation is that the virtual arm can be given high performance much beyond what is available with today's state-of-the-art equipment. Thus, the limits of the amputees can be isolated from the limits imposed by the hardware. Finally, the simulation can be used as an introductory step in familiarizing the amputee with the use of his hardware artificial arm, and at the same time it can help the prothetics technician in chosing the type and number of linkages corresponding to the needs and learning capacity of each individual.

The first step of this research work was a literature review of the various strategies used for the control of artificial arms. Two different schools of thought i.e. Electromyographic Control and Extended Physiological Proprioception were identified and compared. Then, the work of Simpson on gas powered e.p.p. controlled prostheses was presented and its limitations discussed. These limitations were essentially, a single motion, one e.p.p. joint per output joint, and a hardware unbeatable servo feature.

In a desire to investigate the possibilities of providing a user with an artificial arm possessing multiple coordinated motions under microprocessor supervision and control, a Virtual Reality computer simulation of the artificial arm was developed. Arm dynamics were incorporated, and a number of linkages permitting the execution of various tasks modelled. The simulation was placed under test to verify that the visual effect was adequate and that the emulation of various artificial arms (Boston elbow, Utha arm) under various operating conditions (no load, full load, no gravity) was faithful. Specific tests were then performed with seven volunteers using the virtual arm.

There were three broad categories of tests. Here, in summary, are their characteristics and what they consisted on and what their results suggest.

1. The first series of tests was meant to explore whether an e.p.p. controlled arm could be used efficiently with more than one linkage. From the results obtained it is clear that a computer simulation of a dynamic system allows subjects to behave in a way similar to that observed when they are controlling a real physical system. Subjects could control very well the artificial arm consciously using all available sources of feedback. Subconscious control was also adequate in a manner comparable to the subconscious operation of the intact arm. However, a prerequisite to this was the generation and refinement of a mental model of this "extension" to the body formed by the artificial arm. It was also shown, with retention tests, that subjects could learn to use and operate three linkages subconsciously without lost of accuracy in their motions. In fact there is evidence that performance improves as subjects learn more linkages and get better acquinted with system dynamics. Even with several weeks between trials, good subconscious operation of the arm could be

observed.

2. The second series of tests aimed at finding whether subjects could, after learning several linkages, efficiently choose the most appropriate one for the execution of a given task. Results are again very conclusive. After an adaptation time to the testing protocol, a 100% success is obtained. No confusion could be detected at any time. Numerous linkages can and should be used with e.p.p. controlled prostheses.

3. The third series of tests consisted in monitoring the subjects using the various linkages and identifying when the system would be beaten. That happens when the input goes faster than the output can follow. By empirically adjusting the parameters of the equation of motion we could determine how to avoid beating the system. Thus, Simpson's hardware unbeatable servo feature can now be replaced, if at all needed, by a warning feature.

6.2 Contribution

This research work is probably one of the first to combine the exploratory potential of Virtual Reality to the study of adequate control strategies for artificial arms. Futhermore, it the first study to assess the capabilities of a human being to learn programmed linkages, remember them, and use them. Also, it provides valuable data and answers (possible use of multiple linkages, guidelines on the need for a mechanical unbeatable servo) related to the use of extended physiological proprioception as a control strategy for artificial arms. This information was not available in the literature. Other direct contributions of this work are:

- Development of a software simulation as the main research tool. The requirements were to perform the simulation on a Personal Computer which should run in real-time. No commercial software could be used as none could really do what we wanted (in 1989) and moreover the speed constraint was so tight that we had to develop customized software. The software is writen in C and the fast graphics routines

were written in Assembler. System dynamics including approximation to non-linear differential equations are computed in real-time.

- Design of a platform for testing artificial arm parameters such as geometry, size, weight, size of components, motors, motor minimum torque, arm dynamics etc...
- Offering the possibility of varying at will the environmental parameters such as presence or absence of gravity (aerospace applications), different density of medium (under water operation such as sea bottom exploration).
- Formulation of recommendations for the design of future externally powered microprocessor controlled artificial arms.

6.3 Future Work

Adding Depth Cues

We have discussed at length in chapter 3 (section 3.2.1) the various depth cues that the human visual system uses to distinguish the relative positions of objects in a 3-D scene. We also exposed in section 3.2.2 that because of various constraints, we had to make a trade off in the various depth cues that we used for the Virtual Reality. In chapter 5, before offering the results obtained, we elaborated on the acceptance of the Virtual Reality simulation by the subjects and we mentioned that in some specific cases the presence of steroscopic vision (providing binocular disparity) would have helped in giving the subject a better quality depth cue. To be more specific, stereoscopic vision would have reinforced the subject's perception of whether the target is in front or behind the virtual hand and how close it is. In this section we would like to propose an immediate solution that would drastically improve depth perception in the Virtual Reality. This solution is based on our observation of the subjects using the system, thus posterior to the implementation of the simulation. We analyzed this feature, acknowledged its benefits and propose that it is included as part of future work.

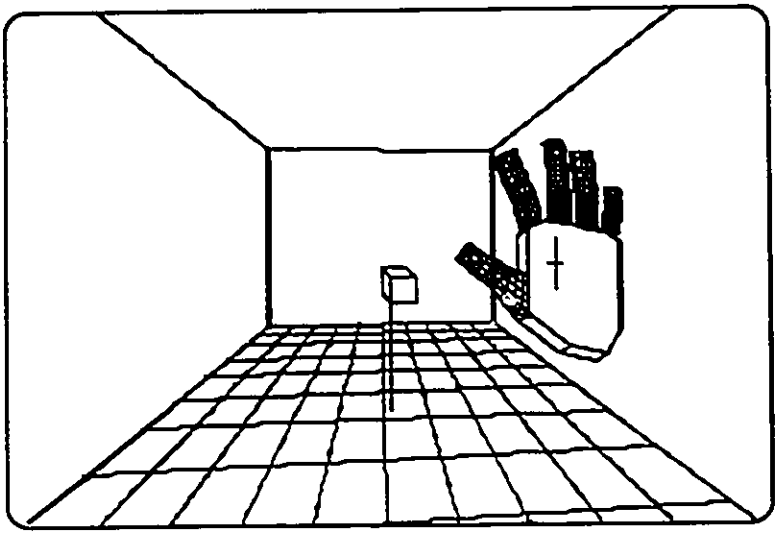

Figure 6.1: The virtual hand .

This new depth cue is based essentially on one of the psychological depth cues discussed in chapter 3: interposition, also called occlusion. This occurs when an object hides or overlaps another. Our suggestion is to use this property in a slightly different way. In the present situation, the hand of the subject in the Virtual Reality is shown in figure 6.1. The palm of the hand is not shaded, it is transparent. Because of that, when the target overlaps the hand, there is an ambiguity in deciding where the target is: behind or in front as shown in figure 6.2 (a). During our tests, we had to teach the subjects to rely on e.p.p., the chessboard floor and the anchor point to help in deciding; but the ambiguity can be removed if the palm of the hand is assumed opaque. When the hand is between the target and the observer, normal interposition is used and the target is either partially or totally hidden as shown in figure 6.2 (b). As the hand is moved closer and closer to the target, contact takes place and the target is allowed to penetrate through the hand as shown in figure 6.2 (c). This latter case will also help the subject in deciding when he is on target. In the situation depicted in figure 6.2 (a) we now know that the target is closer to the observer than the hand.

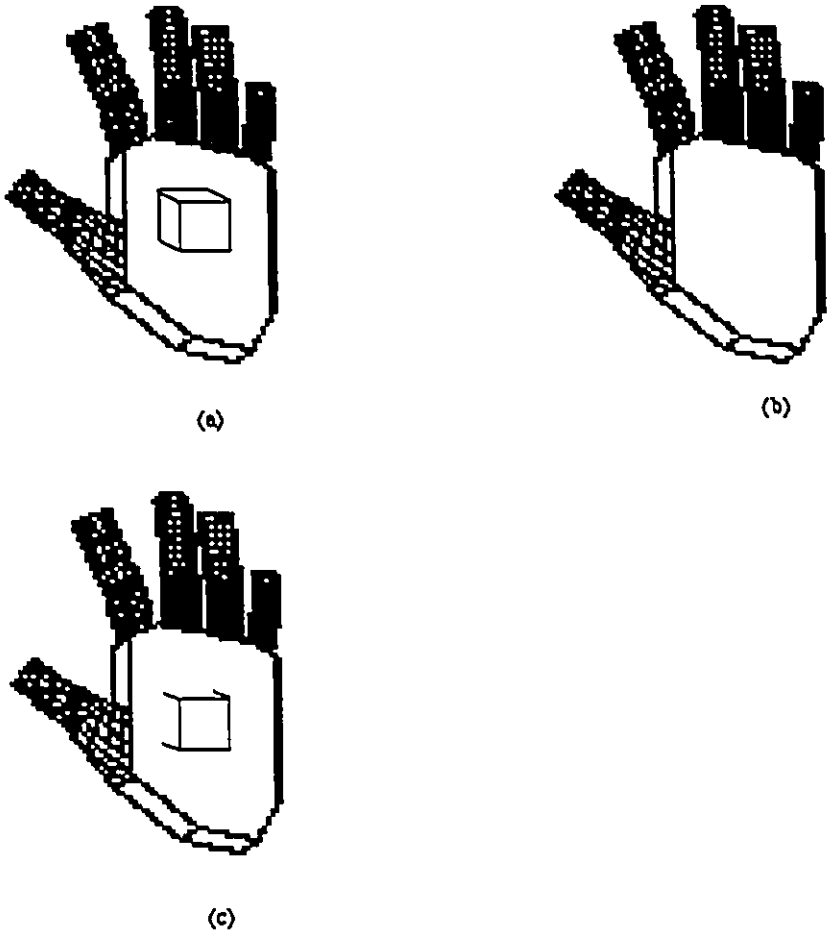

Figure 6.2: The opaque virtual hand and the dissolving target.

The implementation of this feature that we termed: the "dissolving target" will not require too much coding and thus CPU time such that the screen refresh rate will not be altered. The coordinates and specifically the depth (z) coordinates of the hand and the target are readily available at all times. Keeping this in mind, we could use any of the hidden surface algorithms detailed in [31, 19] to implement the dissolving target feature. The only change we would probably have to make is to allow for penetrating faces as this is a deviation from classical hidden line removal algorithms.

Because of the relatively simple scenario we are dealing with here, a straight forward algorithm given in Appendix C will perfom the required task.

From Simulation to Hardware

Now that some of the key questions concerning e.p.p. controlled artificial arms have been answered, further work can be invested in developing a hardware artificial arm. To do so, answers will have to be provided for some practical considerations such as:

- Adequate harnessing of artificial arm to the amputee.
- Reliable measurement of e.p.p. joint displacement.
- Artificial arm architecture.
- Choice of electrical (motors, electronics) and mechanical components (composite materials for the frame, gears).
- Choice of various useful linkages.

The simulation developed should also be a valuable tool in assisting the design and testing of such an arm.

6.4 Final Considerations

It is indeed a difficult task to provide amputees with an adequate replacement for their lost limbs. It is the author's opinion that with today's available technology, researchers should not aim at designing the perfect artificial arm that would mimic as closely as possible the intact arm. Trying to integrate the dexterity, the precision, wide varity of movements, the power of the human arm in an artificial arm is difficult for now. However, the design of the artificial arm should be viewed in the perspective of providing an assistive device helping a disabled person in performing a number of useful tasks. Furthermore, the device should be easy to use, and allow subconscious operation. If this last condition is not met, the disabled person would have to devote much of his attention to operate the artficial arm. But the focus should not be to operate the tool but rather perform the task. The author beleives that an e.p.p. controlled artificial arm possessing multiple linkages embodies that ideology and is a viable tool.

Appendix A

The Dynamics Equation for Joint 1

This appendix develops the dynamics equation for joint 1. In the case of our work where the artificial arm is attached above the elbow, joint 1 is the intact shoulder of the patient and is also the input of the system; so it does not have to be modelled. In the case where it is needed to simulate a complete artificial arm for a shoulder disarticulated amputee it would be of use.

The Lagragian L is given by:

$$\begin{aligned} L &= \sum K_i - \sum P_i \\ L &= \frac{1}{2}(m_1 + m_2)l_1^2\dot{\theta}_1^2 + \frac{1}{2}m_2 l_2^2\dot{\theta}_2^2 + m_2 l_1 l_2 \cos(\theta_1 + \theta_2)\dot{\theta}_1\dot{\theta}_2 \\ &\quad + (m_1 + m_2)gl_1\cos\theta_1 - m_2 g l_2 \cos\theta_2 \end{aligned} \tag{A.1}$$

To obtain the dynamics equation for joint 1 the Lagragian L is differentiated with respect to the first coordinate as expressed in equation (A.2):

$$F_1 = \frac{d}{dt}\frac{\partial L}{\partial \dot{q}_1} - \frac{\partial L}{\partial q_1} \tag{A.2}$$

Differentiating the Lagrangian with respect to $\dot{\theta}_1$ and θ_1 we get:

$$\frac{\partial L}{\partial \dot{\theta}_1} = (m_1 + m_2)l_1^2\dot{\theta}_1 + m_2 l_1 l_2 \cos(\theta_1 + \theta_2)\dot{\theta}_2$$

$$\frac{d}{dt}\frac{\partial L}{\partial \dot{\theta}_1} = (m_1 + m_2)l_1^2\ddot{\vartheta}_1 - m_2 l_1 l_2 \sin(\theta_1 + \theta_2)\dot{\theta}_1\dot{\theta}_2 + m_2 l_1 l_2 \cos(\theta_1 + \theta_2)\ddot{\theta}_2 - m_2 l_1 l_2 \sin(\theta_1 + \theta_2)\dot{\theta}_2^2 \quad \text{(A.3)}$$

$$\frac{\partial L}{\partial \theta_1} = -m_2 l_1 l_2 \sin(\theta_1 + \theta_2)\dot{\theta}_1\dot{\theta}_2 - (m_1 + m_2)g l_1 \sin\theta_1 \quad \text{(A.4)}$$

Now subtracting equation A.4 from equation A.3 we get the Torque at joint 1:

$$T_1 = (m_1+m_2)l_1^2\ddot{\theta}_1 + m_2 l_1 l_2 \cos(\theta_1+\theta_2)\ddot{\theta}_2 - m_2 l_1 l_2 \sin(\theta_1+\theta_2)\dot{\theta}_2^2 + (m_1+m_2)g l_1 \sin\theta_1 \quad \text{(A.5)}$$

Appendix B

More Accurate Curves Of Linkage 2 Learning Phase

This appendix provides more accurate time versus trial curves for the three subjects with different time scales. The linkage under consideration was Linkage 2 and this was during the learning phase.

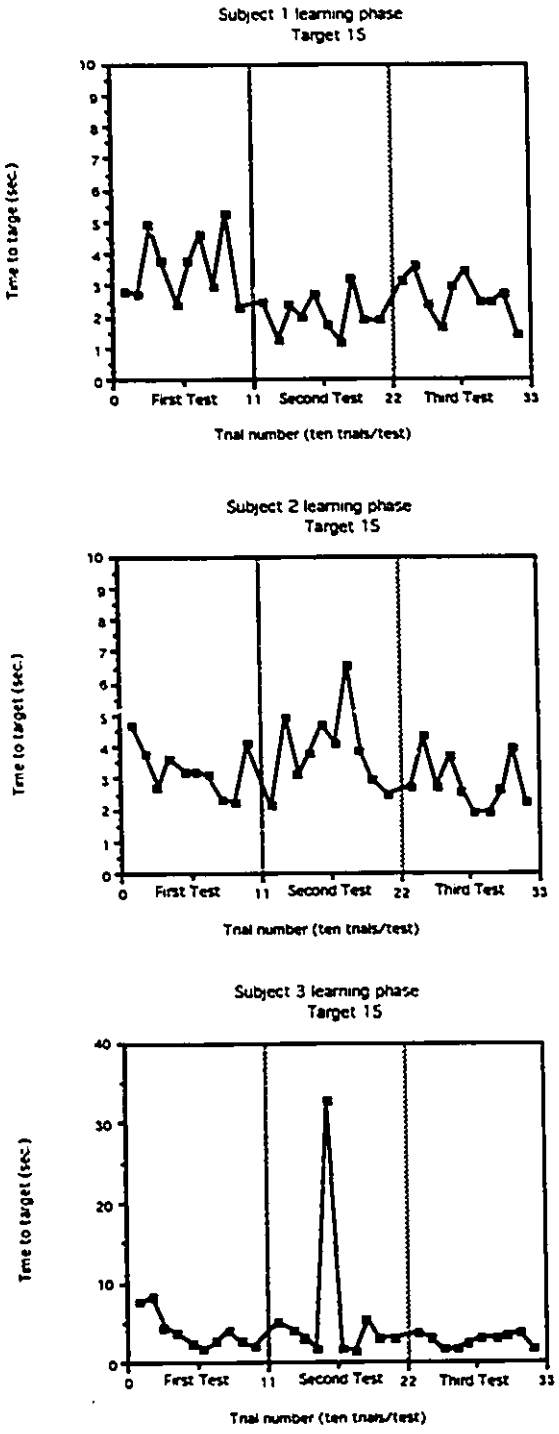

Figure B.1: Time-to-target vs Trial number for Target 15 for three typical subjects.

Appendix C

The Algorithm for The Dissolving Target

This appendix briefly develops the necessary algorithm to implement the dissolving target.

(a) Extreme points (min and max) as shown in figure C.1 for the target and the palm of the hand are identified (using a sort algorithm) for the x, y and z coordinates. The example in figure C.1 shows the Zmin, Zmax and Xmin, Xmax for the target (T) and the hand (H). The coordinate system used is that of the screen as shown in figure C.2 for completeness.

(b) Determination of overlapping in x using XminT, XmaxT and XminH, XmaxH is made.

- If no overlap in x, draw both target and hand.
- else continue with next step.

(c) Determination of overlapping in y using YminT, YmaxT and YminH, YmaxH is made.

- If no overlap in y, draw both target and hand.
- else continue with next step.

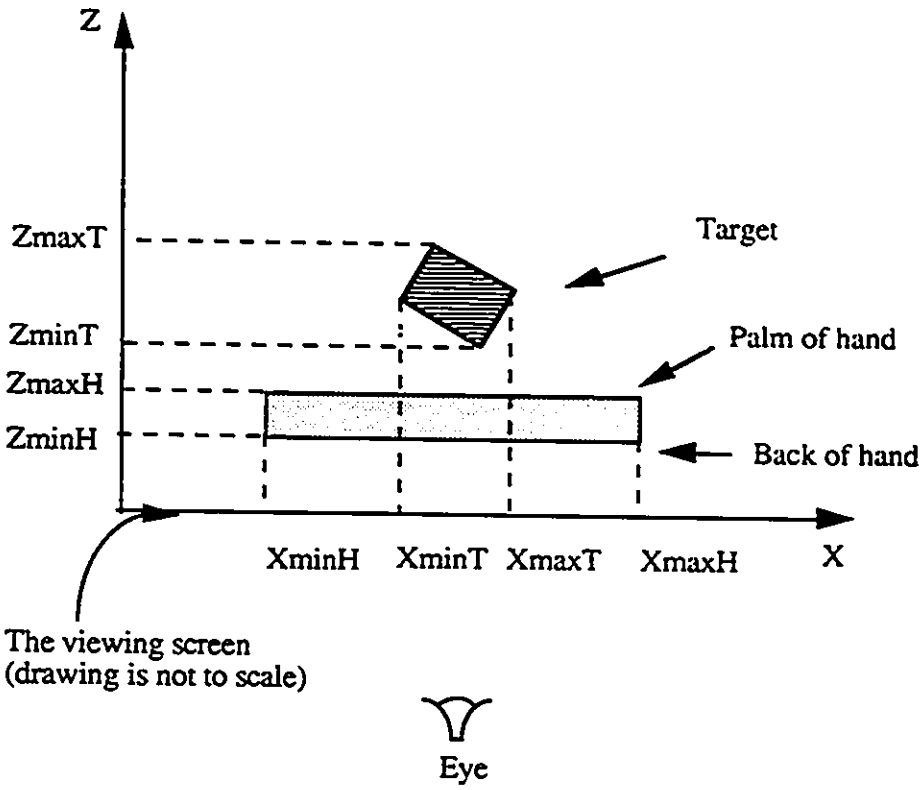

Figure C.1: Top view of a scene representing the target and the hand.

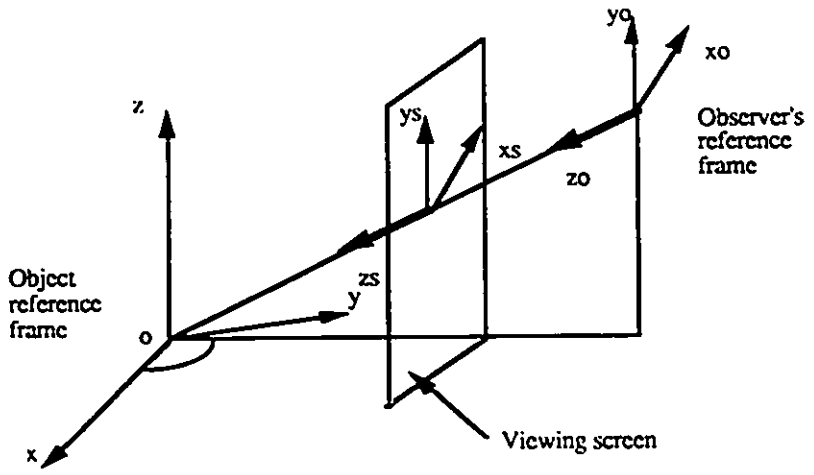

Figure C.2: Representation of the reference frame for object, observer and the viewing screen.

(d) Determination of any penetration of the target in the hand in z using ZminT, ZmaxT and ZminH, ZmaxH is made. In this case all points on the target with a z less or equal to ZminH will be drawn.

(e) Algorithm should take care of partial interposition.

This algorithm is very simple and does not really need optimization for speed because of the simplicity in rendering of the objects in the scene implying a very limited number of points going through sorting and comparisons.

Bibliography

[1] Abul-Haj, C. and Hogan, N., "An Emulator System for Developing Improved Elbow-Prosthesis Designs," IEEE Trans. Biomed. Eng., vol. BME-34, no. 9, pp. 724-736, September. 1987.

[2] Asada, H., Youcef-Toumi, K., Direct-Drive Robots, Theory and practice, The M.I.T. Press Cambridge, Massachusetts, London, England.

[3] Brookes, B.C. and Dick, W.F.L., An introduction to STATISTICAL METHOD, Sec. Ed., HEINEMANN. LONDON, 1969.

[4] Burdea, G. and Zhuang, J., "Dextrous telerobotics with force feedback-an overview." Part 1: Human factors. Robotica. Cambridge, UK., 9, pp. 171-178, 1991a.

[5] Burdea, G. and Zhuang, J., "Dextrous telerobotics with force feedback-an overview." Part 2: Control and implementation. Robotica. Cambridge, UK., 9, pp. 291-298, 1991b.

[6] Burdea, G., Zhuang, J., Roskos, E., Silver, D. and Langrana, N., "A Dextrous Master with Force Feedbask," Presence: vol. 1, no. 1, pp. 18-28, Massachusetts Institute of Technology, 1992.

[7] Carrabine, L., "Plugging into the Computer to Sense Virtual Reality," Computer-Aided Engineering, pp. 18-24, June 1990.

[8] Childress, D.S. (1972) Northwestern Universities. Chicago (unpublished communication).

[9] Childress, D.S., Holmes, D.W. and Billock, J.N, "Ideas on Myoelectric Prosthesic Systems For Upper-Extremity Amputees," in The Control of Upper-Extremity Prostheses and Orthoses, P. Herberts, R. Radefors, R. Magnusson and I. Petersen, Eds. Springfields, IL: Charles C. Thomas, 1974, Ch. 15.

[10] Childress, D.S., "Historical Aspect of Powered Limb Prostheses," Clin. Prosthet. Orthot. vol. 9, no. 1, pp. 2-13, Winter 1985.

[11] Clark, J., "Roots and branches of 3-D," BYTE, pp.153-164 May 1992.

[12] C.N., "Entering Virtual Reality," Computing NOW, Vol.12, pp. 12-16, September 1992.

[13] Crossman, E.R. and Cooke, F.W., "Manual control of slow response systems," in The Human Operator in Process Control, E. Edwards and F. Lees, Eds. London: Taylor and Francis, 1974, pp. 51-66.

[14] DesignCAD 3-D, Pofessional CAD System, American Small Business Computers, Inc., V2.1, 1987-1989.

[15] Doubler, J.A. and Chidress, D.S., "Design and Evaluation of a Prosthesis Control System Based on the Concept of Extended Physilogical Proprioception," Journal of Rehab. Research and Dev., vol.21, no.1, BPR 10-39, pp. 19-31.

[16] Doubler, J.A. and Chidress, D.S.,"An Analysis of Extended Physilogical Proprioception as a Prosthesis-Control Technique," Journal of Rehab. Research and Dev., vol.21, no.1 BPR 10-39, pp. 5-18.

[17] Dunfiel, V. and Shwedyk, E., "Digital E.M.G. Processor," Med. & Biol. Eng. & Comput., 1978, vol. 16, pp. 745-751.

[18] Ellis, S.R., " Nature and Origins of Virtual Environments: a Bibliographic Essay," Computing Systems in Engineering vol.2, no.4, pp. 321-347, 1991.

[19] Foley, J.D. and Van Dam, A., Fundamentals of Interactive Computer Graphics, Addison-Wesley Pul. Comp., 1982.

[20] Gibbons, D.T., O'Riain, M.D. and Philippe-Auguste, S. "An Externally Powered Prosthesis Employing Programmed Linkages," IEEE Trans. Biomed. Eng., vol. BME-34, pp. 493-498, July 1987.

[21] Graupe, D. and Cline, W.K., "Functional Separation of EMG Signals Via ARMA Identification Methods for Prosthesis Control Purposes," IEEE Trans. Syst., Man and Cybern., vol. SMC-5, pp. 252-259, March 1975.

[22] Hollerbach, J.M., "A recursive Lagrangian formulation of manipulator dynamics and a comparative study of dynamics formulation complexity," IEEE Trans. Syst., Man and Cybern., vol. 10, November 1980.

[23] Kruger, M.W., "Responsive environments," NCC Proceedings, pp. 375-385, 1977.

[24] Kruger, M.W., Artificial Reality, Addison-Wesley, Reading, Massacheusetts, 1983.

[25] Kruger, M.W., "VIDEOPLACE-An Artificial Reality," SIGCHI 85 Proceedings, pp. 35-40, April 1985.

[26] Kuo, B.C., Automatic Control Systems. 5th ed., Englewood Cliffs: Prentice-Hall, 1987.

[27] Lee, S., and Saridis, G.N., "The Control of a Prosthesic Arm by EMG Pattern Recognition," IEEE Trans. on Automat. Contr., vol AC-29, no. 4, April 1984.

[28] Lyman, J.H., Freedy, A., Prior, R. and Solomonow, M., " Studies Toward a Practical Computer-Aided Arm Prosthesis System": Bull. of Prosthetics Research. pp. 231-225, 1974.

[29] McAllister, D.F., "3-D DISPLAYS," BYTE, pp. 183-188 May 1992.

[30] Moray, N., Loosteen, P. and Pajak, J., "Acquisition of Process Control Skills," IEEE Trans. on Sys., Man, and Cyb., vol. SMC-16, no. 4, July/August 1986.

[31] Newman, M.W., Sproull and F.R., Principles of interative computer graphics, second ed., McGRAW-HILL, 1979.

[32] Newquist, H.P., "A Computer-Generated Suspension of Disbelief," AI EXPERT, pp. 34-39, August 1991.

[33] Nugent, W.R., "Virtual Reality: Advanced Imaging Special Effects Let You Roam in Cyberspace," Journal of The American Society for Information Science, Vol. 42(8), pp. 609-617, September 1991.

[34] O'Riain, M.D. and Gibbons, D.T., "Position Proprioception in a Microcomputer-Controlled Prosthesis," Med. & Biol. Eng. &Comput., Vol. 25, pp. 294-298, May 1987.

[35] Paul, R.P., Robot manipulators: mathematics, programming, and control. The computer control of robot manipulators, Cambridge, Mass., MIT Press, 1981.

[36] Philippe-Auguste, J.S., "A Microcomputer Controlled Above-Elbow Prosthesis using Extented Physiological Proprioception," Masters thesis, Dep. Elec. Eng., University of Ottawa, Ont. Canada, Fall 1986.

[37] Philippe-Auguste, J.S. and Gibbons, D.T., "Simulation and modelling of a microm-puter controlled controlled above-elbow prosthesis," Automed., vol. 11, pp. 99-109, 1989.

[38] Philippe-Auguste, J.S., "Performance Evaluation of a Computer Simulation of a Robotic Arm using the Principle of Extented Physiological Proprioception," Candidacy paper, Dep. Elec. Eng., University of Ottawa, Ont. Canada, 1989.

[39] Philipson, L. and Söbye, R., "Control Accuracy And Response Time in Multiple-State Myoelectric control of Upper-Limb Prostheses. Initial Results in Nondisabled Volunteers," Med. & Biol. Eng. & Comput., vol. 25, pp. 289-293.

[40] Proakis, J.G., Digital Communication, 2nd Ed., New York:MacGraw-Hill, 1989.

[41] Raitt, D., "The Electronic Library Manager's Guide to Virtual Reality," The Electronic Library, vol. 9, no. 1, pp. 3-5, February 1991.

[42] Scott, R.N., Parker, P.A. and Dunfield, V.A. (1974) Myoelectric control. In: IEE Medical Electronics Monograph 7-12 (Eds. D.W. Hill and B.W. Watson) Peter Peregrinus Ltd.

[43] Shannon, C.E., "A Mathematical Theory of Communication," Bell Syst Tech J 27(3): 379-423, 623-656, 1948.

[44] Simpson, D.C. and Lamb, D.W. (1965). "A System of Powered Prostheses For Severe Bilateral Upper Limb Deficiency," Journal of Bone And Joint Surgery, 47B, pp. 442-447.

[45] Simpson, D.C. "Functional Requirements and Systems of Control for Powered Prostheses," Bio-Medical Engineering, vol. 1, pp. 250-254, 265, 1965.

[46] Simpson, D.C. "The control and supply of a multi-movement externally powered upper limb prosthesis," Proc. 4th Intl. Symp. External Control of Human Extremities, Belgrade, pp. 247-254, 1973.

[47] Simpson, D.C. and Kenworthy, G., "The Design of a Complete Arm Prosthesis," Bio-Medical Engineering, 1973, vol.-8(2), pp. 56-59, February.

[48] Simpson, D.C., "The choice of control system for the multimovement prosthesis: extended physiological proprioception (e.p.p.) ", in "The Control of Upper-Extremity Prostheses and Orthoses", Eds. P. HERBERTS, R. KADEFORS, R. MAGNUSSON, and I. PETERSEN, pub. C.C. Thomas, ch.15, 1974.

[49] Snyder, W.E., Industrial Robots: Computer Interfacing and Control, Englewood Cliffs: Prentice-Hall, 1985.

[50] Stanford, D., "The Concise Oxford Dictionary," University Press, Oxford, 1985.

[51] Sutherland, I.E., "The ultimate display," International Federation of Information Processing 2, 506, 1965.

[52] Sutherland, I.E., "Computer displays," Scientific American 222(6), pp. 56-81, 1970.

[53] Watkison, D., "Virtual reality: The ultimate special effect," Videography, pp. 107-111, October 1990.

[54] Wenzel, M., E., "Localization in Virtual Acoustic Displays," Presence: vol.1, no. 1, pp. 80-105, 1991.

[55] Wirta, R.W., Taylor, D.R. and Finley, F.R., "Pattern-Recognition Arm Prosthesis," A Historical Perspective-A Final Report: Bull. of Prosthetic Research. pp. 9-35, 1978.

[56] Wolfram, S., "Mathematica," a System for Doing Mathematics by Computer, Addison-Wesley Publising Compagny, 1988.